THE FLORIDA STATE UNIVERSITY

COLLEGE OF ARTS AND SCIENCES

AN ECOLOGICAL MODEL OF THE LOWER MARINE TROPHIC LEVELS ON THE CONTINENTAL SHELF OFF WEST FLORIDA

By
J. S. WROBLEWSKI

A Thesis submitted to the
Department of Oceanography
in partial fulfillment of the
requirements for the degree of
Master of Science

Approved:

James J. O'Brien
Professor directing Thesis

R. W. Menzel

Robert C. Harriss

Albert Collier

John W. Winchester
Chairman
Department of Oceanography

June, 1972

Department of Oceanography

ABSTRACT

A simulation model of the flow of the biologically limiting nutrient through the lower trophic levels of a marine ecosystem over a continental shelf is presented. The model delineates the concentration of the limiting nutrient dissolved in the water column and in the biological components phytoplankton, zooplankton, pelagic fish, and detritus. Interrelated processes of this time dependent, spatial, nonlinear, physical-chemical-biological model include advection, diffusion, several biotic and abiotic environmental conditions, and numerous biological processes and physiological functions.

Model solutions include specification of steady state values and model responses to pulses of nutrient availability. The necessity of including the effect of advection upon the spatial distribution of the biotic components is demonstrated by comparing model solutions for an upwelling situation and a case where advection is neglected.

The maximum rate of nutrient uptake by phyto-plankton, V_m, is found to be a fundamental time scale to
The maximum rate of nutrient uptake by phyto-plankton, V_m, is found to be a fundamental time scale to

which both physical and biological processes can be related. The value of V_m is dependent on the biologically limiting nutrient; V_m scales the rates of the biological processes such as growth, death, excretion, and regeneration.

A nondimensional parameter S, evolved from the formulation of the model, scales the effects of advection and diffusion relative to the rate of biological turnover in determining the spatial solutions. The magnitude of S is dependent on the value of V_m. The spatial distributions of the biotic components are calculated for both phosphate and nitrate limiting situations. Simulations show major differences in standing stock concentrations and distributions within weeks for these two nutrients. Localities of greater upwelling of nutrient rich waters into the euphotic zone show greater phytoplankton and zooplankton standing stocks.

The rates of the system are explored. Sensitivity analyses are conducted on the model formulation to determine the controlling factors in the system dynamics. Herbivore grazing and excretion rates are found to influence the standing stock concentrations of the
Herbivore grazing and excretion rates are found to
influence the standing stock concentrations of the
biological components to the greatest extent.

ACKNOWLEDGEMENTS

This thesis resulted from the development of a time dependent, spatial plankton model created jointly by Dr. James J. O'Brien and the author.

This research has been supported for the past eighteen months primarily by the Office of Naval Research and the National Science Foundation under Grant # GA-29734. Part of the research was conducted at the National Center for Atmospheric Research in Boulder, Colorado.

The Computer Facility at NCAR provided CDC 7600 and 6600 time and the Florida State University Computing Center provided CDC 6400 time.

Appreciation is extended to my committee members, Professor Albert Collier, Dr. Robert C. Harriss, Dr. R.W. Menzel, and Dr. James J. O'Brien. Special recognition is due Dr. Richard Iverson and Dr. John Winchester for their encouragement toward the modeling approach of studying ecosystems. I wish to thank Murice O. Rinkel, Assistant Director, State University System of Florida Institute of Oceanography, for making possible field observations necessary for this study.
Institute of Oceanography, for making possible field observations necessary for this study.

This research reflects the interdisciplinary interests, ideas, and teamwork which are the qualities of the Mesoscale Atmospheric Oceanic Interaction Research Group directed by Dr. James J. O'Brien. The deepest gratitude is extended to the director and members of this team for their unbounded aid in solving this multi-disciplinary oceanographic problem.

TABLE OF CONTENTS

      Euphotic Zone Calculation

      Photosynthetic Rate as a Function of Time of Day

MODEL. . . . .

6.1 Physical Constants

LIST OF TABLES

LIST OF ILLUSTRATIONS

LIST OF ILLUSTRATIONS - Continued

Figure | Page

16.a and b. Contours of the u velocity (left) and v velocity (right) over the oceanic section. Positive u velocities indicate

LIST OF ILLUSTRATIONS - Continued

longitude at 27° 15' N latitude (see Fig. 2) showing the depth profiles of the chlorophyll a and nutrient concentration data collected during November, 1971 150

LIST OF ILLUSTRATIONS - Continued

1. INTRODUCTION

1.1 Background

The building of mathematical models to understand the processes of ecological systems began with the classic prey-predator equations of Lokta (1925) and Volterra (1928). Since then marine scientists have attempted to describe the processes of biological production in the ocean by deducing equations which represent the interaction of biological elements with their environment. Several fundamental mathematical formulations which theoretically simulate or predict primary and secondary production in the sea have been presented by Fleming (1939), Riley (1946, 1947 a and b), Riley, Stommel, and Bumpus (1949), Steele (1959), Cushing (1959), and Yentsch (1963). Patten (1968) and Raymont (1966) have prepared excellent review articles on this type of mathematical model of plankton production. A scheme of the evolutionary development of modeling plankton systems is shown in Fig. 1. Recently developed models such as Iverson (1972) are not included.

O'Connor and Patten (1968) classify previous plankton models as either (1) the model sacrifices

O'Connor and Patten (1968) classify previous plankton models as either (1) the model sacrifices

Fig. 1 Important citation relations between mathematical plankton models and some of their antecedents. Each reference is coded at the left as follows: (1) the model sacrifices generality to gain realism and precision; (2) the model sacrifices realism to gain generality and precision; (3) the model sacrifices precision to gain realism and generality; and (4) the model exhibits a reasonable balance between realism, generality, and precision. The letter E denotes an extension of a previously formulated model. (Modified from O'Conner and Patten, 1968).

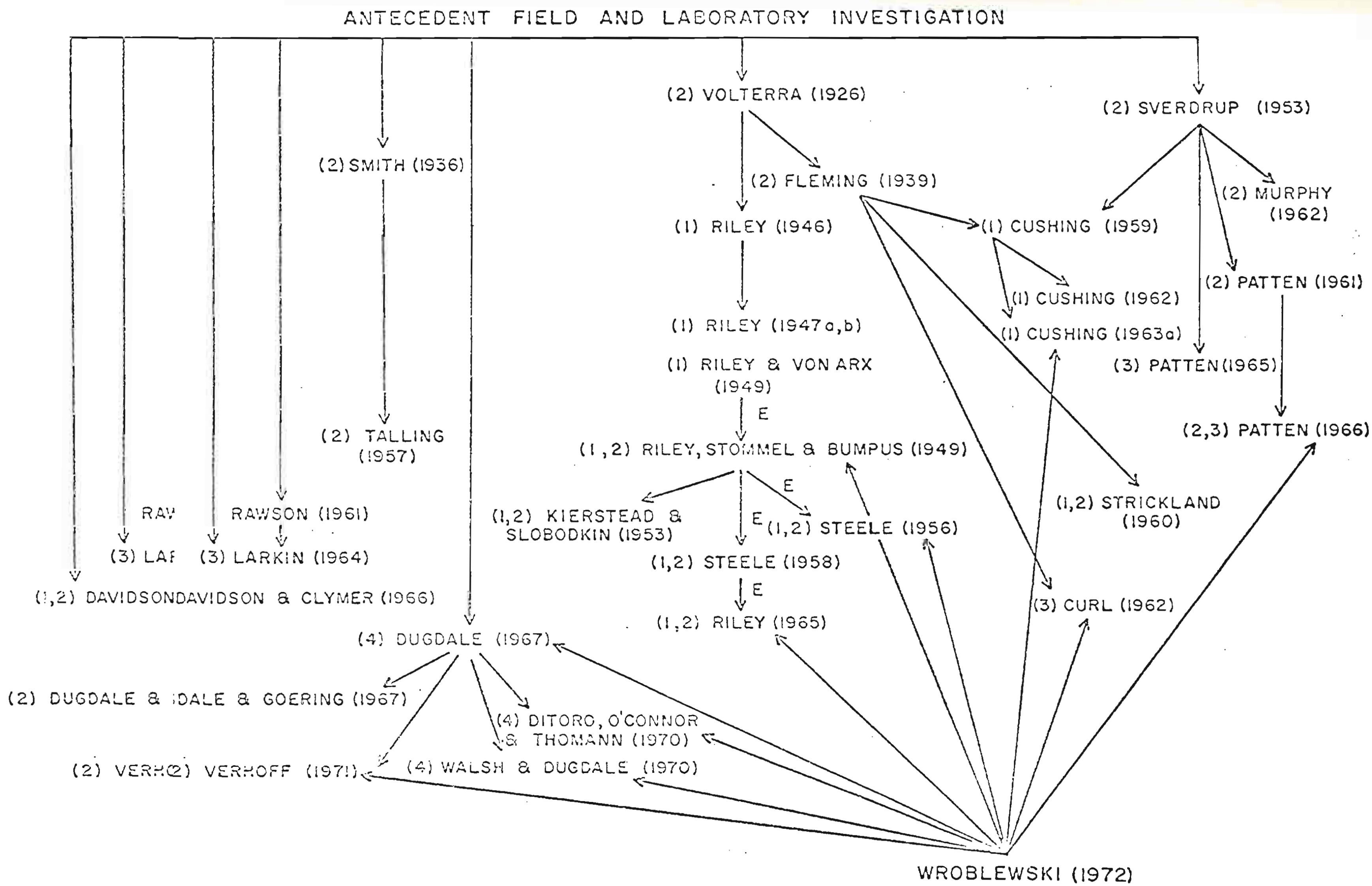
ANTECEDENT FIELD AND LABORATORY INVESTIGATION
(2) VOLTERRA (1926)
(2) SVERDRUP (1953)
(2) SMITH (1936)
(2) FLEMING (1939)
(2) MURPHY (1962)
(1) RILEY (1946)
(1) CUSHING (1959)
(1) CUSHING (1962)
(2) PATTEN (1961)
(1) RILEY (1947a,b)
(1) CUSHING (1963a)
(1) RILEY & VON ARX (1949)
(3) PATTEN (1965)
E
(2) TALLING (1957)
(1,2) RILEY, STOMMEL & BUMPUS (1949)
(2,3) PATTEN (1966)
E
RAV
RAWSON (1961)
(1,2) KIERSTEAD & SLOBODKIN (1953)
E
(1,2) STEELE (1956)
(1,2) STRICKLAND (1960)
(3) LAI
(3) LARKIN (1964)
(1,2) STEELE (1958)
E
(1,2) DAVIDSONDAVIDSON & CLYMER (1966)
(3) CURL (1962)
(1,2) RILEY (1965)
(4) DUGDALE (1967)
(2) DUGDALE & DALE & GOERING (1967)
(4) DITORO, O'CONNOR & THOMANN (1970)
(2) VERH(2) VERHOFF (1971)
(4) WALSH & DUGDALE (1970)
WROBLEWSKI (1972)

Fig. 1

generality to gain realism and precision; (2) the model sacrifices realism to gain generality and precision; or (3) the model sacrifices precision to gain realism and generality. With the evolution of more complex models, we add the classification (4) the model exhibits a reasonable balance between realism, generality, and precision.

In 1935 Tansley introduced the ecosystem concept. The trophic-dynamic modeling of ecosystems began with Lindeman (1942) whose food chain theories have proven to be fundamentally sound. Early studies of the trophic structure of marine ecosystems include investigations by Odum and Odum (1955), Teal (1962), Riley (1963), Ryther (1963), and Schaeffer (1965).

Investigations of the dynamics of marine ecosystems have followed two approaches. Energy flow studies (e.g. H.T. Odum, 1957; Slobodkin, 1962; and Macfadyen, 1964) have provided significant contributions to the understanding of aquatic ecosystem energetics. The second approach concerns studies of the cycling of material through the biotic and abiotic elements of the system (e.g. Curl, 1962; Gerking, 1962; and Dugdale and
material through the biotic and abiotic elements of the system (e.g. Curl, 1962; Gerking, 1962; and Dugdale and
Goering, 1967). The interconvertability of these approaches

was demonstrated by Odum (1962) who took published data on the production and utilization of organic matter and converted them to an energy flow chart. Material turnover studies differ in time scale and magnitude from energetic investigations. A comparison of the two approaches can be found in Mann (1969).

Within the last decade, the systems analysis approach of engineering has been applied to the investigation of ecosystems. In his book Systems Analysis in Ecology Watt states, "for ecologists, a suitable definition of a system is an interlocking complex of processes characterized by many reciprocal cause-effect pathways". Systems as these have analogies in the engineering sciences. Watt continued to observe, "a principle attribute of a system is that we can only understand it by viewing it as a whole". This is the philosophy of the systems approach.

Several texts discussing the application of this approach to ecology in general include those by Watt (1962), Pielou (1969), and Patten (1971).

1.2 Purpose of the Study

The intent of this study is to introduce a quantitative simulation of the flow of the biologically

quantitative simulation of the flow of the biologically
limiting nutrient through the lower marine trophic levels

in the waters over a continental shelf. The study area is the Gulf of Mexico waters off West Florida during the winter and spring months of the year. Dugdale's (1967) concept of estimation of biomass in terms of content of the biologically limiting nutrient is the basis of this simulation. Specifically, the relative proportion of the limiting nutrient in each of the biotic components (phytoplankton, zooplankton, pelagic fish, organic detritus, and dissolved nutrients) is calculated.

Conservation of mass within the marine ecosystem is a basic assumption. The total amount of limiting nutrient in the system is accounted for by either mass transport into or out of the area, or uptake and release by biological components within the system. The objective is to demonstrate that reasonable spatial distributions of the average concentration of the limiting nutrient in the lower marine trophic levels can be simulated.

Present biological and physical oceanographic conceptions about the area are incorporated into this study. The mechanism of current-induced upwelling is used to generate a circulation pattern over the shelf such that nutrient rich bottom waters are brought into

used to generate a circulation pattern over the shelf such that nutrient rich bottom waters are brought into

the euphotic zone. This addition of limiting nutrient enables greater biological production in these otherwise nutrient poor waters.

Fig. 2 is a map of the Gulf of Mexico waters under consideration. The shelf region is of considerable width. Bottom topography consists of a gently sloping bottom extending to approximately 200 kilometers seaward where a sharp continental shelf break is encountered. Here the bottom rapidly plunges to depths of greater than 1000 meters. During the winter and spring months storms and winds mix the shelf waters to the bottom. The Florida Loop Current, the major current occurring in the eastern Gulf of Mexico, is found running south close to the shelf break during this period.

Field studies of the area by Bogdanov *et al*. (1968) and Austin (1971) have indicated upwelling occurs offshore during the cold period of the year, accompanied by increases in plankton biomass and concentration of main commercial species of fish on the southwestern part of the Florida Shelf (Figs. 3-5). The commercial importance of these waters is a major consideration for choosing these waters for investigation.

waters for investigation.

Fig. 2 Model area: the continental shelf off West Florida. Transects 1 and 2 are locations of observational data collected for input into the simulation model.

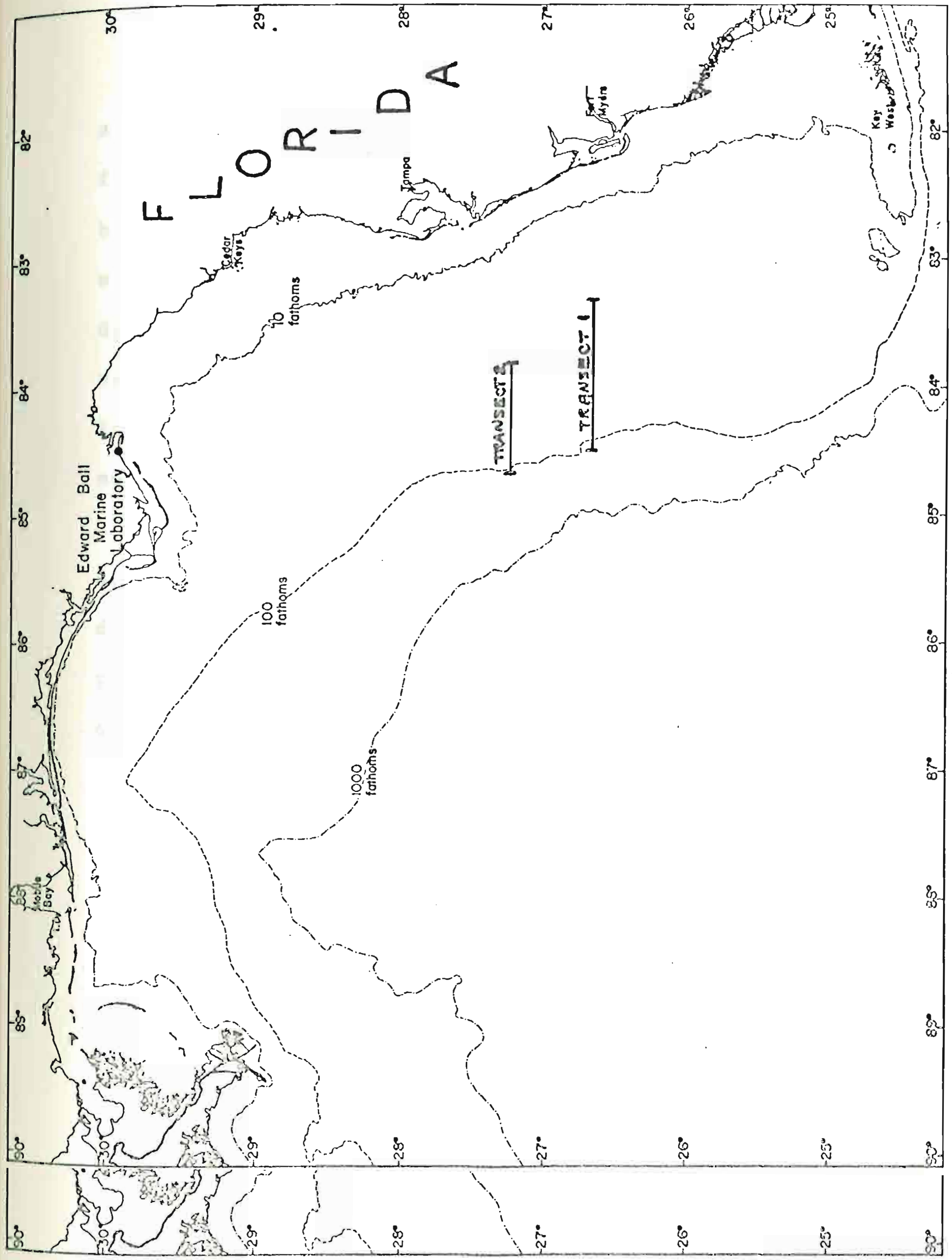
FLORIDA
Cedar Keys
Tampa
Fort Myers
Key West
Edward Ball Marine Laboratory
Mobile Bay
10 fathoms
100 fathoms
1000 fathoms
TRANSECT 1
TRANSECT 2

Fig. 2

The problem consists of integrating the physical and biological dynamics concurrently. The approach followed here is the construction of a composite of the biological, chemical, and physical interrelations into a single system. After formulation of the biological dynamics, physical flow patterns, environmental conditions, and necessary initial conditions, calculations of changes in time and space of the system components are made using numerical techniques.

The constructed model is used for investigation of the rates of the system. Experiments are performed to determine the response of the model to variations in parameters. A sensitivity analysis reveals the importance of individual mechanisms on biological components and on the system as a whole.

Simulation is only the first step in understanding the biological production of the area. This study is presently concerned with an attempt to understand the system dynamics. Fig. 6 (from Van Dyne, 1969) contrasts the classical scientific method applicable to biology with the model approach as adopted in the research. An intent of this study is to define the objectives of subsequent
the model approach as adopted in the research. An intent
of this study is to define the objectives of subsequent
field research programs. Insufficient knowledge of the

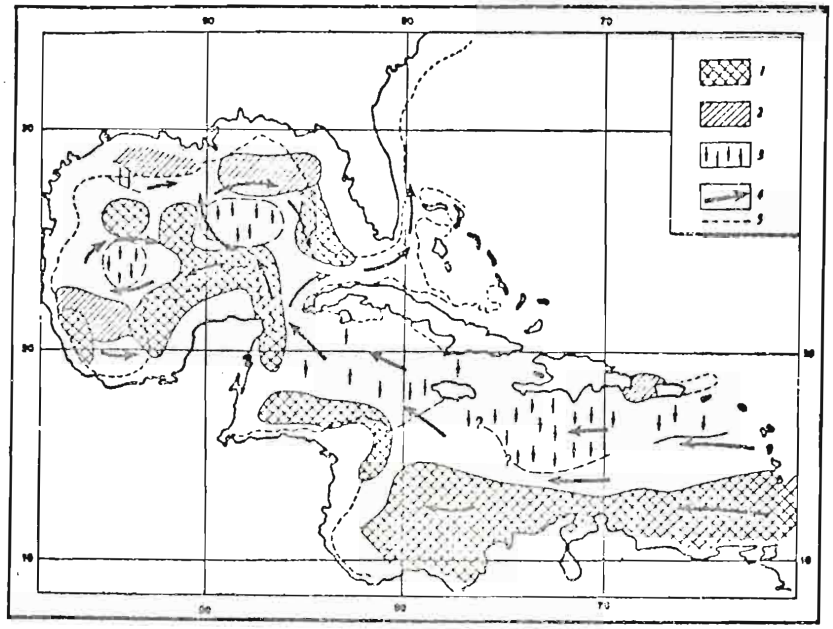

Fig. 3 Regions of upwelling and regions of descending waters in the Gulf of Mexico and Caribbean Sea. 1) upwelling through most of the year; 2) upwelling in summer; 3) predominance of descending waters; 4) main surface currents (summer); 5) edge of shelf. (from Bogdanov,1968).

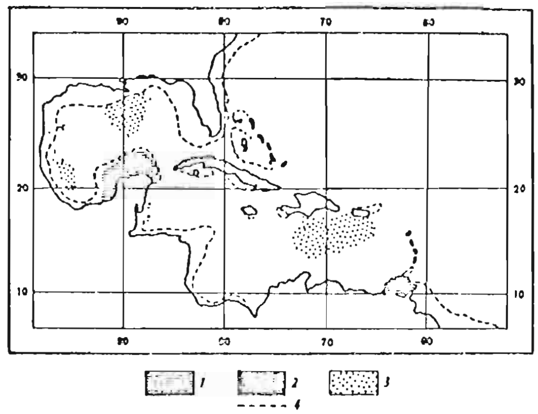

Fig. 4 Main concentrations of commercial species of fish in the Gulf of Mexico and Caribbean Sea in the warm part of the year. 1) concentrations of bottom fish; 2) regions of commercial bottom fishing; 3) regions of tuna concentration and commercial fishing; 4) edge of shelf. (from Bogdanov, 1968).

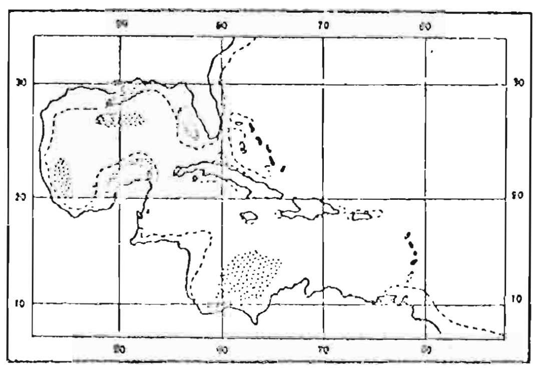

Fig. 5 Regions of concentration of the main commercial species of fishes in the Gulf and Caribbean Sea in the cold part of the year. Notation as in Fig.4

in the cold part of the year. Notation as in Fig.4

(from Bogdanov,1968).

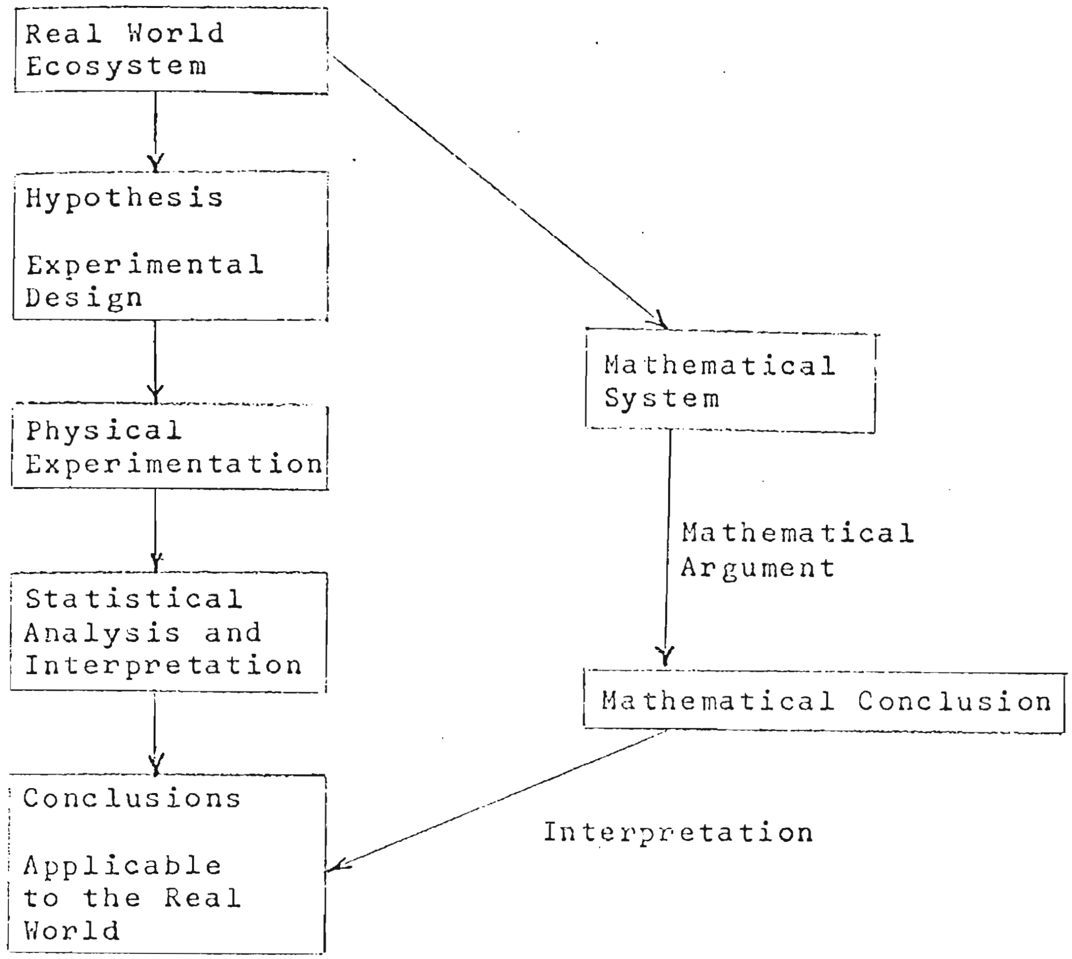

Fig. 6 The conventional approach in studying ecosystems or ecosystem components is shown on the left and includes processes of formulating hypothesis, designing and conducting experiments, and analyzing and interpreting results. A second and new approach to studying natural resource problems involves the abstraction of the system into a model. (from Van Dyne,1969).

Van Dyne,1969).

physiological processes and food chain dynamics limits our understanding of the marine ecosystem. It is hoped this research will identify the important biological processes which govern the continental shelf ecosystem. Future feedback between field observations and model development is intended.

2. SYSTEM REPRESENTATION AND FORMULATION

The idealized model area is shown in cross section in Fig. 7. The oceanic section is generalized as a two dimensional box with the top a free surface and the bottom bounded by a flat continental shelf. A straight vertical coast constitutes the right hand boundary and the seaward boundary of integration is at the continental shelf break. The x direction is taken as positive towards the coast and the depth z as positive upwards. An assumption necessary for computational economy is that there are no longshore variations; i.e., any variation in the north-south is small compared to those in the x-z plane (mathematically, $\partial/\partial y = 0$.)

The cross section is divided into a grid of 41 by 82 rectangles in the x and z directions respectively. The dimensions of each grid box are approximately 2.5 meters in depth by 5 kilometers in width. A theoretical flow field is specified at each grid point. The onshore water velocity u is taken as positive along x towards the coast, the vertical velocity w is positive upwards,

the coast, the vertical velocity w is positive upwards,

Fig. 7 The idealized oceanic area in cross section with the top a free surface, the bottom a flat continental shelf, the right hand boundary the vertical coast, and the seaward boundary at the continental shelf break. The water column is divided into a euphotic and an aphotic zone.

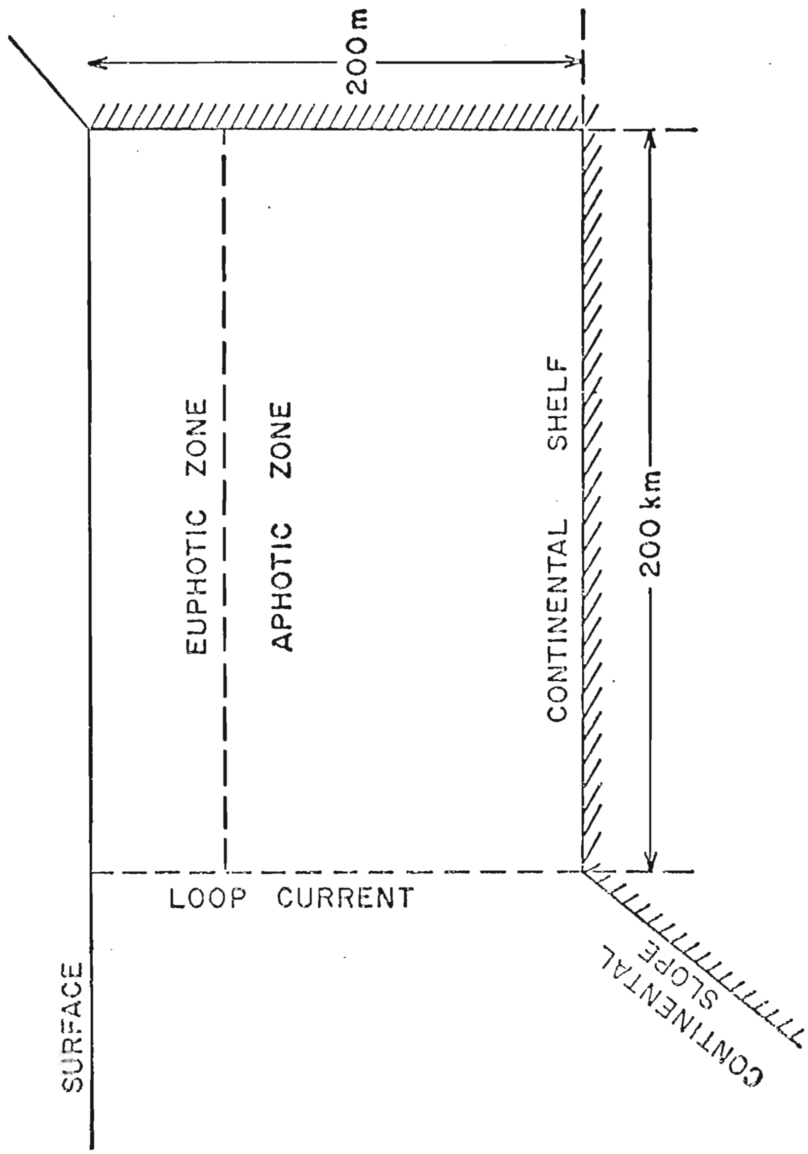
200 m
EUPHOTIC ZONE
APHOTIC ZONE
CONTINENTAL SHELF
200 km
LOOP CURRENT
SURFACE
CONTINENTAL SLOPE

Fig. 7

and the longshore horizontal velocity v is negative in a southerly direction along the coast.

2.1 System Processes

Let us consider the biomass concentration of the phytoplankton component P at an arbitrary point on the spatial grid. We will assume that the phytoplankton dynamics P(x, z, t) are governed by

$$\frac{DP}{Dt} \equiv \frac{\partial P}{\partial t} + u\frac{\partial P}{\partial x} + w\frac{\partial P}{\partial z} - \frac{\partial}{\partial x}\left[\nu_h \frac{\partial P}{\partial x}\right] - \frac{\partial}{\partial z}\left[\nu_v \frac{\partial P}{\partial z}\right] = \underset{\text{biological terms}}{\text{---}} \qquad (1)$$

The first three terms on the left hand side represent collectively the change of P following a water parcel moving within the ocean. The first term is the local change and the other terms are the advective changes. The last two terms on the left hand side are the turbulent diffusion terms where ν_h and ν_v are the horizontal and vertical eddy diffusivities, respectively. These diffusion terms represent collectively, the diffusion of P by chaotic motion and motion whose time and space scales are smaller than those which can be resolved by the grid size used in the model. These five terms define the operator on the extreme left.

These five terms define the operator on the extreme left.

The biological terms include any biotic processes which might be included in a marine food chain model. Formulations for phytoplankton growth, processes which diminish the phytoplankton stock (predation by higher trophic levels, excretion, mortality, etc.) and any losses or additions to the phytoplankton component which are biological in nature are included here. Equations similar to (1) can be written for zooplankton, detritus, and dissolved nutrients.

If advection and diffusion are neglected, then $\frac{DP}{Dt} = \frac{\partial P}{\partial t}$. The local derivative $\frac{\partial P}{\partial t}$ is the time dependent change in the component resulting from biological, chemical, and environmental considerations. In this case the local derivative is identical to the total derivative since only time is an independent variable. This is always the situation when spatial distributions of the biological components are omitted in models. The biological processes we are including are indicated in (2)-(6).

$$\frac{DP}{Dt} = \underset{\mathrm{I}}{\text{growth of P from N uptake}} - \underset{\mathrm{II}}{\text{extracellular release}}$$

$$- \underset{\mathrm{III}}{\text{grazing by Z}} - \underset{\mathrm{IV}}{\text{predation by F}} \qquad (2)$$

$$- \underset{\mathrm{III}}{\text{grazing by Z}} - \underset{\mathrm{IV}}{\text{predation by F}} \qquad (2)$$

$$\frac{DZ}{Dt} = \text{growth of Z by } \underbrace{\text{grazing on P}}_{\text{III}} \text{ and } \underbrace{\text{D}}_{\text{V}} - \underbrace{\text{excretion}}_{\text{VI}} - \underbrace{\text{natural death}}_{\text{VII}} - \underbrace{\text{predation by F}}_{\text{VIII}} \qquad (3)$$

$$\frac{DD}{Dt} = \text{input from Z } \underbrace{\text{natural death}}_{\text{VII}} - \underbrace{\text{grazing by Z}}_{\text{V}} - \underbrace{\text{bacterial regeneration}}_{\text{IX}} - \underbrace{\text{sinking}}_{\text{XI}} \qquad (4)$$

$$\frac{DF}{Dt} = \text{growth of F by } \underbrace{\text{predation on P}}_{\text{IV}} \text{ and } \underbrace{\text{Z}}_{\text{VIII}} - \underbrace{\text{excretion}}_{\text{X}} \qquad (5)$$

$$\frac{DN}{Dt} = \text{loss from } \underbrace{\text{uptake by P}}_{\text{I}} + \underbrace{\text{extracellular release by P}}_{\text{II}} + \text{excretion by } \underbrace{\text{Z}}_{\text{VI}} \text{ and } \underbrace{\text{F}}_{\text{X}} + \underbrace{\text{input of decomposed D}}_{\text{IX}} \qquad (6)$$

where P is phytoplankton, Z is zooplankton, D is zooplankton detritus, F is pelagic fish, and N is limiting nutrient dissolved in the water column. The specific formulation of Roman numeralled terms I-X will be discussed in the next section, while the sinking term XI is formulated in 5.3.

Fig. 8 summarizes the system dynamics allowed within any single spatial block. The biological processes are shown as transfers (arrows) between components. The advective and diffusive fluxes between spatial blocks are

advective and diffusive fluxes between spatial blocks are

Fig. 8 Biological processes within a spatial block. The model's biotic components include phytoplankton, zooplankton, pelagic fish, detritus, and the biologically limiting nutrient dissolved in the water column. Light arrows denote flow pathways of the limiting nutrient between trophic levels and the dissolved nutrient. Heavy arrows indicate fluxes between spatial blocks.

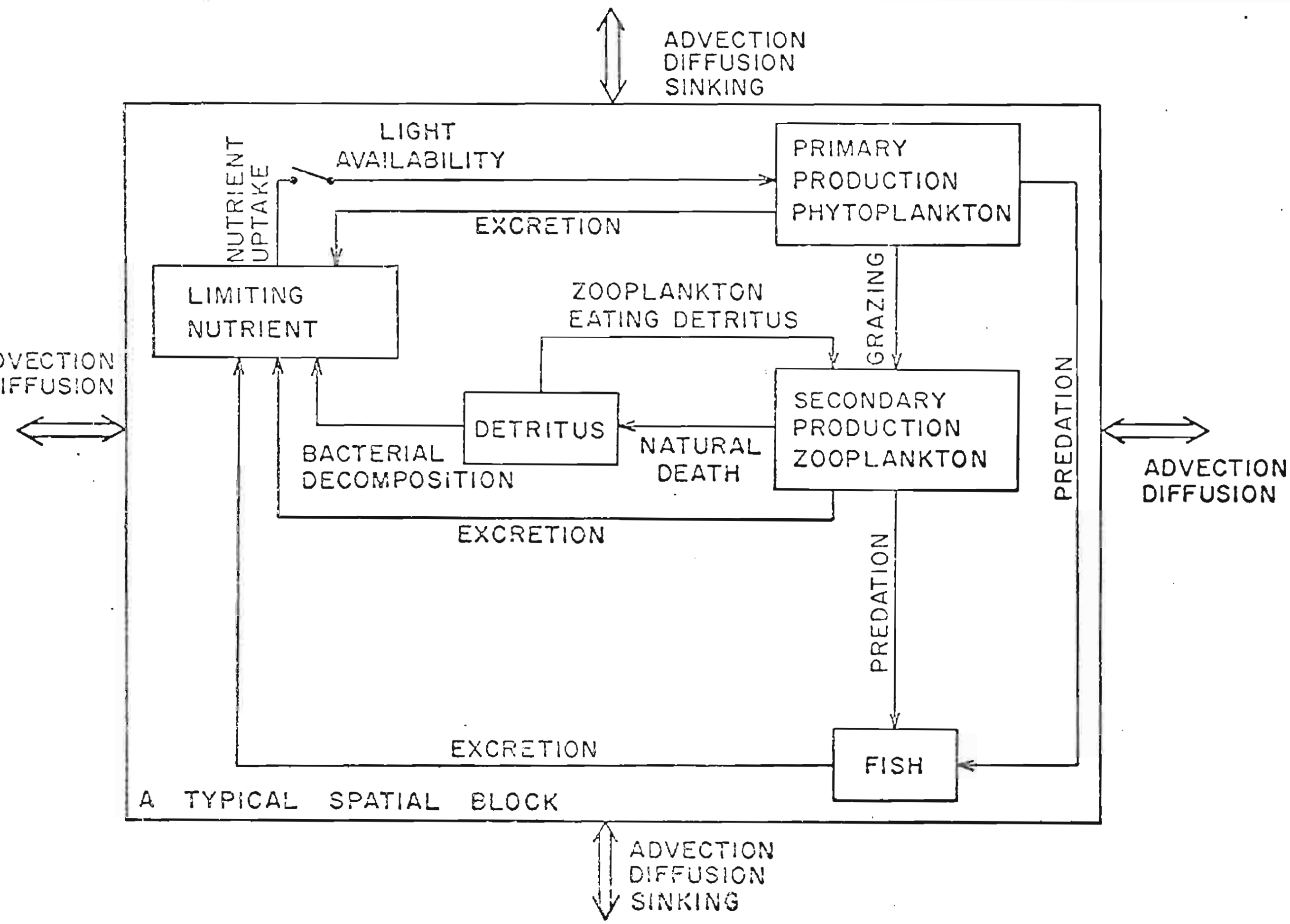
ADVECTION
DIFFUSION
SINKING
LIGHT
AVAILABILITY
NUTRIENT
UPTAKE
EXCRETION
PRIMARY
PRODUCTION
PHYTOPLANKTON
LIMITING
NUTRIENT
ZOOPLANKTON
EATING DETRITUS
GRAZING
ADVECTION
DIFFUSION
DETRITUS
NATURAL
DEATH
SECONDARY
PRODUCTION
ZOOPLANKTON
PREDATION
ADVECTION
DIFFUSION
BACTERIAL
DECOMPOSITION
EXCRETION
PREDATION
EXCRETION
FISH
A TYPICAL SPATIAL BLOCK
ADVECTION
DIFFUSION
SINKING

Fig. 8

Fig. 9 Relationships between three typical spatial blocks in the euphotic zone and three spatial blocks in the aphotic zone. The letters P,Z,N, and D represent the local concentration of phytoplankton, zooplankton, dissolved nutrient, and detritus within a single block. The arrows indicate flux processes between spatial blocks. Light availability defines the euphotic zone.

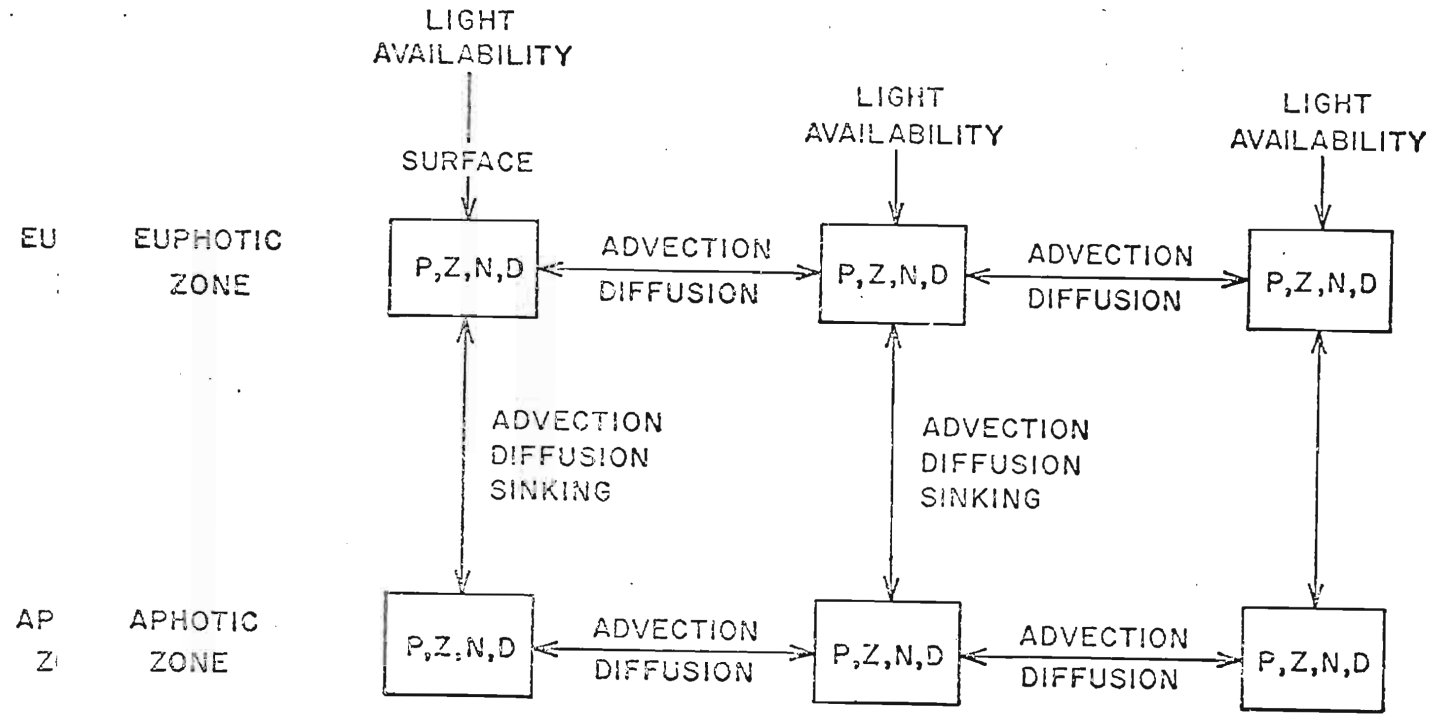
LIGHT AVAILABILITY
SURFACE
LIGHT AVAILABILITY
LIGHT AVAILABILITY
EUPHOTIC ZONE
APHOTIC ZONE
P,Z,N,D
P,Z,N,D
P,Z,N,D
P,Z,N,D
P,Z,N,D
P,Z,N,D
ADVECTION DIFFUSION
ADVECTION DIFFUSION
ADVECTION DIFFUSION SINKING
ADVECTION DIFFUSION SINKING
ADVECTION DIFFUSION
ADVECTION DIFFUSION

Fig. 9

represented by heavy arrows. Fig. 9 shows the flux processes occurring between three spatial blocks in the euphotic zone and their relationships with three blocks in the aphotic region.

2.2 The Mathematical Simulation of Biological Dynamics

Simulations are limited by the ability to represent accurately the biological processes as they occur in nature. However, mathematical representation of the biological functions enable us to understand the system more quantitatively than a purely descriptive approach.

We treat collectively the marine species which have feeding habits in common and can be assigned to one trophic level; therefore, species composition is not considered. We deal here with a simple food chain of three trophic levels. In addition, the amount of detritus and the concentration of limiting nutrient in the water column are considered. We investigate the dynamics of each biotic component, namely the nutrient uptake and turnover rates, the feeding dynamics, the nutrient exchanges between trophic levels, and the effect of changes in food supply.

The simulation quantitatively traces the biologically

in food supply.

The simulation quantitatively traces the biologically

limiting nutrient's flow within and between the phytoplankton, zooplankton, detritus, fish, and the nutrient dissolved in the water column. In addition, the time dependent, spatial distributions of the standing stock of phytoplankton, zooplankton, dissolved nutrient, and detritus within the regions of the water column are determined.

The five biotic components are expressed in concentration of the biologically limiting nutrient. The combined amount in the phytoplankton, zooplankton, detritus, fish, and the nutrient dissolved in the water column is defined as N_t, the average amount of limiting nutrient on the continental shelf area amongst all components. Since N_t is assumed constant,

$$N_t = N' + P' + Z' + D' + F'$$

where primes denote dimensional quantities. In this case, the units are concentration, e.g. μ gm atom NO3-N/liter. We will subsequently elect to non-dimensionalize all quantities. These will be denoted by the absence of primes.

The amount of the limiting nutrient in P,Z,D, and F is often expressed as μ gm atom nutrient/gm biomass. One

The amount of the limiting nutrient in P,Z,D, and
F is often expressed as μ gm atom nutrient/gm biomass. One

can obtain the units used in this study upon multiplying by gm biomass/liter to give μgm atom nutrient/liter.

The Phytoplankton Equation

As this is a material flow study, we consider the biological processes which deal with uptake, release, and transfer of the limiting nutrient. Dugdale (1967) has demonstrated the applicability of Monod enzyme kinetics to the uptake of limiting nutrients by marine phyto-plankton. Subsequent laboratory and field work (Eppley and Coatsworth, 1968; Thomas and Dodson, 1968; MacIssac and Dugdale, 1969; Eppley *et al.*, 1969; Dugdale and MacIssac, 1971) support the hypothesis that uptake rates of nitrate, ammonia, and phosphate by phytoplankton are hyperbolic functions of nutrient concentration.

The Michaelis-Menton formulation of Monod (1942) kinetics is

$$V = \frac{V_m N'}{K + N'}$$

where V is the specific uptake rate (hr^{-1}) of nutrient N' (concentration), V is the maximum uptake rate, and K is the Michaelis constant or half-saturation constant. K is

the Michaelis constant or half-saturation constant. K is

the concentration supporting half the maximum uptake rate (Fig. 10).

The dynamic equation for phytoplankton growth is

$$\frac{DP'}{Dt'} = \underset{\text{I}}{\frac{V_m N'P'}{K+N'}} \; \underset{\text{II}}{- BP'} \; \underset{\text{III}}{- E_z(1 - e^{-d_p P'})Z'} \; \underset{\text{IV}}{- \Phi F' \frac{\sigma P'}{(\sigma P' + Z')}} \qquad (8)$$

where the numbered terms correspond to those of the descriptive equations (2) - (6). The first term on the right represents the uptake of the limiting nutrient N' by phytoplankton P' according to Michaelis-Menton kinetics. A fundamental assumption in this research is that growth of phytoplankton by nutrient uptake is governed by Michaelis-Menton kinetics.

Term II represents the collective losses of limiting nutrient from the phytoplankton component. It encompasses the processes of extracellular release by phytoplankton, cell breakage and release of cytoplasm by mechanical disruption, the death and autolysis of senescent cells, etc. Phytoplankton excretion is usually expressed as a percentage of the carbon fixed by photosynthesis (Watt, 1966). We consider phytoplankton excretion as the extracellular release of amino acids

photosynthesis (Watt, 1966). We consider phytoplankton excretion as the extracellular release of amino acids

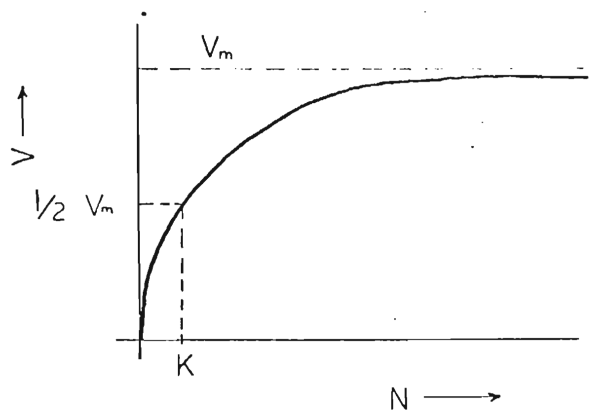

$$V = \frac{V_m \, N}{K + N}$$

Fig. 10 Rate of nutrient uptake V as a function of limiting nutrient concentration N according to the Michaelis-Menton expression. V_m is the maximum rate of uptake. K is the nutrient concentration at which V is 1/2 V_m.

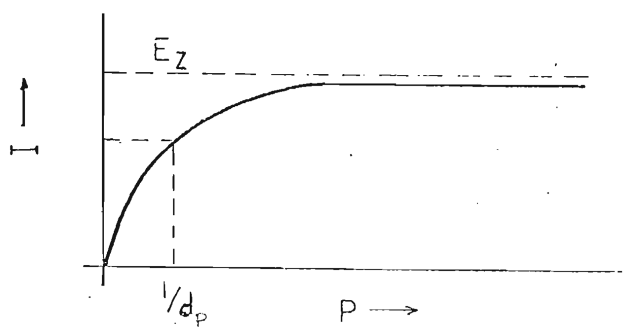

$$I = E_Z(1 - e^{-d_p P})$$

Fig. 11 Zooplankton grazing rate I as a function of phytoplankton concentration P. E_z is the maximum ingestion rate.(after McAllister,1970).

phytoplankton concentration P. E_z is the maximum ingestion rate.(after McAllister,1970).

containing the limiting nutrients considered in this model, namely phosphate and nitrate.

The third term represents zooplankton predation; E is a grazing coefficient with units of hr^{-1} Ez McAllister (1970) documents the utility of this nonlinear phytoplankton dependent formulation (term III) of herbivorous grazing, this is discussed further below. The fourth term of equation (7) describes fish predation upon phytoplankton. This formulation will be discussed in context with the fish dynamics.

The Zooplankton Equation

Cushing (1963) expressed the need for a model giving an estimate of zooplankton grazing capacity as a function of algal density over the range of the productive cycle. It should account for superfluous feeding, and describe the behavior of the herbivores. Laboratory studies have indicated zooplankton grazing rates to be a linear function of phytoplankton density for low concentrations of phytoplankton. When phytoplankton are abundant there exists a maximum rate of grazing attainable by the zooplankton (McAllister, 1970).

Parsons, *et al*. (1967) have modified the expression of Ivlev (1945),

Parsons, *et al*. (1967) have modified the expression of Ivlev (1945),

$$I = E_Z(1 - e^{-d_p(P' - P^*)})$$

where I is the rate of ingestion per unit concentration of grazer at phytoplankton concentration P' (the mean concentration during periods of grazing); E_Z is the maximum rate of ingestation attainable by the zooplankton; d_p is a constant which modifies the rate of change of ingestion with food concentration; and P^* is the small concentration of phytoplankton at which feeding begins. At concentrations below P^*, the zooplankton starve.

For very small P^*, grazing is approximately (Fig. 11),

$$I = E_Z(1 - e^{-d_p P'}).$$

In the euphotic zone of our model, P' never approaches concentration values which would dictate the inclusion of P^*. The constant $1/d_p$ is the concentration of P' at which the specific ingestion rate, I, is approximately two thirds of the maximum rate, E_Z.

The zooplankton dynamics in the model is governed by

governed by

$$\frac{DZ'}{Dt'} = \underbrace{E_Z(1 - e^{-d_P P'})Z'}_{\text{III}} + \underbrace{E_D D'Z'}_{\text{V}} - \underbrace{\Gamma\left[E_Z(1 - e^{-d_P P'})Z'\right]Z'}_{\text{VI}}$$

$$- \underbrace{d_D Z'}_{\text{VII}} - \underbrace{\Phi F'\left(\frac{Z'}{gP' + Z'}\right)}_{\text{VIII}} \qquad (9)$$

where D' (term V) is the detritus component which serves as a partial food source for zooplankton. The parameter d_D (term VII) is the natural death rate for zooplankton. The term VII is the flux of the zooplankton biomass being transferred to the detritus component. Coefficient E_D (term V) is the grazing coefficient (conc.$^{-1}$ hr.$^{-1}$) for zooplankton on detritus. This grazing rate is $E_D D$.

Field and laboratory studies (Cushing, 1969; Parsons et al., 1967) have indicated that zooplankton excrete more of the material ingested when phytoplankton are abundant. We therefore assume a direct relationship between zooplankton grazing on phytoplankton and excretion. Term VI is linearly related to term V by the excretion coefficient Γ. Thus the zooplankton excretion varies with the rate of zooplankton predation on phytoplankton.

with the rate of zooplankton predation on phytoplankton.

When ingestion of phytoplankton is small, zooplankton excretion is small.

The Detritus Equation

Detritus consists of dead zooplankton biomass and is grazed upon by living zooplankton.

$$\frac{DD'}{Dt'} = \underset{\text{VII}}{d_D Z'} - \underset{\text{V}}{E_D Z' D'} - \underset{\text{IX}}{\ell D'} - \underset{\text{XI}}{w_s \frac{\partial D'}{\partial z}} \qquad (10)$$

Term VII is the source of detritus; term V is the loss due to zooplankton grazing. The term (IX) is a simple linear parameterization of the regeneration of detritus by bacteria into dissolved limiting nutrient. The sensitivity analysis will demonstrate that the model dynamics are not crucial to the value of ℓ, therefore a more sophisticated formulation does not seem to be appropriate. The time $1/\ell$ may be interpreted as the time for 2/3 of the detritus to be regenerated in the absence of all other loss mechanisms.

Term XI parameterizes sinking of detritus due to gravitational effects. It is discussed in detail in 5.3.

The Fish Equation

In the particular model runs integrated for this

In the particular model runs integrated for this
study, we consider only periods of several days to a few

weeks. Therefore we assume that, although there are omnivorous fish, F, there will be no net increase in F over this short time period. Hence, nekton grazing on P and Z must balance nekton excretion. Fish mortality also occurs on a much longer time than considered. This is expressed as

$$\frac{DF'}{Dt'} = \Phi F' - HF' = 0$$

where Φ is the nekton grazing rate and H is the nekton excretion rate (hr.$^{-1}$). The fish are not affected by the water movement or turbulent diffusion as are the other biotic components. We also ignore fish mobility in this preliminary ecosystem model. The fish in the model always exist where there are available food sources.

The species composition of the nekton trophic level is not considered, but the pelagic fish are regarded as planktivores, i.e. omnivorous filter feeders. Fish grazing is a function of gill raker efficiency. We assume that θ' percent of the phytoplankton and all the zooplankton are within sizes retainable by the filtering mechanism. The grazing rate on zooplankton is

The grazing rate on zooplankton is

$$\Phi \frac{Z'}{\theta P' + Z'}$$

and the grazing rate on phytoplankton is

$$\Phi \frac{\theta P'}{\theta P' + Z'}$$

The sum of these is Φ . The fish dynamics equation is

$$\frac{DF'}{Dt'} = \Phi F' \frac{\theta P'}{\theta P' + Z'} + \Phi F' \frac{Z'}{\theta P' + Z'} - H F'$$

IV VII X

or

$$\frac{DF'}{Dt'} = \Phi F' - H F'$$

and, as indicated above $\Phi = H$ in the model. Term IV is the rate of ingestion of P by F. Term VIII is the rate of ingestion of Z by F and term X is the subsequent (and instantaneous) excretion by F to dissolved nutrients.

<u>The Nutrient Equation</u>

The local change in the dissolved limiting nutrient N' is the sum of all nutrient excretion processes (terms II, VI, and X), plus nutrient regenerated from

(terms II, VI, and X), plus nutrient regenerated from

detritus (term IX), minus that taken up by the phytoplankton (term I):

$$\frac{DN'}{Dt'} = -\underbrace{\frac{V_m N' P'}{K + N'}}_{\mathrm{I}} + \underbrace{BP'}_{\mathrm{II}} + \underbrace{\Gamma E_z(1 - e^{-d_p P'}) Z'^2}_{\mathrm{VI}} + \underbrace{HF'}_{\mathrm{X}} + \underbrace{\ell D'}_{\mathrm{IX}} \qquad (12)$$

2.3 Nondimensionalization of Biological Dynamics

In the physical sciences, researchers find it rewarding to nondimensionalize their equations. This approach is sometimes an enigma to those unfamiliar with the procedure. We have chosen to solve equations (8) - (12) after scaling by the Michaelis-Menton parameter V_m and the total amount of limiting nutrient N_t. In this section we nondimensionalize equations (8) - (12) and explain the utility and benefits of this approach.

The biological formulation contains explicitly the parameters V, K, B, d, Γ, ℓ, E, E, d, Φ, H, and θ, and implicitly the initial concentrations of N', P', Z', D', and F'. We anticipate that by nondimensionalizing the equations the number of parameters will be reduced. Solving one nondimensional case is then equivalent to solving many dimensional cases. To transform

will be reduced. Solving one nondimensional case is then
equivalent to solving many dimensional cases. To transform

back to dimensional units one multiplies the nondimensional solutions by the scaling parameters.

We are fundamentally interested in the role of the Michaelis-Menton kinetics within the phytoplankton trophic level. The flow of nutrient material through the primary producers is a function of the initial uptake of nutrient by phytoplankton from the water column. The maximum rate of nutrient uptake by phytoplankton, V_m, may be measured in concentrations of the limiting nutrient or as the doubling rate of phytoplankton per 24 hours. It is a fundamental rate to which all other biological rates may be related. Thus we let time be scaled by V_m, $t' = t/V_m$, where t' has units of hours, t is nondimensional, and V_m has units of $hr.^{-1}$. Let P', N', D', F', and Z' be scaled by N_t, the amount of limiting nutrient in all biological components averaged over the entire continental shelf region.

Using these scaling relationships, (8) - (12) become,

$$\frac{DP}{Dt} = \frac{NP}{\alpha \cdot N} - \beta P - \epsilon_Z(1-e^{-\delta_P P})Z - \phi F\left(\frac{\theta P}{\theta P+Z}\right) \qquad (13)$$

$$\frac{DZ}{Dt} = \epsilon_Z(1-e^{-\delta_P P})Z + \epsilon_D ZD - \gamma\epsilon_Z(1-e^{-\delta_P P})Z^2 - \delta_D Z - \phi F\left(\frac{Z}{\theta P+Z}\right) \qquad (14)$$

$$\frac{DD}{Dt} = \delta_D Z - \lambda D - \epsilon_D Z D \qquad (15)$$

$$\frac{DF}{Dt} = \phi F\left(\frac{\theta P}{\theta P+Z}\right) + \phi F\left(\frac{Z}{\theta P+Z}\right) - \eta F \qquad (16)$$

$$\frac{DN}{Dt} = -\frac{NP}{\alpha+N} + \beta P + \gamma\epsilon_Z(1-e^{-\delta_P P})Z^2 + \eta F + \lambda D \qquad (17)$$

where

$$N = \frac{N'}{N_t}; \quad P = \frac{P'}{N_t}; \quad Z = \frac{Z'}{N_t}; \quad D = \frac{D'}{N_t}; \quad F = \frac{F'}{N_t}$$

$$\alpha = \frac{K}{N_t}; \quad \beta = \frac{B}{V_m} \quad \epsilon_Z = \frac{E_Z}{V_m} \quad \delta_P = d_P N_t$$

$$\phi = \frac{\Phi}{V_m}; \quad \delta_D = \frac{d_D}{V_m} \quad \lambda = \frac{\ell}{V_m} \quad \epsilon_D = \frac{E_D N_t}{V_m}$$

$$\phi = \frac{\Phi}{V_m}; \quad \delta_D = \frac{d_D}{V_m} \quad \lambda = \frac{x}{V_m} \quad \epsilon_D = \frac{E_D N_t}{V_m}$$

$$\gamma = \Gamma N_t; \quad \eta = \frac{H}{V_m} \quad t = t' V_m; \quad \theta = \theta$$

As an illustrative example, consider the simplified equation $\frac{DP'}{Dt'} = -B P'$ where primes denote dimensional quantities. Scaling P' and time t' by N_t and V_m respectively and dividing by $N_t V_m$,

$$\frac{DP}{Dt} = -\frac{B}{V_m} P$$

which says $\beta = \frac{B}{V_m}$.

All quantities in (13) - (17) are nondimensional. P, Z, N, F, and D are all fractions; if multiplied by 100 they are percent of N_t in the system at any time, i.e. a standing stock. One time unit equals V_m in hours. The reader must bear in mind these scaling relationships when comparing our results with real oceanographic process rates. The scaling relationships are summarized for the reader's convenience in Table 1.

If we were not concerned with spatial effects, this would be the complete formulation of a one box model, as discussed by Verhoff (1971). The formulation and subsequent nondimentionalization of the physical processes will be discussed in 5.

2.4 Environmental Considerations

The model is designed to apply to the shelf

2.4 Environmental Considerations

The model is designed to apply to the shelf

Table 1. Dimensional and Non-Dimensional Quantities

Dimensional	Scaling Factor	Non-Dimensional
Dependent Variables		
P'	N_t^{-1}	P
Z'	N_t^{-1}	Z
F'	N_t^{-1}	F
D'	N_t^{-1}	D
N'	N_t^{-1}	N
u'	C^{-1}	u
v'	C^{-1}	v
w'	$C^{-1}(A_v/A_h)^{-\frac{1}{2}}$	w
Independent Variables		
t'	V_m	t
x'	$(A_h/f)^{-\frac{1}{2}}$	x
z'	$(A_v/f)^{-\frac{1}{2}}$	z
Biological Parameters		
B	V_m^{-1}	β
d_D	V_m^{-1}	δ_D
d_P	N_t	δ_P
E_D	$N_t\ V_m^{-1}$	ϵ_D
E_Z	V_m^{-1}	ϵ_Z
H	V_m^{-1}	η
E_Z	V_m^{-1}	ϵ_Z
H	V_m^{-1}	η
k	N_t^{-1}	α
ℓ	V_m^{-1}	λ

Table 1 (cont.)

Dimensional	Scaling Factor	Non Dimensional
Biological Parameters (cont.)		
Γ	N_t	γ
τ'	$V_m/24$	τ
Φ	V_m^{-1}	ϕ
Physical Parameters		
b'	$(A_h/f)^{-\frac{1}{2}}$	b
d'	$(A_v/f)^{-\frac{1}{2}}$	d
w_s'	$C^{-1}\ S^{-1}(A_v/A_h)^{-\frac{1}{2}}$	w_s
ς'	$-g\ C^{-1}(f\ A_h)^{-\frac{1}{2}}$	ς
ν_h'	$(V_m\ A_h/f)^{-1}$	ν_h
ν_v'	$(V_m\ A_v/f)^{-1}$	ν_v

waters during late fall to early spring, when the winds due to northers and cool atmospheric temperatures have created a homogeneous well-mixed water column.

The attenuation of light in the water column must be considered. A euphotic zone, defined as the part of the water column within which any photosynthesis can take place, is assumed to extend to a maximum depth of 40 meters (Yentsch, 1963).

As photosynthesis is a function of light intensity and light attenuates with depth, the rate of photosynthesis with depth in the euphotic zone is not constant. In the spatial model the growth rate of phytoplankton is subjected to a photosynthesis-depth curve (Fig. 12).

We define a photosynthesis-depth function, E(z) which approximates Curve II (Yentsch, 1963) of Fig. 12,

$$E(z) = 0.5\ [1 + \tanh\ (10[z-z\ ])]$$

where z is approximately 30 m. To account for light inhibition of photosynthesis in the upper five meters of the water column, we redefine

$$E\ (0 - 2.5\ m) = 0$$

$$E\ (0 - 2.5\ m) = 0$$

$$E\ (2.5 - 5\ m) = 0.5$$

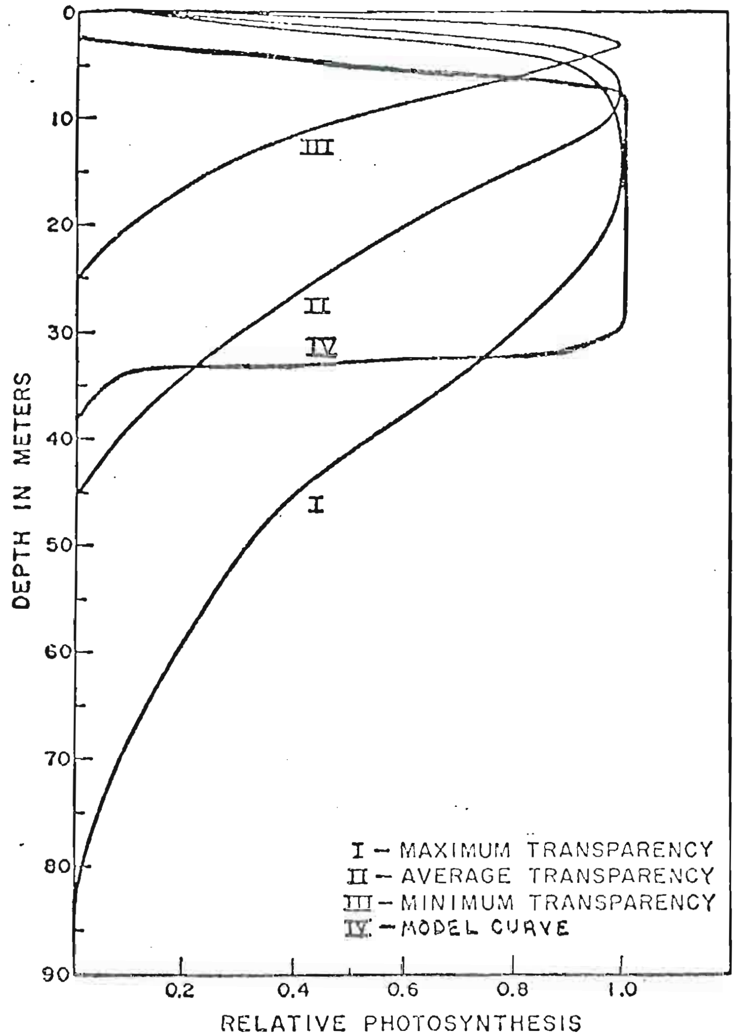

Fig. 12 Relative photosynthesis as a function of depth for a homogeneously distributed phyto-plankton population under bright sunlight in the open ocean (after Yentsch,1963). Curve IV defines the euphotic zone and the relative the open ocean (after Yentsch,1963). Curve IV defines the euphotic zone and the relative rate of photosynthesis in the spatial model.

$E(Z) < 0.01$ below 35 m. There is considerable room for improvement in the specification of this important environmental parameter.

The Michaelis-Menton uptake term in (13) and (17) is multiplied by this dimensionless function thereby restricting increases in phytoplankton to the defined euphotic zone. The phytoplankton equation in the euphotic zone becomes

$$\frac{DP}{Dt} = E(z)\,\frac{NP}{\alpha + N} - \beta P - \epsilon_z (1 - e^{-\delta_p P}) Z - \phi F\left(\frac{\theta P}{\theta P + Z}\right) \quad (18)$$

Phytoplankton advected or diffused below 40 meters experience only losses due to excretion and predation, since $E(z) = 0$. Zooplankton grazing is allowed to take place wherever phytoplankton occur.

Another form of light limitation of phytosynthesis is the diurnal variation of sunlight. Phytoplankton existing in the portion of the water column where light attenuation or inhibition is not a factor are affected by this diurnal variation. This effect upon the phytoplankton dynamics is discussed in 3.

3. NON-SPATIAL BIOLOGICAL DYNAMICS

3.1 Values for the Variable Biological Parameters

We integrate the model using specific values of the parameters α, β, ϵ_Z, ϵ_D, λ, δ_D, γ, ϕ, η, δ_P, and σ which are based on oceanographic measurements. In some cases we must resort to food chain theory as a guide to the appropriate parameter value. This section outlines the rational for selecting the specific values of the parameters used in this study.

ALPHA

Dugdale (1967) and Eppley, et al. (1969) document the Michaelis constant, K, as a small concentration of the limiting nutrient for which the specific uptake rate is one-half the maximum uptake rate. MacIsaac and Dugdale (1969) present euphotic zone values of the order of 10 μ moles/liter in nitrogen poor regions which experience seasonal upwelling of water with concentrations of 10-20 μ moles/liter of nitrate. Thomas (1970) has found a Michaelis constant of 0.75 μgm atom NO3-N/liter for natural tropical Pacific phytoplankton populations
found a Michaelis constant of 0.75 μgm atom NO3-N/liter for natural tropical Pacific phytoplankton populations
limited by nitrogen.

If we assume an N_t of 30 μgm atom NO_3-N/liter for a nitrate limited system (see Appendix I) then in our model,

$$\alpha = \frac{K}{N_t} = \frac{0.75 \text{ gm atom } NO_3\text{-N/liter}}{30 \text{ gm atom } NO_3\text{-N/liter}} = 0.025$$

Thomas and Dodson (1968) have reported a K value of 0.12 μgm atom PO_4-P/liter for tropical waters where phosphate is limiting. Assuming the total amount of biologically available phosphate to be 4.0 μgm atom PO_4-P/ liter (see Appendix I) then

$$\alpha = \frac{K}{N_t} = \frac{0.12 \text{ gm atom PO -P liter}}{4 \text{ gm atom PO -P liter}} = 0.030$$

A range of α values (10^{-1} to 10^{-2}) has been investigated. Lower values of α correspond to phyto-plankton utilizing extremely low concentrations of the limiting nutrient, permitting a higher percent of limiting nutrient in the phytoplankton component. A larger value of α results in less efficient uptake.

BETA

The coefficient β parameterizes the combined

BETA

The coefficient β parameterizes the combined losses of the limiting nutrient by P not accounted for by zooplankton grazing and fish predation. A major loss process is extracellular release. The magnitudes published for excretion are controversial due to experimental difficulties, but a significant portion of the compounds excreted may be amino acids. Fogg (1966) has found the proportion of photosynthesis production lost through extracellular release to range from 5 to 34 percent in natural phytoplankton populations. Watt (1966), Fogg (1966), and Thomas (1970) found that nutrient deficiencies, as nitrogen starvation, cause an increase in the release of dissolved organic matter from algae.

Consider the loss of phytoplankton biomass due to the excretion process alone, $\frac{DP}{Dt} = -\beta P$. The solution is $P = P_o e^{-\beta t}$. At $t = 1/\beta$, $P \approx P_o/3$. Thus $t = 1/\beta$ is the e-folding time taken for the process $-\beta$ P to reduce P to 1/3 P_o . A typical model value for β is 0.25. If V_m is of the order 10^{-1} hr^{-1} for nutrient limited systems (Eppley, <u>et al</u>., 1969) then the real time scale for loss of absorbed nutrient is

$$t' = t/V_m = 1/\beta\ /V_m \approx 40 \text{ hours} \approx 2 \text{ days.}$$

$$t/V_m = 1/\beta\ /V_m \approx 40 \text{ hours} \approx 2 \text{ days.}$$

We know that the excretion time scale β^{-1} must be longer than the growth time scale or else the phytoplankton population will collapse. The time scale for biological turnover of the phytoplankton population by nutrient excretion is indeed longer than the growth time scale, V_m^{-1} , in the ocean.

<u>The Zooplankton Parameters EPSILON-Z, EPSILON-D, and DELTA-P</u>

The determination of grazing rates of zooplankton in the sea is very difficult. Laboratory measurements by Parsons, *et al*. (1969) of the grazing ration expressed as a ratio of the weight of phytoplankton carbon ingested to the weight of the animals varied from 10 to 60 percent for varying concentrations of phytoplankton. It is not obvious what value the nondimensional grazing coeffient, E_z, should attain. We choose the value of parameters E_z and E_z to give us a reasonable ecological efficiency by zooplankton at equilibrium (see 3.4).

The expression for phytoplankton-dependent zooplankton grazing in the model $E_z[1- \exp(-\delta pP)]Z$ yields a curve whose slope initially depends on δp and asymptotically reaches the maximum E_z(Fig. 11). The quantity δp is the concentration at which the zooplankton grazing rate is approximately 2/3 of the
quantity δp is the concentration at which the
zooplankton grazing rate is approximately 2/3 of the
maximum allowable rate E_z. In the model δp is taken

to be 1.2, giving a grazing rate of 2/3 E_z at a non-dimensional phytoplankton concentration of 0.83. Since the model solutions almost always yield $P < 0.8$, the model utilizes the nonlinear part of the curve (Fig. 11).

<u>Zooplankton Excretion and Death Coefficients GAMMA and DELTA-D</u>

A correct formulation of zooplankton excretion processes is essential for marine ecosystem models, because this is an important mechanism by which nutrients are recycled back into the water column (Cushing, 1969). Much of the phytoplankton grazed passes through the zooplankton gut undigested, especially in regions of high phytoplankton concentration.

Parameter γ of the term $\gamma \epsilon_Z [1 - \exp(-\delta_P P) Z] Z$ linearly relates zooplankton excretion to zooplankton grazing. In the model, the amount grazed minus the amount excreted equals the nutrient assimilated by the zooplankton. Neglecting the relatively small detritus food source for illustrative purposes, the limiting nutrient assimilated by the zooplankton is

$$\frac{DZ}{Dt} = \epsilon_Z (1 - e^{-\delta_P P}) Z - \gamma \epsilon_Z (1 - e^{-\delta_P P}) Z^2$$

$$\frac{DZ}{Dt} = \epsilon_Z (1 - e^{-\delta_P P}) Z - \gamma \epsilon_Z (1 - e^{-\delta_P P}) Z^2$$

If we divide both sides of the equation by the quantity grazed, we have

$$\frac{1}{\epsilon_Z(1 - e^{-\delta_P P})Z} \frac{DZ}{Dt} = 1 - \gamma Z .$$

For growth of zooplankton, γZ must be less than 1. As zooplankton concentrations are typically less than 0.25 N_t, γ may be estimated to be approximately 4.0.

Upon death the zooplankton becomes part of the detritus component. The limiting nutrient within the detritus component may be directly utilized by zooplankton, or regenerated to dissolved nutrient by bacterial decomposition. The value of δ_D is taken as 0.10. Thus 2/3 of the Z population dies in time $t = 1/\delta_D$ or 10/Vm hours. If Vm is of the order 10^{-1} to 10^{-2} hour (Eppley, et al., 1969), then the e-folding time is on the order of $\approx$ 4 to 40 days, i.e., the Z population will collapse in 4-40 days if its food source is absent.

LAMBDA

The coefficient of bacterial decomposition of detritus into limiting nutrient is λ . In (15) λ is nondimensionalized by V_m . The loss of detritus due to decomposition is

nondimensionalized by V_m . The loss of detritus due to decomposition is

$$\frac{DD}{Dt} = -\lambda D$$

which has the solution $D = D_o e^{-\lambda t}$. At $t = 1/\lambda$, $D \approx D_o/3$. The biological system's response was investigated for this e- folding time lag of $t = 1/\lambda$. A $\lambda = 0.5$ would be equivalent to a regeneration time lag of the order of one or two days. This seemed appropriate regeneration times for the limiting nutrients (phosphate and nitrate) considered in the model (Steele, 1959).

Fish Grazing, Excretion, and Gill Raker Efficiency Coefficiencts PHI, ETA, and THETA

Omnivorus fish grazing is formulated as $\phi F \left(\frac{\theta P}{\theta P + Z}\right)$ and grazing on zooplankton as $\phi F \left(\frac{Z}{\theta P + Z}\right)$. Coefficient ϕ is taken to be 0.25 based on ecological efficiency considerations (see 3.4). As fish biomass is constant in this model, the excretion coefficient is identical to the grazing rate, ϕ.

Gill raker efficiency coefficient θ is arbitrarily set at 0.10. This value means that 90 percent of the phytoplankton is passed by the gill rakers.

3.2 Steady State Values of the Biological Components

We have formulated in 2. a complex system

3.2 Steady State Values of the Biological Components

We have formulated in 2. a complex system
describing the spatial distributions and dynamics of the

biological components. In order to interpret the spatial effects, it is desirable to first understand the system within the classical one box framework, where most physical processes can be ignored. In this respect, equations (13) - (17) describe the dynamics of a nutrient limited biological system. The properties of the system are determined by investigating the time dependent solutions of the biotic components as governed by these equations. An analytical solution is not possible due to the nonlinearity of the relationships. Equations (13) - (17) are consequently integrated numerically using an Euler finite difference scheme on a high speed digital computer for the range of parameter values discussed in 3.1.

Fig. 13 is one time dependent solution of these equations. The abscissa is nondimensional time. One time unit is V_m hrs. and is of the order of one day (25 hrs. for $V_m = 0.04$ hr^{-1}). The curves express the standing stock of each biotic component as a percent of N_t . We assume at t = 0, the onset of intense upwelling or deep mixing by a storm injects an excess amount of the limiting nutrient, N = 0.25, into the closed system. We arbitrarily choose P = 0.33, Z = 0.33, F = 0.09, and

the limiting nutrient, N = 0.25, into the closed system. We arbitrarily choose P = 0.33, Z = 0.33, F = 0.09, and

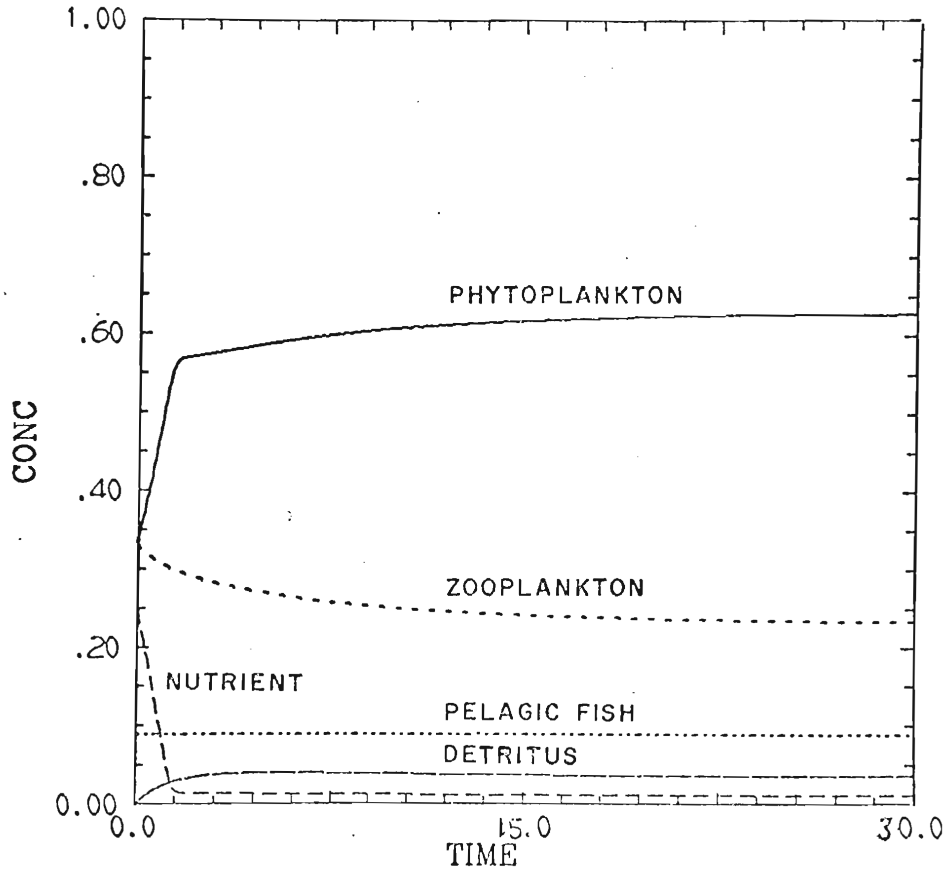

Fig. 13 Time dependent standing stock concentrations of the biotic components P, Z, N, D, and F. The abscissa is nondimensionalized time ($t = t' V_m$). The ordinate is the concentration of the biotic component as a fraction of the total amount of limiting nutrient in the system ($N_t = 1.0$). The parameter values for this solution are:

$\alpha = 0.02$, $\beta = 0.25$, $\epsilon_Z = 0.63$, $\epsilon_P = 0.60$, $\xi_F = 1.20$,

$\gamma = 2.30$, $\lambda = 0.50$, $\xi_Z = 0.10$, $\theta = 0.10$, $\phi = \eta = 0.25$

$\gamma = 2.30$, $\lambda = 0.50$, $\xi_Z = 0.10$, $\theta = 0.10$, $\phi = \eta = 0.25$

D= 0.0 as our other initial concentrations.

Fig. 13 shows the rapid growth of phytoplankton by uptake of the limiting nutrient. The dissolved nutrient decreases accordingly.

The zooplankton curve asymptotes to a steady state standing stock value. Detritus increases from zero at time t = 0 to a small percent (4%) of N_t. Fish biomass remains constant. Note that $P + N + Z + D + F = N_t = 1$ for all time.

The overall model behavior is not critically dependent on the initial conditions. The biotic components approach the same steady state values, when initial concentrations are changed. This result is not shown for brevity.

Each of the eleven parameters can be varied, and different solutions obtained. As the dynamics of two different limiting nutrients are considered in the complete spatial model, the nondimensionalized Michaelis-Menton constant is of special interest. The model response to a three fold increase in α is shown by a comparison of Fig. 14 and 13. A higher α corresponds to a smaller utilization of low concentrations of
a comparison of Fig. 14 and 13. A higher α corresponds
to a smaller utilization of low concentrations of
dissolved limiting nutrient by the phytoplankton. A

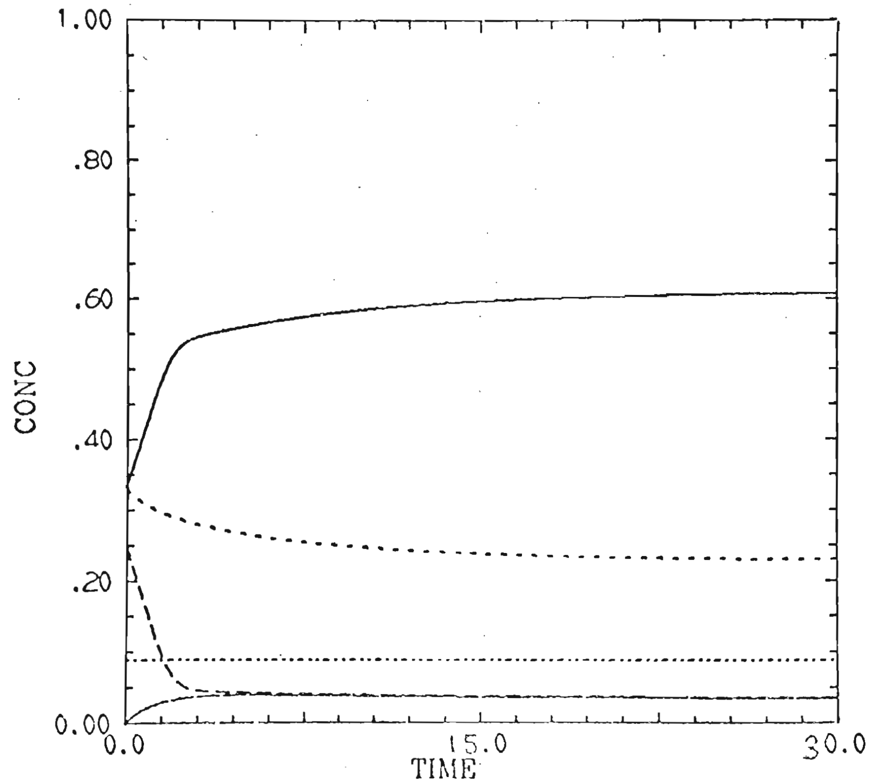

Fig. 14 Time dependent standing stock concentrations of the biotic components upon a three fold increase in the value of α . Line representations and all other parameter values are the same as in Fig.13.

greater concentration of N remains biologically unavailable in the water column. The phytoplankton standing stock in Fig. 14 is proportionately smaller. The zooplankton and detritus components are also slightly smaller concentrations than in Fig. 13.

The response of the one box system to fluctuations in environmental conditions is of interest. Since in nature the rate of photosynthesis varies with light intensity, we simulate the effect of diurnal variation of sunlight upon the growth kinetics of the phytoplankton. The phytoplankton nutrient uptake term is multiplied by a periodic function such that the rate of phytoplankton growth becomes a function of time of day.

Optimal light conditions initiates an increased photosynthetic rate by the plants, but the duration of this peak is only for several hours of the day. Sufficient anabolism may be accomplished within this short period of maximum nutrient uptake to sustain the phytoplankton over the twenty-four hour period (Russel-Hunter, 1970).

We choose a periodic function which gives the same averaged amount of nutrient uptake as would a constant
We choose a periodic function which gives the same averaged amount of nutrient uptake as would a constant
rate over twenty four hours. We define

$$f(t) = \pi \tau^{-1} \sin(2\pi t/\tau)$$

where t is nondimensional time equal to $t'V_m$ and τ represents one nondimensional day. Parameter τ' has units of 24 V_m^{-1} . When $f(t) \leq 0$, we set $f(t) = 0$ to simulate night conditions.

Note that

$$\int_0^{\tau} f(t) = 1$$

which states that, over one nondimensional day, τ , the amount of nutrient uptake is exactly equal to the uptake with or without diurnal variation if N is a constant over the entire period.

A one box solution including this diurnal variation of nutrient uptake rate by the phytoplankton is presented in Fig. 15. The value of τ used here is 1.0. Each time unit on the abscissa of Fig. 15 is one Vm^{-1}. All other parameter values are the same as in Fig. 13.

The daily fluctuations in the phytoplankton standing stock result in a negatively correlated oscillation of the dissolved nutrient concentration. The phytoplankton standing stock result in a negatively correlated oscillation of the dissolved nutrient concentration. The phytoplankton oscillations are damped out by the numerous feedbacks of

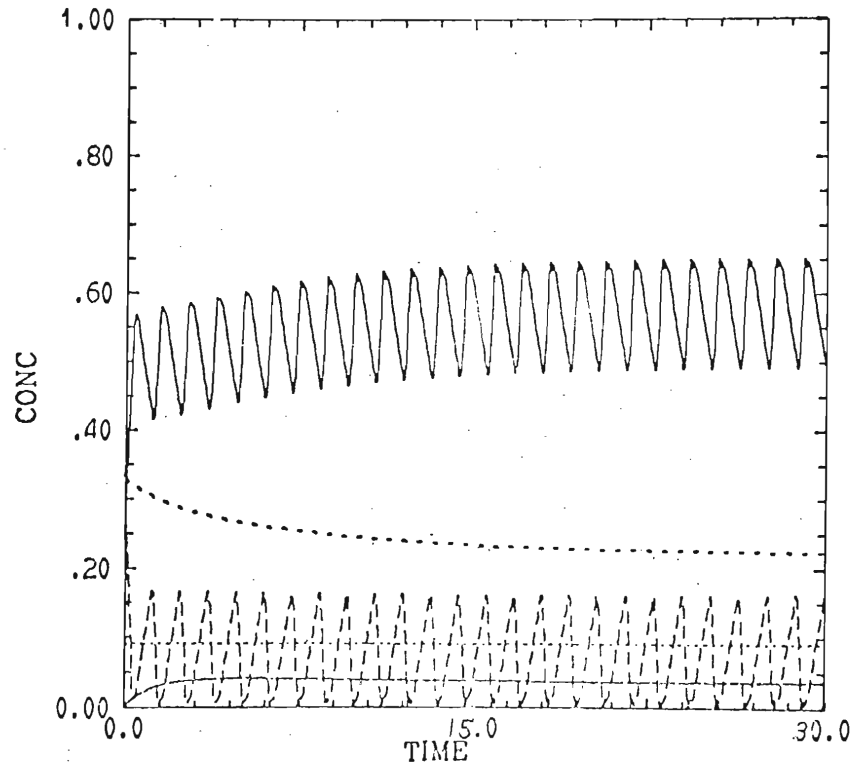

Fig. 15 Effect of diurnal photosynthetic rate variation upon the standing stock concentration of phytoplankton, zooplankton, dissolved nutrient, detritus, and pelagic fish. The solution includes the diurnal photosynthetic rate function with parameter $\tau = 1.0$. Line representations and all parameter values are the same as in Fig.13.

the food chain system, such that the zooplankton and detritus components show no daily fluctuations.

McAllister (1970) has shown that nocturnal zooplankton grazing behavior places a greater stress upon the phytoplankton standing crop than does a constant grazing or grazing only during the day. A stress upon the system such as this has yet to be investigated with this model.

3.3 Standing Stocks and Ecological Efficiencies of the Food Chain Model

In 1962 Curl attempted to measure the standing crops of carbon, nitrogen, and phosphorus and their transfer between marine trophic levels in continental shelf waters south of New York. Sampling errors introduced poor measurements of phytoplankton, herbivore, and carnivore standing stocks. By incorporating a large number of assumptions, Curl was able to arrive at a ratio of primary to herbivore production, but he found it difficult to extend his calculations to the carnivores (Mann, 1969).

In view of the complexity of the food web structure and the rapid changes in species composition that takes place in nature, it is doubtful that a complete picture

and the rapid changes in species composition that takes place in nature, it is doubtful that a complete picture

of the biological dynamics of an area can be attained by sampling alone. An approximate model of biological production as is presented here may provide the basis for understanding the factors which cause changes in standing stocks (Paloheimo and Dickie, 1970).

Major fluctuations in phytoplankton standing stock reflect the availability of nutrient in the water column. Zooplankton and fish production are dependent on the extent of their food supply. This model permits a study of the effect of nutrient limitation on the standing stock of the phytoplankton, zooplankton, and detritus.

A standing stock is defined as the concentration of the limiting nutrient in a trophic level at a certain time. In this model trophic level biomass or standing stock is a function of assimilated rather than merely ingested food.

Thus

standing stock = nutrient gains - nutrient losses.

The amount of food intake by a trophic level is proportional to its biomass.

proportional to its biomass.

Due to the confusion of terminology of various authors on the trophic level concept, we follow Kozlovsky's

(1967) lead in explicitly defining <u>net</u> <u>productivity</u> as the energy, or here limiting nutrient accumulation which occurs in a trophic level. <u>Production</u> is explicitly defined as <u>that portion of the productivity of a trophic level which is passed on to the next trophic level</u>. In other words, production is less than productivity since some of the net productivity is lost through processes such as death or excretion. It should be remembered that a closed system is assumed with no losses to the system. Slobodkin's (1960) definition of ecological efficiency originally formulated for energy transfers can be directly applied to nutrient transfer systems. We define

$$\text{ecological efficiency} = \frac{\text{production}}{\text{food intake}} = \frac{\text{energy passed to the next higher trophic level}}{\text{ingestion at the trophic level}}$$

For simplicity only a single food source is assumed for each trophic level, i.e. the standing stock of the lower trophic level.

It follows that

$$\text{ecological efficiency} = \begin{array}{c} \text{nutrient gain terms} \quad -\text{nutrient loss terms (other than predation)} \\ \hline \text{nutrient gain terms} \quad -\text{nutrient loss terms (other than predation)} \\ \hline \text{nutrient gain terms} \quad -\text{nutrient loss terms (other than predation)} \end{array}$$

For example, the ecological efficiency between the phytoplankton and the zooplankton in the model from (13) and (14) using steady state values from Fig. 13 is

$$\frac{\text{production of Z}}{\text{P available for Z consumption}} = \frac{\epsilon_Z(1-e^{-\delta_P P})Z - \gamma\epsilon_Z(1-e^{-\delta_P P})Z^2 - \delta_D Z}{\frac{NP}{\alpha+N} - \beta P}$$

$$= 0.1583$$

This means that 6.3 times as much phytoplankton is being produced than zooplankton in terms of biomass. This value is within the limits established in present food chain theory. A simplified 10% ecological efficiency between trophic levels of an aquatic food chain has been postulated by Lindeman (1942). Slobodkin (1962) suggests higher ecological efficiencies of 20-25% in general for herbivores and Ryther (1969) postulates 20% efficiency for zooplankton in upwelling areas.

Let us examine the model's ecological efficiency of zooplankton production when both the phytoplankton and detritus components are considered as food sources.

$$\frac{\text{production of Z}}{\text{P and D available to Z}} = \frac{\epsilon_Z(1-e^{-\delta_P P})Z + \epsilon_D Z D - \gamma\epsilon_Z(1-e^{-\delta_P P})Z^2 - \delta_D Z}{\frac{NP}{\alpha+N} - \beta P + \delta_D Z - \lambda D}$$

$$= 0.2071$$

$$= 0.2071$$

Thus we have an increase in zooplankton production efficiency by increasing the food chain complexity.

The ecological efficiency for fish production using model equations (13), (14), and (16) and steady state values from Fig. 13 is

$$\frac{\text{production of F}}{\text{P and Z available to F}} = \frac{\phi F\left(\frac{\theta P}{\theta P+Z}\right) + \phi F\left(\frac{Z}{\theta P+Z}\right)}{\frac{NP}{\alpha+N} - \beta P + \epsilon_Z(1-e^{-S_P P})Z + \epsilon_D Z D - S_D Z - \gamma\epsilon_Z(1-e^{-S_P P})Z^2}$$

$$= 0.2295$$

This fish production efficiency is quite acceptable, especially in light of work by Gulland (1970) and Lasker (1970). It is the steady state standing stock which determines the efficiencies, and the standing stocks are not known until the model is run. We have varied the parameter values to study the effect of the food supply on the steady state standing stocks and the resulting ecological efficiencies. In the development of the model, the tendency has been for more realistic ecological efficiencies following the specification of more realistic model formulation.

The conclusion must be that reasonable efficiencies

The conclusion must be that reasonable efficiencies
are obtained with the existing model, (13) - (17), within

the range of parameter values deduced in 3.1.

The Daily Zooplankton Nutrient Requirement

Ecological efficiencies have shown the production of zooplankton in the model to be reasonable in terms of food chain theory. Let us now compare our daily production of zooplankton with field and laboratory measurements. We relate actual grazing rates to measurement of V_m and N_t. The dimensional quantity of food grazed by the zooplankton may be expressed as

$$Q = E_z d_p P' Z'/Zn' = (\varepsilon_z \delta_p V_m/N_t)(PN_t)(ZN_t)/Z_n' \qquad (19)$$

where Q is the average daily amount of the limiting nutrient grazed by a zooplankter; Z_n' is the average number of zooplankton per unit volume. Typical units of Q are μgm atom of nutrient/dy/copepod.

Let us compare the prediction of this formula with laboratory measurements made by Parsons et al. (1969) and Corner and Cowey (1964). Using our model's steady state values of P and Z (Fig. 13), the corresponding values of V_m, ε_z, and δ_p assuming N_t = 30 μgm atom
values of V_m, ε_z, and δ_p assuming N_t = 30 μgm atom
NO_3-N/liter, and taking Parsons' (1969) value for Z_n,

$$Q = (0.63)(1.22\ dy^{-1})(0.619)(0.230)(N_t)/1\ \text{zooplankter}\ /\text{liter})$$
$$= (0.073\ dy^{-1})(30\ \mu\text{gm atom}\ NO_3\text{-N/liter})/(1\ \text{zooplankter/liter}$$
$$= 2.2\mu\text{gm atom}\ NO_3\text{-N/dy/copepod.}$$

Parsons has found a value of 20 μgm atom carbon/dy/copepod which converted to total nitrogen by a ratio of N/C of 0.1375 (Curl, 1962) gives Q = 2.75 μgm atom total nitrogen/dy/copepod. Corner and Cowey (1964) cite an annual mean daily requirement of nitrogen by the zooplankton (mainly copepods) in Long Island Sound as 1.06 μgm atom nitrogen/mg. dry weight copepod. Taking Parsons' et al. (1969) average zooplankton body dry weight of 0.10 mg. carbon, this gives a Q of approximately 0.1 μgm atom nitrogen/dy/copepod.

The amount of limiting nutrient consumed by a zooplankter within one day in our model is within this range of observations.

4. SENSITIVITY ANALYSIS

In this section we attempt to obtain some indication of the relative importance of the biological processes occurring within the ecosystem. We employ the technique of sensitivity analysis (Tomovic, 1963) to determine the importance of the biological model's parameters in determining the model solution.

Model sensitivity is defined as the displacement from equilibrium the model experiences due to a quantitative variation in an individual parameter. If a model component or the whole system changes substantially to a small variation in a particular parameter, then the value of that parameter is important and must be estimated with precision (Smith, 1970). Any continuing research on the system should focus on the study of mechanisms found highly influential in the simulation model. On the other hand, sensitivity analysis is no panacea. It can only sort out important processes already included in the model. It can not anticipate which additional processes should be included.

included.

Model sensitivity is investigated both empirically and analytically. First, the steady state values of the model components are empirically computed in a simulation run. One parameter is increased by a fixed percent, and the model solution recalculated. The process is repeated for each parameter. The empirical result yields the change in each biological component as a function of the change in each parameter. These may be regarded as estimates of quantities such as

$$\frac{\partial P}{\partial \beta}, \quad \frac{\partial N}{\partial \alpha}, \quad \text{etc.}$$

The method for analytical sensitivity analysis involves derivation of partial differential equations describing the rate of change of the components with respect to a change in the individual parameters. These simultaneous equations are then solved for the values of the partial derivatives $\frac{\partial P}{\partial \beta}$, $\frac{\partial N}{\partial \alpha}$, etc. The two methods of analysis may be compared; to within round-off error they should be identical.

4.1 Analytical Sensitivity Analysis

As an example of the procedure of calculating model sensitivities, let us assume a system much simplier

As an example of the procedure of calculating
model sensitivities, let us assume a system much simplier
but similar in form to the one presented in 2.

Consider a three component system with linear simultaneous equations at steady state

$$\frac{DP}{Dt} = \alpha N - \beta P - \gamma Z = 0$$
$$\frac{DZ}{Dt} = -\delta Z + \gamma Z = 0$$
$$\frac{DN}{Dt} = -\alpha N + \beta P + \delta Z = 0$$

where N, P, and Z are the dependent variables and α, β, γ, and δ are the system parameters. Since these three steady-state equations conserve mass, they sum to zero. Therefore, we may only use two of the above and the following closure relationship

$$N + P + Z = 1.$$

In the example below we shall use the steady-state equations for P and Z plus the closure relationship. We first differentiate the above equations with respect to each parameter, the independent variable for this analysis. The results are represented by a square coefficient matrix A. For example, differentiation with respect to α yields:

$$
\begin{array}{ccc}
A & X & B \\
\begin{bmatrix} -\beta & -\gamma & \alpha \\ 0 & (\gamma - \delta) & 0 \\ 1 & 1 & 1 \end{bmatrix} &
\begin{bmatrix} \frac{\partial P}{\partial \alpha} \\ \frac{\partial Z}{\partial \alpha} \\ \frac{\partial N}{\partial \alpha} \end{bmatrix} = &
\begin{bmatrix} N \\ 0 \\ 0 \end{bmatrix}
\end{array}
$$

Matrix A is always the same upon differentiation with respect to any parameter. We then have the matrix equation $AX = B$. The solution to the set of simultaneous equations for the rate of change of the components with respect to a change in the individual parameters is

$$X = A^{-1} B$$

where A^{-1} is the matrix inverse. The same general procedure is followed in calculating the sensitivity of our model's biotic components to changes in the system's parameter values. At steady state, equations (13) - (17) become

$$\frac{DP}{Dt} = \frac{N\Gamma}{\alpha + N} - \beta P - \epsilon_Z (1 - e^{-\delta_P P}) Z - \phi F\left(\frac{\theta P}{\theta P + Z}\right) = 0$$

$$\frac{DZ}{Dt} = \epsilon_Z (1 - e^{-\delta_P P}) Z - \gamma \epsilon_Z (1 - e^{-\delta_P P}) Z^2 - \epsilon_D Z D - \delta_D Z - \phi F\left(\frac{Z}{\theta P + Z}\right)$$

$$\frac{DD}{Dt} = -\epsilon_D Z D + \delta_D Z - \lambda D = 0$$

$$\frac{DD}{Dt} = -\epsilon_D Z D + \delta_D Z - \lambda D = 0$$

$$\frac{DF}{Dt} = \phi F\left(\frac{\theta P}{\theta P + Z}\right) + \phi F\left(\frac{Z}{\theta P + Z}\right) - \eta F = 0$$

and

$$\frac{DN}{Dt} = -\frac{NF}{\alpha + N} + \beta P + \gamma \epsilon_Z (1 - e^{-S_P P}) Z^2 + \lambda D + \eta F = 0$$

As in the previous example, the sum of these equations is zero, therefore, we must use the simple closure relationship

$$N + P + Z + D + F = 1$$

in the sensitivity analysis.

We arbitrarily neglect the nutrient equation. The same solutions would result if the phytoplankton, zooplankton, or detritus equation was chosen to be neglected. Since the fish biomass is constant, we disregard the fish equation as trivial.

Differentiating the remaining equations with respect to α, for example, gives us our square coefficient matrix A.

$$\begin{bmatrix} A_{11} & A_{12} & A_{13} & A_{14} \\ A_{21} & A_{22} & A_{23} & A_{24} \\ A_{31} & A_{32} & A_{33} & A_{34} \\ A_{41} & A_{42} & A_{43} & A_{44} \end{bmatrix} \begin{bmatrix} \frac{\partial P}{\partial \alpha} \\ \frac{\partial Z}{\partial \alpha} \\ \frac{\partial D}{\partial \alpha} \\ \frac{\partial N}{\partial \alpha} \end{bmatrix} = \begin{bmatrix} \frac{N}{(\alpha + N)^2} \\ 0 \\ 0 \\ 0 \end{bmatrix}$$

where $A_{11} = \frac{N}{\alpha + N} - \beta - \delta_P \epsilon_Z Z e^{-\delta_P P} + \frac{\theta^2 \phi F P}{(\theta P + Z)^2} - \frac{\theta \phi F}{(\theta P + Z)}$

$$A_{12} = -\epsilon_Z (1 - e^{-\delta_P P}) + \frac{\theta \phi F P}{(\theta P + Z)^2}$$

$$A_{13} = 0$$

$$A_{14} = \frac{\alpha}{(\alpha + N)^2}$$

$$A_{21} = (\delta_P \epsilon_Z Z e^{-\delta_P P})(1 - \gamma Z) + \frac{\theta \phi F Z}{(\theta P + Z)^2}$$

$$A_{22} = \epsilon_Z (1 - e^{-\delta_P P})(1 - 2\gamma Z) + \epsilon_D D + \frac{\phi F Z}{(\theta P + Z)^2} - \delta_D - \frac{\phi F}{\theta P + Z}$$

$$A_{23} = \epsilon_D Z$$

$$A_{24} = 0$$

$$A_{31} = 0$$

$$A_{32} = -\epsilon_D D + \delta_D$$

$A_{33} = -\epsilon_D Z - \lambda$

$A_{34} = 0$

and $A_{41} = A_{42} = A_{43} = A_{44} = 1$

A standard Gaussian elimination subroutine is used to solve for A^{-1}. The column vector B for α is shown above.

Table 2 is the result of the matrix solution of the vector for each parameter column vector. The values in the table are the evaluated partial derivatives of P, Z, N, and D with respect to the parameters α, β, ϵ_Z, λ, γ, δ_D, θ, ϕ, ϵ_D, and δ_P using the parameter and steady state values of Fig. 13. Component F is not included as it has a constant concentration of limiting nutrient in the model. As fish grazing coefficient ϕ is equivalent to fish excretion coefficient η, only ϕ is considered in the analysis. For definition purposes, we refer to the quantitative change in a biotic component for a fixed variation in a parameter as the component's sensitivity to that particular parameter. The sensitivity of the greatest magnitude (-1.320) is that by Z for δ_P. Thus for a one percent change in zooplankton death

of the greatest magnitude (-1.320) is that by Z for δ_P.
Thus for a one percent change in zooplankton death

Table 2. Sensitivity Analysis. Partial derivative values of the biotic components with respect to the biological parameters.

	P	Z	N	D
α	-0.402	-0.186	0.610	-0.023
β	-0.042	-0.019	0.064	-0.002
ϵ_Z	-0.449	0.376	0.027	0.046
λ	0.098	-0.035	-0.001	-0.061
γ	0.136	-0.117	-0.004	-0.014
δ_D	1.160	-1.320	-0.048	0.199
θ	-0.294	0.250	0.013	0.031
ϕ	0.549	-0.475	-0.015	-0.058
ϵ_D	-0.042	0.047	0.002	-0.007
δ_P	-0.159	0.133	0.009	0.016

Table 3. Normalized Sensitivity Analysis. Values of Table 2 normalized by multiplying by 100 times the parameter value and dividing by the component's steady state value.

	P	Z	N	D
α	-2.60	-3.23	99.29	-2.53
β	-1.70	-2.12	65.18	-1.66
ϵ_z	-45.67	102.80	68.79	80.52
λ	7.88	-7.63	-3.20	-84.32
γ	50.50	-116.90	-41.40	-91.62
δ_D	18.81	-57.11	-19.57	55.26
σ	-4.75	10.85	5.44	8.50
φ	22.17	-51.53	-16.21	-40.37
ϵ_D	-4.07	12.37	4.24	-11.97
δ_P	-30.79	69.28	46.37	54.28

coefficient S_D , the steady state zooplankton standing crop would decrease by 1.32%. The smallest sensitivity (0.001) indicates minimum fluctuations in dissolved limiting nutrient for changes in λ.

To get a comparative picture of the changes of the components, we have normalized the values of Table 2 as follows. We multiply each partial derivative value by the value of the parameter under consideration, divide by the steady state value of the component, and multiply by 100. Then the first row of Table 3 contains the quantities

$$\frac{\alpha}{P}\frac{\partial P}{\partial \alpha} \times 100; \quad \frac{\alpha}{Z}\frac{\partial Z}{\partial \alpha} \times 100; \quad \frac{\alpha}{N}\frac{\partial N}{\partial \alpha} \times 100; \quad \frac{\alpha}{D}\frac{\partial D}{\partial \alpha} \times 100$$

Rows 2 through 10 are similarly normalized.

4.2 Relative Sensitivity

Relative sensitivity is obtained by setting the largest change equal to one, and expressing all other sensitivities as a percent of this largest change (Smith, 1970). Upon observation of which normalized value in Table 3 is the greatest, we divide all other Table 3 values by this quantity. Table 4 is the result of this

Table 3 is the greatest, we divide all other Table 3
values by this quantity. Table 4 is the result of this

procedure. All values of Table 3 have been divided by the quantity $|(\gamma/Z)(\partial Z/\partial\gamma) \times 100|$. We denote the total operations upon the original partial derivative thus far as the partial derivative with an asterisk, e.g. $(\partial P/\partial\alpha)^*$.

The largest relative change of all components is that of zooplankton as effected by its excretion coefficient γ . The negative sign (-1.0) indicates a decrease in Z if γ is increased. Higher values of γ mean less assimilation. The next largest normalized sensitivity (0.879) is $(\partial Z/\partial\epsilon_Z)^*$, the positive effect of zooplankton grazing on the zooplankton standing crop. A larger maximum grazing coefficient results in more zooplankton biomass, as one would expect. The third greatest sensitivity (0.849) is the dependence of the dissolved limiting nutrient upon the nondimensionalized Michaelis-Menton constant α . A higher α indicates a less efficient uptake of the nutrient by the phytoplankton, a greater concentration of N remaining in the water column biologically unavailable.

The magnitude of the $(\partial D/\partial\gamma)^*$ relationship between detritus and the zooplankton excretion coefficient γ is (-0.783). The effect is indirect, but understandable. The more the zooplankton excrete, the less zooplankton

(-0.783). The effect is indirect, but understandable. The more the zooplankton excrete, the less zooplankton

biomass is available to eventually become detritus. The effect (-0.721) of the bacterial regeneration rate coefficient λ upon the detritus component is to lower the amount of D in the system. A higher λ shortens the time for regeneration of detritus into available nutrient, as the e-folding time scale for detritus is λ^{-1} . The dependence of detritus concentration upon the zooplankton grazing coefficient ϵ_Z (0.688) is again related to zooplankton standing stock.

The seventh largest sensitivity is that by zooplankton biomass for the parameter describing phytoplankton-dependent changes in Z grazing. The $(\partial Z/\partial S_P)^*$ relationship (0.592) indicates the importance of nonlinear zooplankton grazing formulation. The indirect dependence of N upon ϵ_Z (0.588) is obscure except in light of the coupling of system processes. Greater zooplankton grazing results in fewer phytoplankton and more nutrient in the water column.

The amount of dissolved limiting nutrient would expectantly increase (0.557) with greater phytoplankton extracellular release and the zooplankton biomass decrease (-0.488) with a greater death rate.

The above are the ten largest normalized sensitivities. Also of interest are the parameters

The above are the ten largest normalized sensitivities. Also of interest are the parameters

with the least influence upon the component value. It is enlightening to discover that the effect of parameters α and β, the phytoplankton nutrient uptake and extracellular release coefficients, have the smallest effect upon the standing stocks of phytoplankton, zooplankton, and detritus. Consider the normalized sensitivities

$$\left(\frac{\partial P}{\partial \alpha}\right)^* = -0.022 \quad \left(\frac{\partial D}{\partial \alpha}\right)^* = -0.022; \quad \left(\frac{\partial Z}{\partial \beta}\right)^* = -0.018$$

$$\left(\frac{\partial P}{\partial \beta}\right)^* = -0.014; \quad \left(\frac{\partial D}{\partial \beta}\right)^* = -0.014$$

These indicate the system is least responsive to variations in the α and β parameter values.

There are forty relationships expressed in each of the Tables 2 through 4, all of which can be interpreted in terms of food chain relationships or physiological processes. The relative sensitivities of Table 4 express the importance of system processes without regard to the magnitude of the coefficients or components involved. Using the normalized sensitivities we can estimate the overall importance of the parameters by assigning

Using the normalized sensitivities we can estimate the overall importance of the parameters by assigning

Table 4. Relative Sensitivity Analysis. Table 3 values divided by $(\gamma/Z)(\partial Z/\partial\gamma)\times 100$.

	P	Z	N	D
α	-0.022	-0.028	0.849	-0.022
β	-0.014	-0.018	0.557	-0.014
ϵ_Z	-0.390	0.879	0.588	0.688
λ	0.067	-0.065	-0.027	-0.721
γ	0.432	-1.000	-0.354	-0.783
S_D	0.161	-0.488	-0.167	0.473
θ	-0.041	0.093	0.046	0.073
ϕ	0.190	-0.441	-0.139	-0.345
ϵ_D	-0.035	0.106	0.036	-0.102
S_P	-0.263	0.592	0.397	0.464

Table 5. Overall Importance of Parameters. Ordering of the forty model sensitivity values of Table 4. High relative sensitivities are given low order assignments.

	ϵ_Z	γ	S_P	S_D	ϕ	λ	α	θ	ϵ_D	β
P	16	14	19	22	20	28	36	31	33	39
Z	2	1	7	10	13	29	34	26	24	38
N	8	17	15	21	23	35	3	30	32	9
D	6	4	12	11	18	5	37	27	25	40
	32	36	53	64	74	97	110	114	114	126
D	6	4	12	11	18	5	37	27	25	40
	32	36	53	64	74	97	110	114	114	126

each scaled partial derivative an order from one to forty based on its absolute value in Table 4.

Table 5 shows the order assignment of these forty partial derivatives. For example, the order of the normalized $(\partial Z/\partial \gamma)^*$ is read under the γ parameter column along the Z component row. Next we sum the columns. Using high relative sensitivities for low order assignment, the lowest column totals represent overall importance of parameters. "Overall" means the summed influence of the parameter on the standing stocks of the system's biotic components.

We see from Table 5 that the zooplankton grazing coefficient ϵ_Z is the most important parameter in the biological dynamics. Closely following is the zooplankton excretion coefficient γ . The zooplankton grazing parameter δ_P and the zooplankton death coefficient δ_D are also highly influential on the system's steady state. Clearly, the system is very sensitive to the zooplankton dynamics.

The fish grazing coefficient ϕ is fifth in importance. The regeneration rate parameter λ has the next overall importance on the system, followed by the nondimensionalized Michaelis-Menton constant α . The
next overall importance on the system, followed by the nondimensionalized Michaelis-Menton constant α . The

fish gill raker efficiency constant θ is followed by ε_D and finally β. The parameter with the lowest sensitivity in Table 5, namely β is indicated to have the least overall effect upon the system.

4.3 Comparison of Analytical and Empirical Model Sensitivities

The analytical sensitivity analysis has served to predict the change in biotic model components due to changes in the model parameters. Model simulation runs were next performed to determine if the analytical predictions were correct. A ten percent change was made in each parameter and the steady state values of P, Z, N, D, and F found after each parameter change. By computed sensitivity analysis, the phytoplankton component was predicted to experience the largest deviation from its steady state value upon a variation in γ, i.e. $\gamma(\partial P/\partial\gamma) = 0.393$. A 10% increase in γ gave a steady state value for P such that

$$\gamma \frac{\Delta P}{\Delta \gamma} = 0.363$$

This was indeed the greatest change in the model relative to ten percent changes in all other parameters. Table 6

This was indeed the greatest change in the model relative to ten percent changes in all other parameters. Table 6

Table 6. Analytical Sensitivity Analysis. Predicted biotic component displacements (percent) for a ten percent increase in each parameter value.

	P	Z	N	D
α	-2.02	-0.40	2.46	-0.05
β	-1.32	-0.26	1.62	-0.03
ϵ_Z	-35.60	29.80	2.12	3.66
λ	6.13	-2.81	-0.15	-3.17
γ	39.30	-33.60	-1.49	-4.13
S_D	14.70	-15.70	-0.66	1.68
σ	-3.71	3.14	0.18	0.39
ϕ	17.30	-14.90	-0.61	-1.83
ϵ_D	-3.17	3.40	0.14	-0.36
S_P	-8.08	6.77	0.48	0.83

Table 7. Empirical Sensitivity Analysis. Observed biotic component displacements (percent) for a ten percent increase in each parameter value.

	P	Z	N	D
α	-2.02	-0.40	2.46	-0.05
β	-2.23	-0.44	2.72	-0.05
ϵ_Z	-31.28	24.77	3.53	2.97
λ	5.71	-2.57	-0.23	-2.92
γ	36.28	-30.42	-2.03	-3.83
δ_D	15.51	-15.93	-1.05	1.44
θ	-3.56	2.93	0.27	0.36
ϕ	18.42	-15.51	-0.99	-1.92
ϵ_D	-3.15	3.30	0.22	-0.38
δ_P	-7.19	5.78	0.69	0.71

shows the analytical prediction of percent changes in the biotic components with respect to a ten percent change in all parameter values. Table 7 shows the percent changes observed from simulation runs. The similarity of the values of the two tables indicate the analytical sensitivity analysis has been done properly.

4.4 Interpretation of Sensitivity Analysis

Sensitivity analysis gives us an indication of which of the included processes greatly affect the system's steady state. To achieve a better understanding of the system, the processes characterized as important should then be studied more closely in the laboratory and in the field. In our formulated food chain model, zooplankton and fish dynamics are paramount. The importance of zooplankton grazing in marine plankton systems has been documented by Cushing (1963), Riley (1946), and Steele (1959). Observations of herbivore excretion enhancing the growth of phytoplankton have been recorded (Cushing, 1969; Walsh and Dugdale, 1971).

The availability of a nutrient to phytoplankton after it has been excreted by the secondary producers has been explained in terms of chemistry by marine scientists. It has been postulated (Walsh and Dugdale,
has been explained in terms of chemistry by marine scientists. It has been postulated (Walsh and Dugdale,

1971) that for a nitrate limiting situation, for example, excretion of ammonia by zooplankton and herbivorous fishes promotes phytoplankton growth. The preferential uptake of ammonia across the cell wall may be regarded as the functional basis for enhanced phytoplankton blooms.

This model has found an enhancement of phytoplankton standing stock for any limiting nutrient which is returned to the water column via secondary trophic level excretion. It appears to be an inherent property of the system. Perhaps Patten (1971) best explains the result:

> Feedback control may not be directly related to specific recognizable structures or physiological functions, but that regulation may come out of a dynamic interplay of processes when systems are complex enough.

The sensitivity analysis implies the parameters needed to be most accurately measured for this system are those of zooplankton grazing, excretion and death, and fish predation. Current research is concerned with their estimation.

5. WATER CIRCULATION ON THE SHELF

A known physical circulation is essential to any spatial description of biological productivity. Hsueh and O'Brien (1970) have developed a theoretical model of the circulation of the continental shelf waters of the eastern Gulf of Mexico. It is this circulation pattern together with the postulated biological and chemical dynamics which leads to a hypothetical spatial picture of the lower marine trophic levels in the model area.

The West Florida coastal water is influenced by the presence of a strong (50 to 100 cm sec^{-1}) southerly flow, the Loop Current, located off the continental shelf break. It occurs approximately 200 to 250 kilometers off the west coast of Florida during the winter season (Leipper, 1970). Where the Loop Current meanders against the continental shelf, bottom friction results in shoreward transport of water along the continental shelf bottom. Conservation of mass requires displaced bottom water to be forced upward and offshore. This process is termed "current-induced upwelling" (Hsueh and O'Brien, 1970).

process is termed "current-induced upwelling" (Hsueh and O'Brien, 1970).

Oceanographic surveys in the area have indicated evidence of this theoretical upwelling (Bogdanov, et al, 1968). Oxygen isopleths have been observed to rise to the surface in this region and temperature and salinity data also support the theory (Austin, 1971).

5.1 Formulation of the Flow Field

A simple linear model of a homogeneous ocean with a straight vertical coast and a flat continental shelf (Fig. 7) is employed. Boundary constraints placed upon the flow are

a) flow at the coast is zero; i.e., u = v = 0

b) flow at the bottom is zero, i.e., u = v = 0

c) there is no wind stress at the free surface; i.e.,

$$\frac{\partial u}{\partial z} = \frac{\partial v}{\partial z} = 0$$

At the seaward edge of the shelf region, the horizontal velocity of the offshore current is prescribed as a function of depth. The magnitude of the v' velocity at the shelf break boundary is described by the cosine function

$$v' = -C \cos(3\pi z/2d)$$

$$v' = -C \cos(3\pi z/2d)$$

simulating a southerly (negative) flow in the upper layers and a countercurrent northerly (positive) flow above the bottom. The maximum speed is C and the depth of the water column is d.

Upon neglecting the nonlinear acceleration terms, assuming constant density and hydrostatic equilibrium, and taking $\partial/\partial y = 0$, the steady state u momentum equation can be written,

$$f v' - g \frac{\partial \zeta'}{\partial x'} + A_h \frac{\partial^2 u'}{\partial x'^2} + A_v \frac{\partial^2 u}{\partial z'^2} = 0 \qquad (26)$$

where primes denote dimensional terms, $\frac{\partial \zeta'}{\partial x'}$ is the sea slope in the x direction, f is the Coriolis parameter, g is the acceleration of gravity, and A_v and A_h are the assumed constant vertical and horizontal eddy viscosities.

The v momentum equation at steady state can be written,

$$-f u' + A_h \frac{\partial^2 v'}{\partial x'^2} + A_v \frac{\partial^2 v'}{\partial z'^2} = 0 \qquad (27)$$

We can reduce the parameter space by nondimensionalizing these equations. We let

alizing these equations. We let

$u' = C u$ $\qquad\qquad$ $v' = C v$

$$x' = (A_h/f)^{1/2} x \qquad w' = (A_v/A_h)^{1/2}\, C\, w$$

$$z' = (A_v/f)^{1/2} z \qquad \zeta' = \frac{(f\, A_h)^{1/2}\, C}{g}\, \zeta$$

where C is the typical horizontal speed of the Loop Current. The nondimensionalized equations of motion for the cross section of the ocean shown in Fig. 7 is,

$$-v = -\frac{\partial \zeta}{\partial x} - \frac{\partial^2 u}{\partial x^2} - \frac{\partial^2 u}{\partial z^2}$$

and

$$u = \frac{\partial^2 v}{\partial x^2} - \frac{\partial^2 v}{\partial z^2}$$

Since $\partial v/\partial y$ is taken to be zero, the continuity equation

$$\frac{\partial u}{\partial x} + \frac{\partial w}{\partial z} = 0$$

may be used to calculate w.

At the surface, the Coriolis force, fv, balances the pressure gradient force $\frac{\partial \zeta}{\partial x}$. However, within the bottom Ekman layer, the friction along the bottom decreases the v velocity. The geostrophic balance is bottom Ekman layer, the friction along the bottom decreases the v velocity. The geostrophic balance is upset and water is transported onshore. The water must flow seaward at the top to provide mass balance.

5.2 The Simulated Circulation Pattern

Fig. 16-17 are simulated representations of the physical circulation pattern over the shelf used in this model. Fig. 16a shows contours of the u velocity, the speed of the water flow in the x direction toward the coast. Note the positive onshore flow along the bottom. Offshore flow occurs in the upper region where negative u velocities occur. Contours of the longshore v velocity are presented in Fig. 16b. An equatorward flow (negative velocities) simulates the Loop Current in the upper 60 meters over the shelf break. A poleward flow (positive velocities) is found below.

The vertical velocities are shown in Fig. 17a. Note that the strong positive velocities (upwelling) occur over most of the shelf while negative (downwelling) velocities are found inshore and at the shelf break boundary. Fig. 17b. shows the transverse circulation. The streamfunction is defined as

$$\frac{\partial \Psi}{\partial z} = -u \qquad \text{and} \qquad \frac{\partial \Psi}{\partial x} = w$$

$$\frac{\partial \Psi}{\partial z} = -u \qquad \text{and} \qquad \frac{\partial \Psi}{\partial x} = w$$

Fig. 16a and b. Contours of the u velocity (above) and v velocity (below) over the oceanic section. Each vertical unit is 20 meters and each horizontal unit represents 20 kilometers. Small tick marks denote the location of spatial blocks along the grid edges. There are 82 divisions in the vertical and 41 divisions in the horizontal. Positive u velocities indicate onshore flow; negative u velocities represent offshore flow. Negative v velocity indicates a southerly flow; positive v velocities represent a northerly countercurrent. Fig. 16a contours from -0.66 to 0.44, with a contour interval of 0.06. Fig. 16b contours from -1.0 to 1.0 by 0.1.

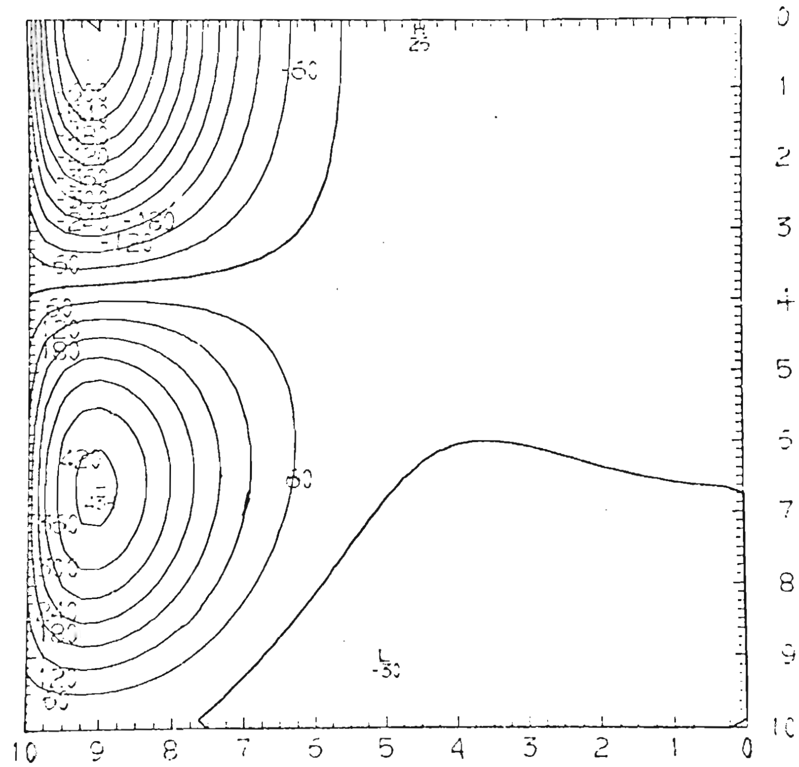

Fig. 16a

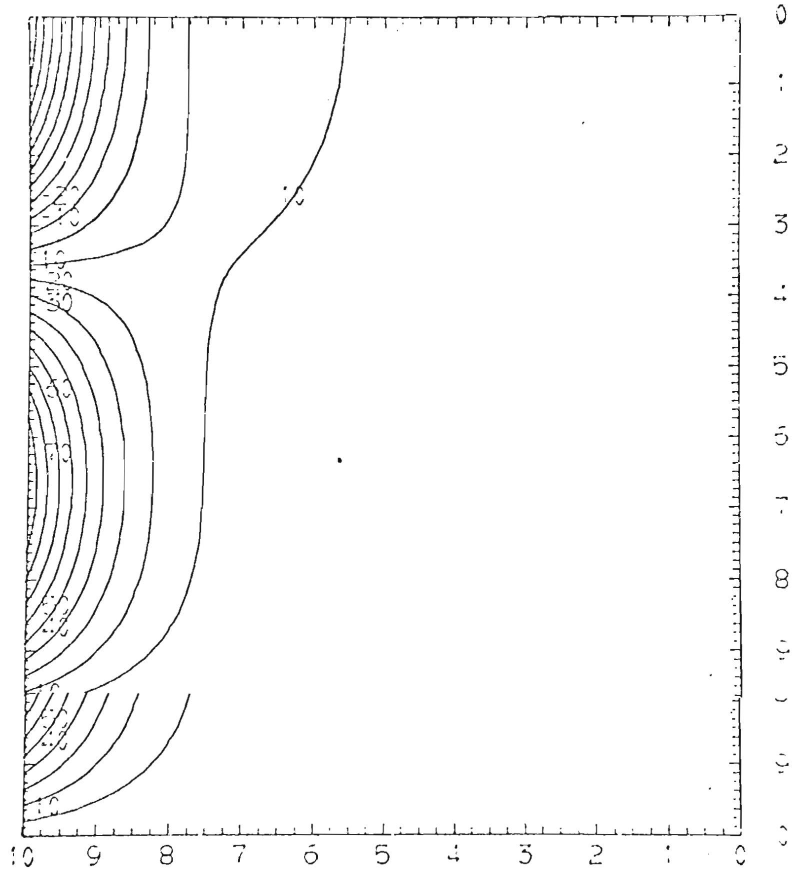

Fig. 16b

Fig. 17a and b. Contours of the vertical w velocities (above) and the streamfunction ψ (below) over the oceanic section. Positive w indicates an upward velocity; negative w represents a downward velocity. Negative ψ values represent a clockwise gyre. Positive ψ values denote a counterclockwise gyre. Strong upwelling is indicated from approximately 120 to 180 kilometers offshore, with downwelling occuring at the coast and seaward boundary. Grid spacings are the same as in Fig. 16. Fig. 17a contours from -2.30 to 0.73, with a contour interval of 0.1. Fig. 17b contours from -0.56 to 0.80 by 0.08.

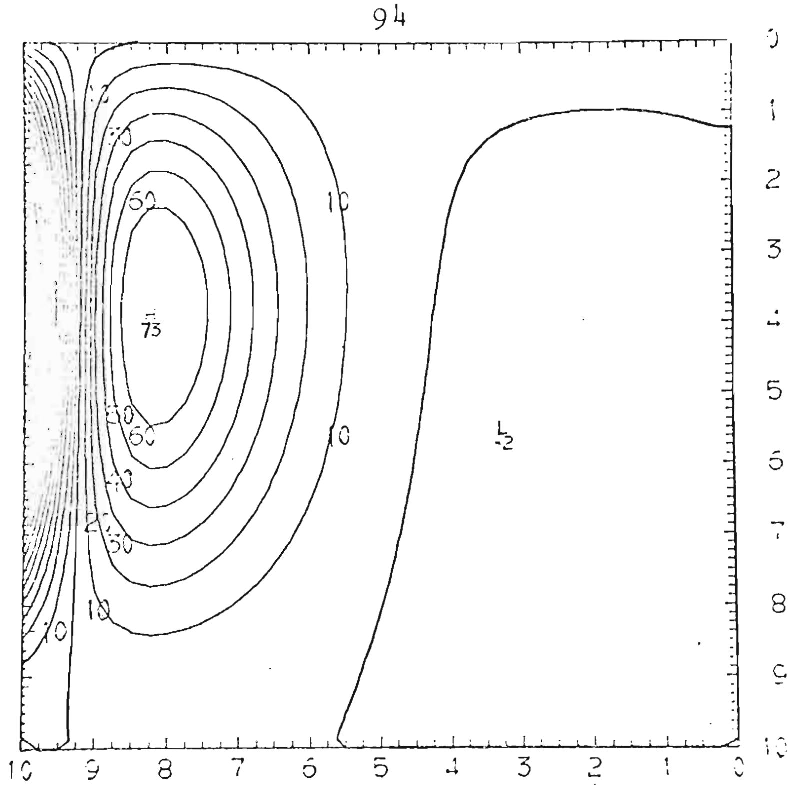

Fig. 17a

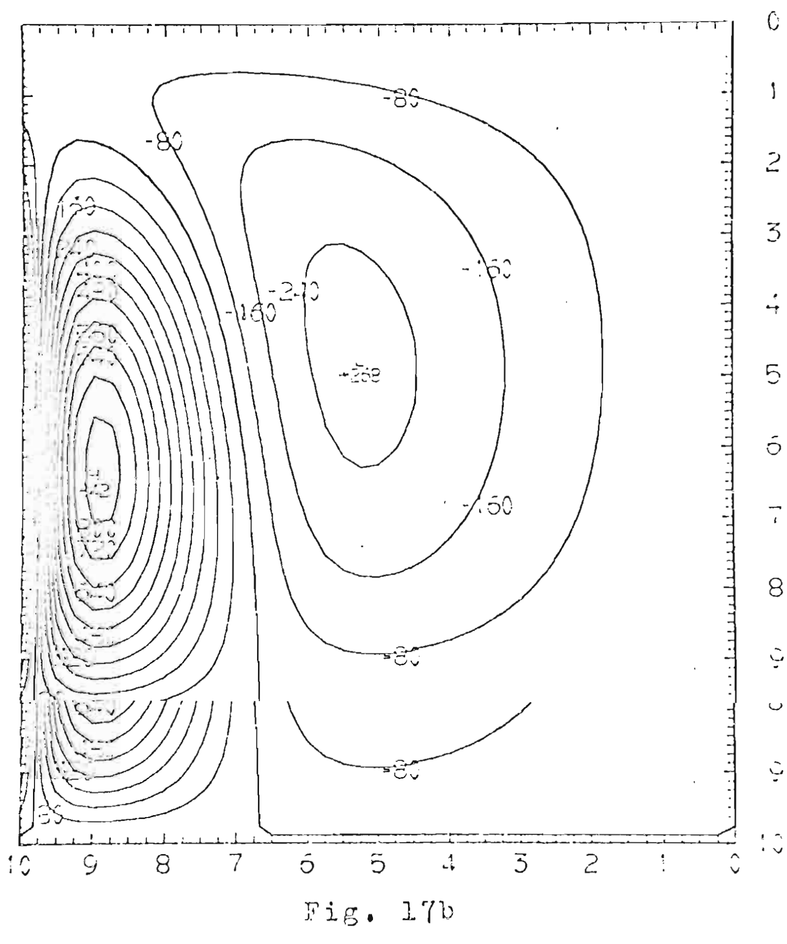

Fig. 17b

since $\frac{\partial u}{\partial x} + \frac{\partial w}{\partial z} = 0$ in this model.

This picture conceptually represents the flow of the ocean in the x-z plane. The magnitude of the flow is proportional to the spacing of the contours, and the sign of the streamfunction specifies direction. The flow is always parallel to the streamfunction contours.

Two gyres over the shelf are found. One gyre weakly spinning in a clockwise direction is located over the shoreward part of the shelf. The second gyre located approximately 130 kilometers offshore spins strongly in a counterclockwise direction. This motion results in strong upwelling of bottom waters from 120 to 180 km offshore and downwelling near the coast and seaward boundary.

5.3 Combination of Biological and Physical Formulations

We are now ready to place the biological dynamics into the simulated physical system. Boundary constraints placed on the advection and diffusion of biotic components are:

a) no transport across the free surface

ponents are.

a) no transport across the free surface

b) no transport through the bottom or coastal boundary

c) transport across the seaward boundary is determined by the flow field.

We scale the physical processes to the biological rates as follows. Consider the dimensional total derivative for phytoplankton dynamics,

$$\frac{DP'}{Dt'} \equiv \frac{\partial P'}{\partial t'} + u'\frac{\partial P'}{\partial x'} + w'\frac{\partial P'}{\partial z} - \nu_h'\frac{\partial^2 P'}{\partial x'^2} - \nu_v'\frac{\partial^2 P'}{\partial z'^2}$$

$$= \frac{V_m P' N'}{K + N'} - \beta P' - E_z(1 - e^{-\delta_P P'})Z' - \Phi F' \frac{\theta P'}{\theta P' + Z'} \qquad (31)$$

Substitution of previously defined scaling relationships into (31), and dividing by Mt V_m, we have

$$\frac{DP}{Dt} \equiv \frac{\partial P}{\partial t} + \frac{C}{V_m(\frac{Ah}{f})}\left(u\frac{\partial P}{\partial x} + w\frac{\partial P}{\partial z}\right) - \frac{1}{V_m(\frac{Ah}{f})}\left(\nu_h'\frac{\partial^2 P}{\partial x^2}\right) - \frac{1}{V_m(\frac{Av}{f})}\left(\nu_v'\frac{\partial^2 P}{\partial z^2}\right)$$

$$= \frac{PN}{\alpha + N} - \beta P - \epsilon_z(1 - e^{-\delta_P P})Z - \phi F\left(\frac{\theta P}{\theta P + Z}\right). \qquad (32)$$

Now we define a nondimensional ratio $S \equiv \frac{C}{V_m(Ah/f)^{\frac{1}{2}}}$ (O'Brien and Wroblewski, 1972), and the Rossby number $R_o \equiv C(A_h f)^{-\frac{1}{2}}$. Substituting into equation (32) we get

$$\frac{DP}{Dt} = \frac{\partial P}{\partial t} + S\left(u\frac{\partial P}{\partial x} + w\frac{\partial P}{\partial z}\right) - \frac{1}{V_m\left(\frac{A_h}{f}\right)}\left(\nu_h'\frac{\partial^2 P}{\partial x^2}\right) - \frac{1}{V_m\left(\frac{A_v}{f}\right)}\left(\nu_v'\frac{\partial^2 P}{\partial z^2}\right)$$

$$= \frac{PN}{\alpha + N} - \beta P - \epsilon_Z(1 - e^{-S_P P})Z - \phi F\left(\frac{\theta P}{\theta P + Z}\right) \tag{33}$$

We nondimensionalize the diffusion coefficients as $\nu_h = \nu_h'\left[V_m(A_h/f)\right]^{-1}$ and $\nu_v = \nu_v'\left[V_m(A_v/f)\right]^{-1}$. Our final nondimensional equation is then,

$$\frac{DP}{Dt} = \frac{\partial P}{\partial t} + S\left(u\frac{\partial P}{\partial x} + w\frac{\partial P}{\partial z}\right) - \nu_h\frac{\partial^2 P}{\partial x^2} - \nu_v\frac{\partial^2 P}{\partial z^2}$$

$$= \frac{PN}{\alpha + N} - \beta P - \epsilon_Z(1 - e^{-S_P P})Z - \phi F\left(\frac{\theta P}{\theta P + Z}\right). \tag{34}$$

The total derivatives for the Z and N components are similar:

$$\frac{DZ}{Dt} = \frac{\partial Z}{\partial t} + S\left(u\frac{\partial Z}{\partial x} + w\frac{\partial Z}{\partial z}\right) - \nu_h\frac{\partial^2 Z}{\partial x^2} - \nu_v\frac{\partial^2 Z}{\partial z^2}$$

$$= \epsilon_Z(1 - e^{-S_P P})Z + \epsilon_D Z D - S_D Z - \gamma(1 - e^{-S_P P})Z^2 - \phi F\left(\frac{Z}{\theta P + Z}\right) \tag{35}$$

and

$$\frac{DN}{Dt} = \frac{\partial N}{\partial t} + S\left(u\frac{\partial N}{\partial x} + w\frac{\partial N}{\partial z}\right) - \nu_h\frac{\partial^2 N}{\partial z^2} - \nu_v\frac{\partial^2 N}{\partial z^2}$$

$$= -\frac{NP}{\alpha + N} + \beta P + \lambda D + \eta F + \gamma\epsilon_Z(1 - e^{-S_P P})Z^2 \tag{36}$$

$$= -\frac{NP}{\alpha + N} + \beta P + \lambda D + \eta F + \gamma\epsilon_Z(1 - e^{-S_P P})Z^2 \tag{36}$$

No spatial distribution of pelagic fish is considered.

Notice that the advection and diffusion processes are scaled by the parameter S. This nondimensional ratio is related to the maximum advection speed in the horizontal, the maximum rate of uptake of limiting nutrient, and the turbulent part of the flow field. The value of the S parameter for the model area is discussed in 6. The rates of the physical-chemical-biological model are all scaled by the biological turnover rate V_m^{-1}.

Sinking of Detritus

The subject of sinking of plankton components is controversial. Field observations of the vertical distribution of phytoplankton are confused by the combined effects of gravitational sinking of senescent phytoplankton cells, neutral buoyancy maintained by actively phytosynthesizing cells, and the vertical advection of the cells by water motion (Steele, 1959).

In this model, phytoplankton and zooplankton are considered neutrally buoyant and thus subject to the effects of vertical advection and diffusion. Only the dead zooplankton, or detritus, is subjected to a gravi-
effects of vertical advection and diffusion. Only the dead zooplankton, or detritus, is subjected to a gravi-
tational sinking velocity.

Laboratory measurements of sinking rates of inactive planktonic material are on the order of 1 to 10m day^{-1} (Steele, 1956). The model is investigated with sinking velocities for detritus within this order of magnitude. The sinking rate is formulated as follows. We assume an average sinking velocity W_s = 7m/day^{-1} or 0.0081 cm sec^{-1}. We scale detritus sinking as

$$w_s' = \left[S(Av/Ah)^{\frac{1}{2}}\ C\right]\ w_s$$

where w_s is the nondimensional sinking rate, C is the maximum horizontal velocity, S is the parameter which scales the effect of advection and diffusion, and $(A_v/A_h)^{\frac{1}{2}}$ is the ratio of the vertical diffusion coefficient to the horizontal diffusion coefficient.

Notice the value of w_s depends on S which is determined by V_m. This is another example of the scaling of the physical processes by the biological turnover rate. A typical value of the sinking parameter for a nitrate limited sea (V_m = 0.05 hr^{-1}) would be

$$w_s = 0.091$$

$$w_s = 0.091$$

while the w_s value for a phosphate limiting situation (V_m = 0.10 hr^{-1}) is

$$w_s = 0.182$$

The total derivative for the detritus component may then be expresses as

$$\frac{DD}{Dt} \equiv \frac{\partial D}{\partial t} + S\left(u\frac{\partial D}{\partial x} + w\frac{\partial D}{\partial z} + \omega_s\frac{\partial D}{\partial z}\right) - \nu_h\frac{\partial^2 D}{\partial x^2} - \nu_v\frac{\partial^2 D}{\partial z^2}$$

$$= S_D Z - \lambda D - \epsilon_D Z D \tag{37}$$

The term for gravitational sinking of detritus is $\omega_s\frac{\partial D}{\partial z}$.

Equations (34) - (37) are expresses in finite differences (Appendix II) and solved for each spatial grid point using the u and w velocities of the simulated circulation pattern. The values of P, Z, N, and D are calculated for each time increment, giving the time dependent, standing stocks of these biotic components and their spatial distributions.

6. PARAMETER VALUES OF THE FLORIDA SHELF MODEL

6.1 Physical Constants

We have proceeded to formulate the model and scale the processes such that a minimum of characteristic values need to be specified. By identifying the region for investigation, a number of physical parameter values are determined.

Model area geometry specifies the depth of the basin d and the width of the basin b. The depth of the water column is taken to be a constant 200 meters over a 200 kilometer wide shelf. The Coriolis parameter, f, is approximately 5 x 10^{-5} sec^{-1} for the 27° N latitude. Observational data provide the maximum horizontal velocity C. The characteristic maximum velocity (Loop Current) used here is 50 cm sec^{-1}. The relationship between the horizontal and vertical diffusivities is taken as proportional to the ratio of the chosen horizontal and vertical Austauch coefficients,

$$\frac{\nu'_v}{\nu'_h} = \frac{A_v}{A_h}$$

$$\frac{\nu'_v}{\nu'_h} = \frac{A_v}{A_h}$$

Specifying A_h equal to 2×10^8 $cm^2\ sec^{-1}$ and A_v equal to 200 $cm^2\ sec^{-1}$, and taking ν_v' as 1 $cm^2\ sec^{-1}$, then ν_h' is 10^6 $cm^2\ sec^{-1}$.

Using these values of C, f and A_h, the Rossby number as defined in 5.3 has a value of 0.5. This low Rossby number validates the Hsueh and O'Brien (1971) theory for a circulation over the shelf driven by offshore currents.

6.2 Variable Biological Parameters

The actual total amount of the limiting nutrient N_t in the real system is not required in the solutions, as final concentrations are expressed as percents of N_t. For conversion to dimensional units, the scaling relationships of Table 1 are used, and N_t is required. Then $N' = N_t N$, where N' is the dimensional concentration of a specific dissolved limiting nutrient found in a particular region of the water column.

The value of the biological turnover rate V_m, characteristic of the model area waters is required by the simulation run. The influence of the advective processes upon the biological spatial distributions is scaled by the parameter $S = \dfrac{C}{V_m (A_h/f)^{\frac{1}{2}}}$. As the

scaled by the parameter $S = \dfrac{C}{V_m (A_h/f)^{\frac{1}{2}}}$. As the

value of V_m is dependent on the biological and chemical characteristics of an area, it is readily seen how different spatial solutions may arise. The standing stock of phytoplankton in the euphotic zone is dependent not only on the cell division rate V_m, but on the magnitude of the advection of cells below the euphotic zone, and the resupplying of nutrients to the euphotic zone by upwelling water.

The limiting nutrient characteristics of the model area also specify the appropriate value of the Michaelis-Menton constant K to be used in the biological dynamics. As K is nondimensionalized by N_t, we need to know an approximate value of the total amount limiting nutrient available to the system. The value of N_t in this model has been estimated by identification of the probable limiting nutrient in the Florida Shelf waters and the measurement of the concentration of this nutrient in biologically inactive waters being supplied to the system.

In summary, the physical constants required by the model are b', d', C, f, A_h and A_v. The biological parameters characteristic of an area which need be supplied are V_m, K, and N_t.

supplied are V_m, K, and N_t.

6.3 The Value of V_m, K, N_t and the S Parameter for the Model Area

As discussed in Section 2, V_m is the maximum (unlimited) doubling rate of the phytoplankton. V_m occurs at the concentration of the limiting nutrient at which phytoplankton growth is no longer inhibited by low nutrient availability (Thomas, 1970). Values of V_m can be expressed in units of nutrient concentration or cell divisions per hour.

Ranges of V_m are dependent on the nutrient considered and the species of phytoplankton grown. Fortunately, work in this area has provided values of V_m and the Michaelis-Menton constant K for specific organisms and mixed populations under various nutrient conditions in several oceanic regions (Caperon, 1967; Eppley and Coatsworth, 1968; Eppley, Rogers, and McCarthy, 1969; MacIssac and Dugdale, 1969; Thomas and Dodson, 1968; and Thomas, 1970).

Recent observations (Appendix I) as well as published data (Bogdanov, 1968; Collier, 1958) indicate that both phosphorus and nitrate concentrations in model area waters are less than their cited V_m values. Water reactive phosphate is almost undetectable in these waters,

reactive phosphate is almost undetectable in these waters,

indicating phosphate may be the limiting nutrient. Values of V_m and K for a phosphate limiting sea were determined by Thomas and Dodson (1968) who experimented with the diatom Chaetoceros gracilis, isolated from the Costa Rica Dome, an upwelling area in the northeastern tropical Pacific. Chaetoceros gracilis occurs in abundance at times in the model area.

The V_m value found by Thomas and Dodson was 0.22 μ gm atom PO_4-P/ liter which gave a growth rate of 2.49 cell divisions/ 24 hours (0.10 hours-1). The K value, the concentration of limiting nutrient at which the phytoplankton growth rate is $V_m/2$, was found to be 0.12 μ gm atom PO_4-P/liter. The corresponding nondimensionalized value of α used in the model is

$$\alpha = \frac{K}{N_t} = \frac{0.12\mu \text{ gm atom } PO_4\text{-P/liter}}{4 \ \mu \text{ gm atom } PO_4\text{-P/liter}} = 0.030$$

estimating N_t as 4.0 μ gm atom PO_4-P/1 for the model area waters (Appendix I).

Phosphate is quickly recycled in aquatic food chains. Regeneration rates of utilizable phosphorus from zooplankton excretion products and phytoplankton cell

zooplankton excretion products and phytoplankton cell

autolysis may be on the order of hours (Steele, 1959). Also, the low concentration of phosphate in the model waters may not be indicative of phosphorus limitation. Phytoplankton require relatively small quantities of the nutrient for unlimited growth.

From observational data, nitrate is a possible limiting nutrient. Thomas (1970) reports a V_m value of 7 μ gm atom NO_3-N/1 which gave 1.22 doublings/24 hours (0.05 hours^{-1}) of a mixed phytoplankton population from the nitrate limited eastern tropical Pacific. Observations show concentrations of less than 2 μgm atom NO_3-N/1 in the euphotic zone waters of the model region. The K value for nitrate is reported by Thomas (1970) as 0.75 μ gm atom NO_3-N/1.

This would give an α value of

$$\alpha = \frac{K}{N_t} = \frac{0.75\mu \text{ gm atom } NO_3\text{-N/liter}}{30\mu \text{ gm atom } NO_3\text{-N/liter}} = 0.025$$

taking N_t equal to 30 μgm atom NO_3-N/1 (Appendix I).

Recent research (O'Brien, 1972) has indicated that while several nutrients may be in low enough concentrations to effect the rate of phytoplankton growth, at steady state generally only one nutrient is

growth, at steady state generally only one nutrient is

found to be limiting. Which nutrient becomes most important is determined primarily by the rate of supply to the rate of withdrawal of the various nutrients. We may be justified in using one specific V_m value in our model dynamics, instead of considering a synergistic combination of several V_m values.

The model formulation contains the nondimensional ratio S which categorizes the importance of advection and disorganized water motion (turbulence) in determining the spatial distributions of the biological components. In general, when $S \gg 1$, advection is the foremost factor in the plankton dynamics; when $S \ll 1$, advection is unimportant. When S is of the order unity, advection plays a strong competing role with the other environmental conditions in the model in determining the spatial distribution of the plankton (O'Brien and Wroblewski, 1972).

The relative importance of advection and diffusion in the spatial, trophic level model is deduced by scale analysis. Consider the S formulation, as derived in 5,

$$S = \frac{C}{V_m (A_h/f)^{1/2}}$$

where C is the average value of the horizontal advective

$V_m(A_h/f)$

where C is the average value of the horizontal advective

flow, A_h is the horizontal eddy viscosity coefficient, f is the Coriolis parameter, and V_m is the maximum (unlimited) growth rate of the phytoplankton.

We see immediately the S parameter is inversely dependent on the value of V_m. If V_m is high, the biological turnover rate is rapid and the importance of advection on the concentration of the biotic component is diminished. A strong turbulence also lowers the effect of advection.

The value of the S parameter used in the model based on the V_m value for a PO_4 limiting sea was $S_{PO_4} = 0.9$. Compare this value to that calculated for a hypothesized NO_3 limiting sea, $S_{NO_3} = 1.8$. We find that the advection effects are twice as important in a nitrate limiting sea than in phosphate limited waters. The high V_m for phosphate results in a higher biological turnover rate. The spatial distribution of the plankton in the phosphate limiting case is then determined more by phytoplankton growth than by advective processes.

The usefulness of the S parameter as developed in this paper lies in its simple formulation and general applicability to any nutrient limited aquatic ecosystem.

7. RESULTS OF THE SPATIAL PHYSICAL CHEMICAL - BIOLOGICAL MODEL

7.1 Spatial Distributions of the Biotic Components in the Absence of Advection

The biological system formulated in 2 is coupled with the simulated circulation pattern described in 5 to give an integrated physical-chemical-biological model. The formulation appears in equations (34) - (37).

It is instructive at this point to run the spatial model considering time dependency and diffusion, but without advection. The u, v, and w velocities of equations (34) - (37) are taken to be zero. The biological components are initialized at nondimensional concentrations of

$$P = 0.33$$

$$Z = 0.33$$

$$N = 0.25$$

$$F = 0.09$$

$$D = 0.00$$

at time t = 0 over all space. The biological parameter values used are the same as in Fig. 13.

at time t = 0 over all space. The biological parameter values used are the same as in Fig. 13.

The spatial solutions for an elapsed model time $t = 8$, equivalent to three to six days in nature, appear in Fig. 18-19. The euphotic and aphotic zones are well defined. The absence of contours except at the upper and lower boundary of the euphotic zone illustrates the homogeneous distributions within the euphotic and aphotic zones. The gradient between the zones arises from the effect of diffusion which acts to make the transition between zones smooth rather than abrupt.

We find the euphotic zone concentrations of the dissolved limiting nutrient, phytoplankton, zooplankton, and detritus components to be identical with the solutions for the one box model (Fig. 13). As the environmental conditions permit only nutrient and sinking detritus to exist below the euphotic zone, the aphotic zone is devoid of phytoplankton and zooplankton.

Phytoplankton (Fig. 18b) are maintained only in the area where the depth-photosynthesis curve is positive. Phytoplankton initially existing below the euphotic zone are grazed to extinction. Zooplankton (Fig. 19a) are confined to the area where their phytoplankton and detritus food sources exist. The zooplankton in the aphotic zone starve to death after consuming all the phytoplankton there.
food sources exist. The zooplankton in the aphotic zone starve to death after consuming all the phytoplankton there.

Fig. 18a and b. Spatial distribution of the dissolved limiting nutrient (above) and phytoplankton standing stock (below) concentrations at time t = 8.0 in the absence of advection. Fig. 18a contours from 0.01 to 1.0, contour interval of 0.05. Fig. 18b contours from 0.0 to 0.63, contour interval of 0.05.

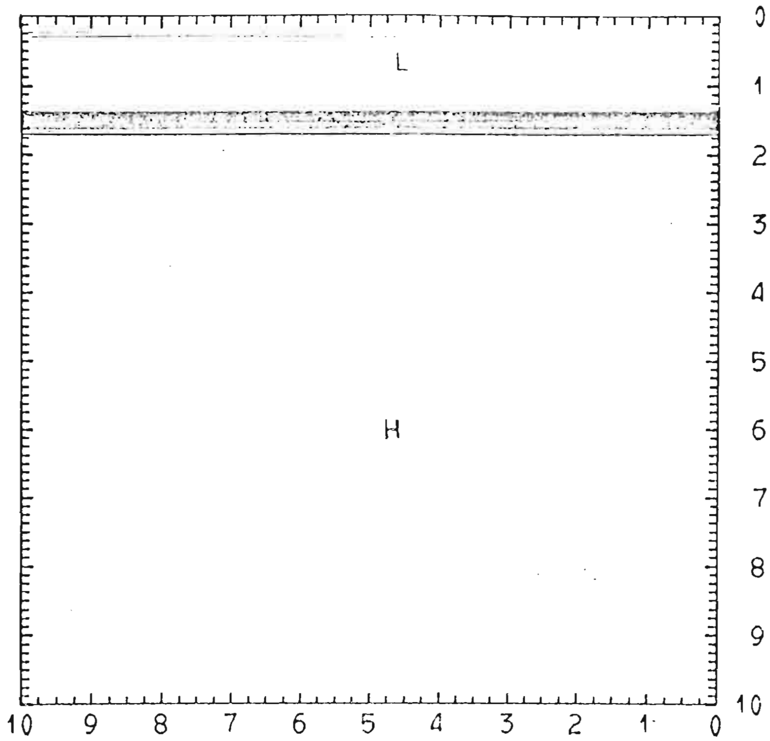

Fig. 18a

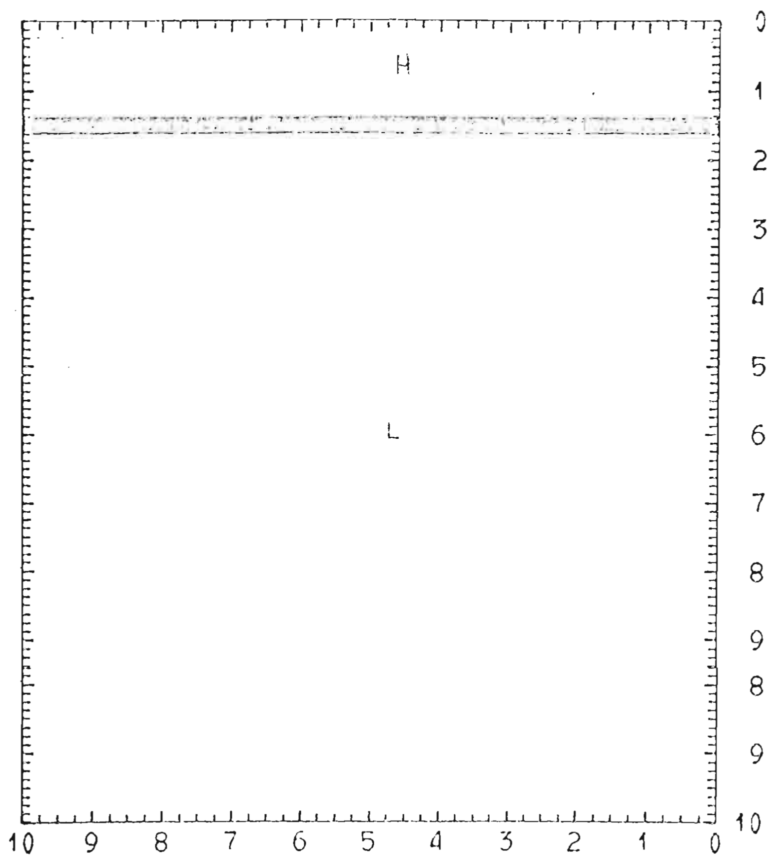

Fig. 18 b

Fig. 19a and b. Spatial distribution of the zooplankton (above) and detritus (below) concentrations at time t = 8.0 in the absence of advection. Fig. 19a contours from 0.0 to 0.24, contour interval of 0.05. Fig. 19b contours from 0.0 to 0.04, contour interval of 0.003.

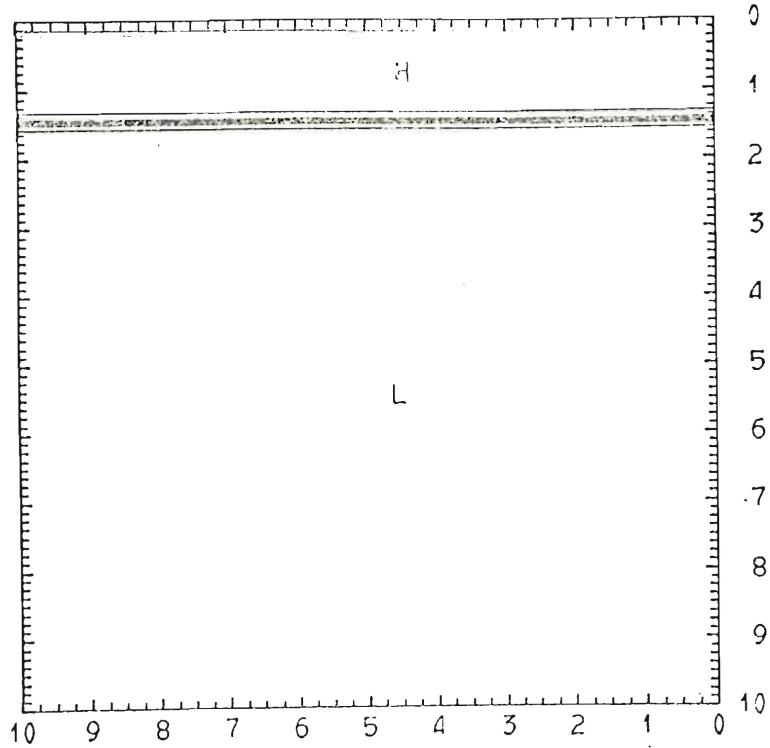

Fig. 19a

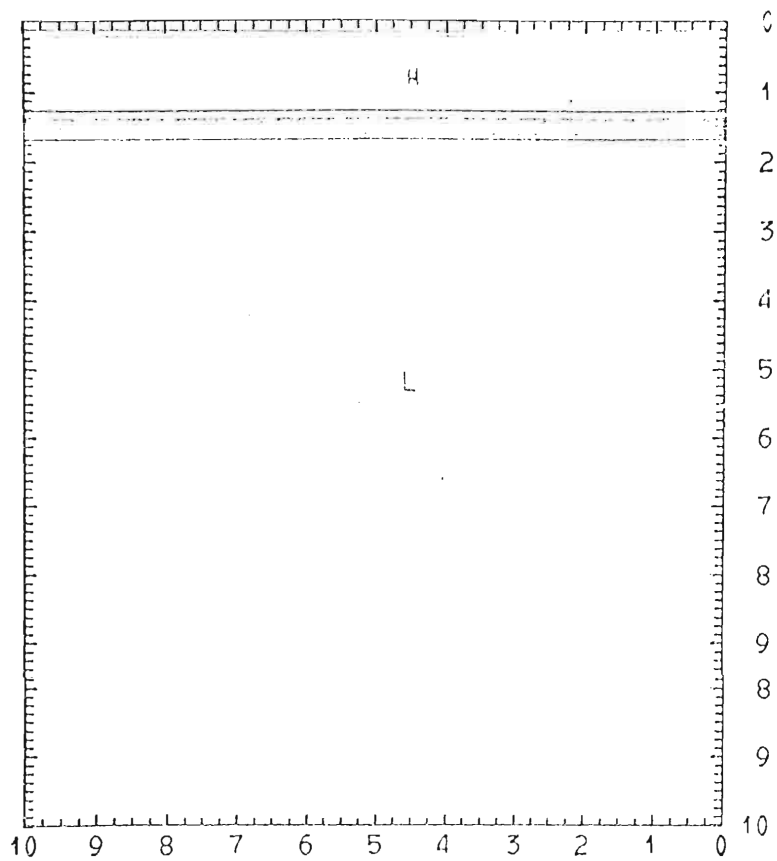

Fig. 19b

The low concentration of dissolved limiting nutrient (Fig. 18a) in the euphotic zone is a consequence of uptake by phytoplankton. Highest concentrations of N occur in the aphotic zone, where sinking detritus is decomposed and there are no nutrient losses. The width of the euphotic-aphotic gradient band in Fig. 19b of the detritus distribution reflects the gravitational sinking of detritus.

The purpose of this exercise has been to demonstrate to the reader the transition from a one box model to one with 3200 boxes. We see that without advection, the zones of biological activity as defined by environmental effects (light, nutrients) are well defined, homogeneous, and generally uninteresting. The use of models with only vertically stacked boxes is thus justified in situations where vertical advection is negligible and diffusion and sinking are the only interchanges between the euphotic and aphotic zones.

The following discussion will illustrate the necessity of including the effect of advection upon the distribution and biological processes of the biotic components in a situation where strong vertical

biotic components in a situation where strong vertical

advection occurs. The case in point is the upwelling of nutrient rich bottom waters over a continental shelf.

7.2 The Spatial Solutions for an Advected Phosphate Limiting Sea

We next consider the effects of advection on the spatial distributions of the biotic components. The u, v, and w velocities of equations (34) through (37) are those predicted from the steady state solution of equations (28) through (30). These specify the magnitude and direction of the water velocity at each point on the spatial grid. (Appendix II). For the following solutions we consider the model waters to be phosphate limited, and use the appropriate values of V_m, K, N_t and S.

Calculations are made of the changes in the spatial distribution of the phytoplankton, zooplankton, dissolved nutrient, and detritus as they are advected and diffused from their initial homogeneous concentrations of P = 0.33, Z = 0.33, N = 0.25, F = 0.09 and D = 0.0. Innovations are the advection of P, Z, N, and D below the euphotic zone and the upwelling of nutrient rich bottom waters. The resulting time dependent solutions are shown in Fig. 20 - 27.

waters. The resulting time dependent solutions are shown in Fig. 20 - 27.

By time t = 0.4 changes from the initial homogeneous distributions have occurred. Fig. 20 - 21 show the spatial distribution and concentration of the dissolved limiting nutrient, phytoplankton, zooplankton and detritus after approximately four hours (since V_m for the PO_4 limiting situation is 0.10 hr^{-1}).

The definition of zones of biological activity is evident at time t = 2.0. Observe in Fig. 22a that the limiting nutrient N is decreasing in the euphotic zone especially from 2.5 to 40 meters, and increasing below it. Close contouring at the euphotic zone's lower boundary indicates rapid changes in concentration. The gradation of the band is the result of both the smooth attenuation of the depth-photosynthesis curve and the effect of diffusion.

In Fig. 22b the phytoplankton standing stock has increased above its initial concentration in the euphotic zone and decreased in the aphotic zone. Fig. 23a shows zooplankton increasing in areas of high phytoplankton concentration and decreasing in the aphotic zone. The concentration of detritus has increased above its initial value of zero to 0.3% in the euphotic zone.

value of zero to 0.3% in the euphotic zone.

Fig. 20a and b. Spatial distribution of the concentration of dissolved limiting nutrient (above) and phytoplankton standing stock (below) at time t = 0.4 for an advected, phosphate limiting sea. Fig. 20a contours from 0.22 to 0.34, contour interval 0.05. Fig. 20b contours from 0.25 to 0.37, contour interval 0.05.

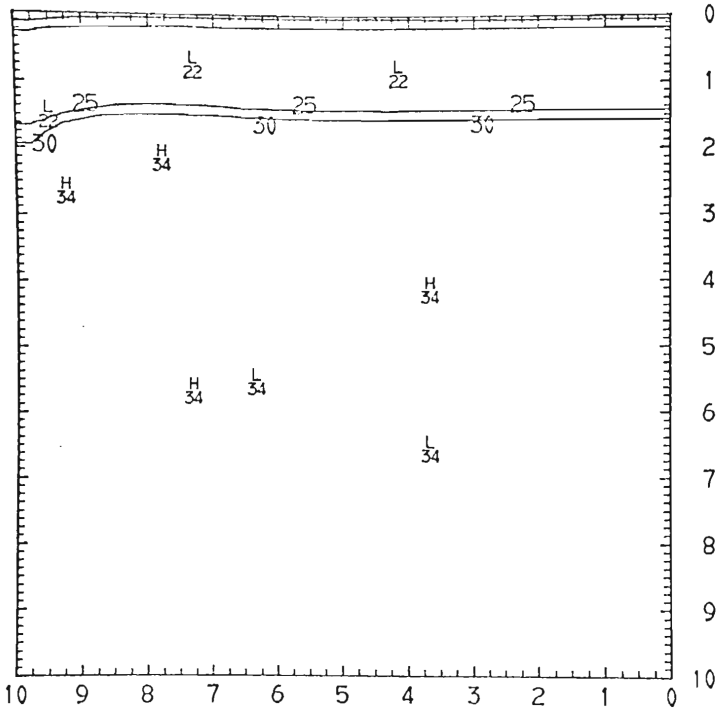

Fig. 20a

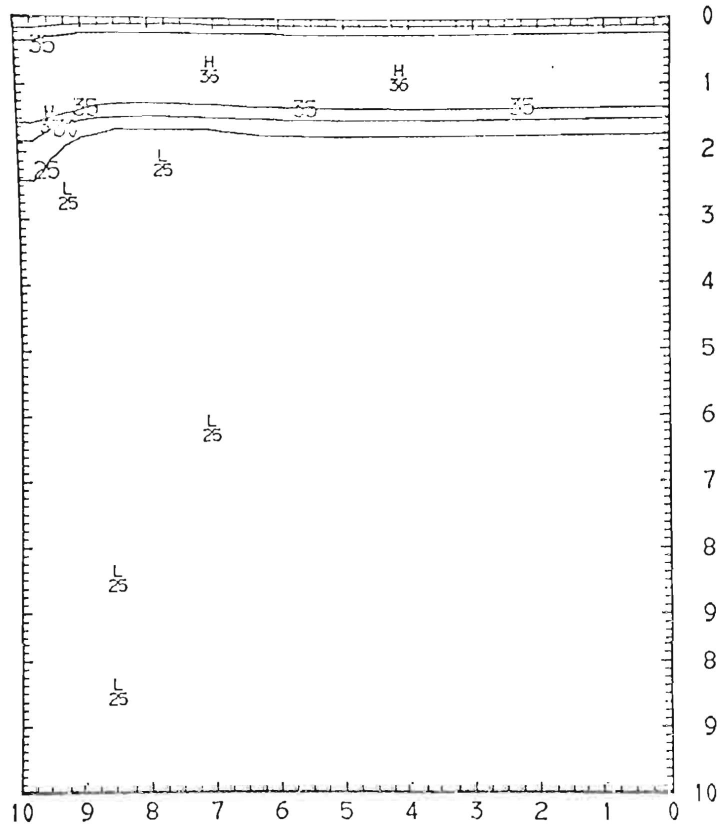

Fig. 20b

Fig. 21a and b. Spatial distribution of the zooplankton (above) and detritus (below) concentrations at time t = 0.4 for an advected, phosphate limiting sea. Fig. 21a contours from 0.31 to 0.32, contour interval of 0.05. Fig 21b contours from 0.0 to 0.012, contour interval of 0.002.

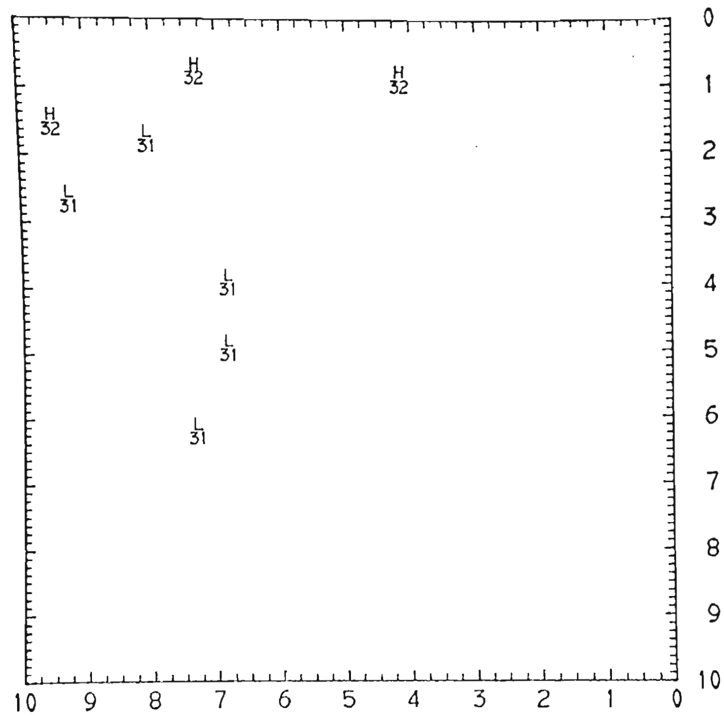

Fig. 21a

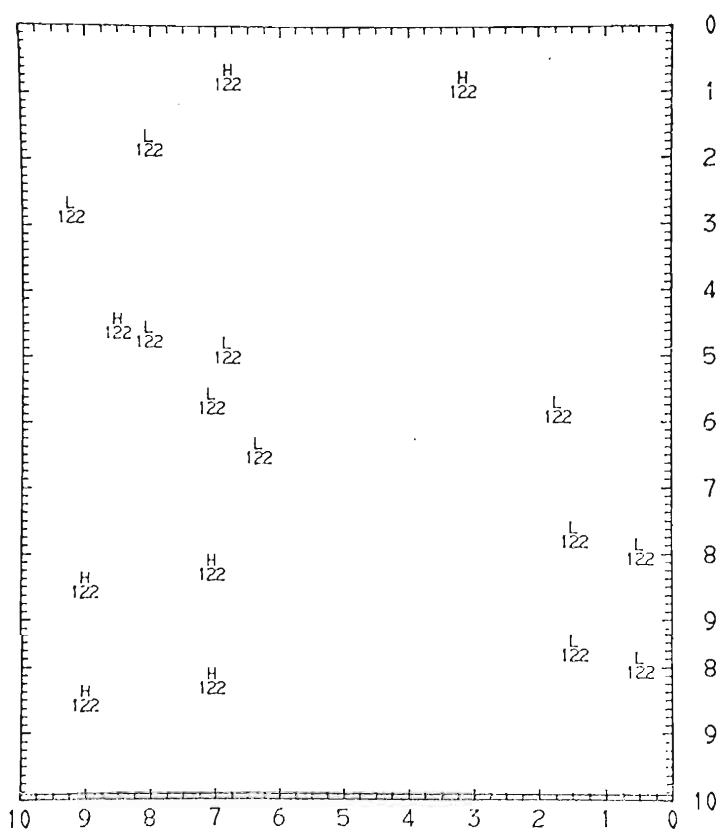

Fig. 21b

Fig. 22a and b. Spatial distributions of the concentration of dissolved limiting nutrient (above) and phytoplankton standing stock (below) at time t = 2.0 for an advected, PO_4 limiting sea. Fig. 22a contours from 0.12 to 0.54, contour interval of 0.05. Fig. 22b contours from 0.08 to 0.48, contour interval of 0.05.

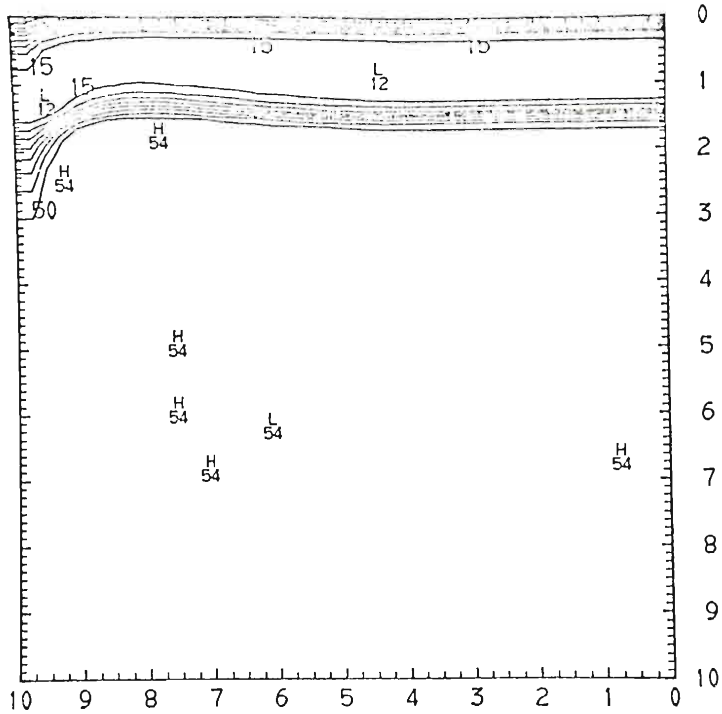

Fig. 22a

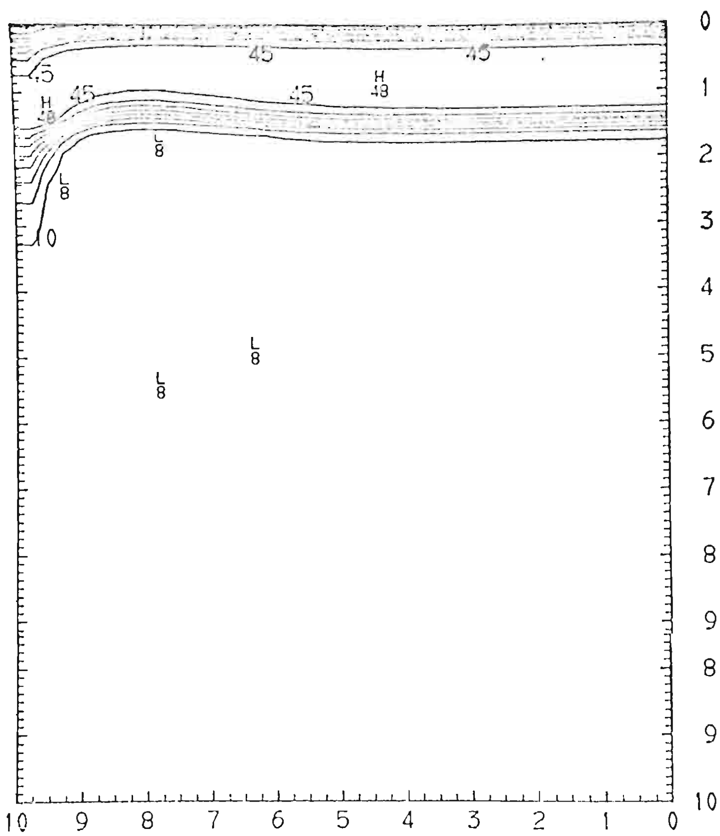

Fig. 22b

Fig. 23a and b. Spatial distribution of the concentration of zooplankton (above) and detritus (below) at time t = 2.0 for an advected, PO_4 limiting sea. Fig. 23a contours from 0.26 to 0.28, contour interval of 0.05. Fig. 23b contours from 0.03 to 0.03, contour interval of 0.002.

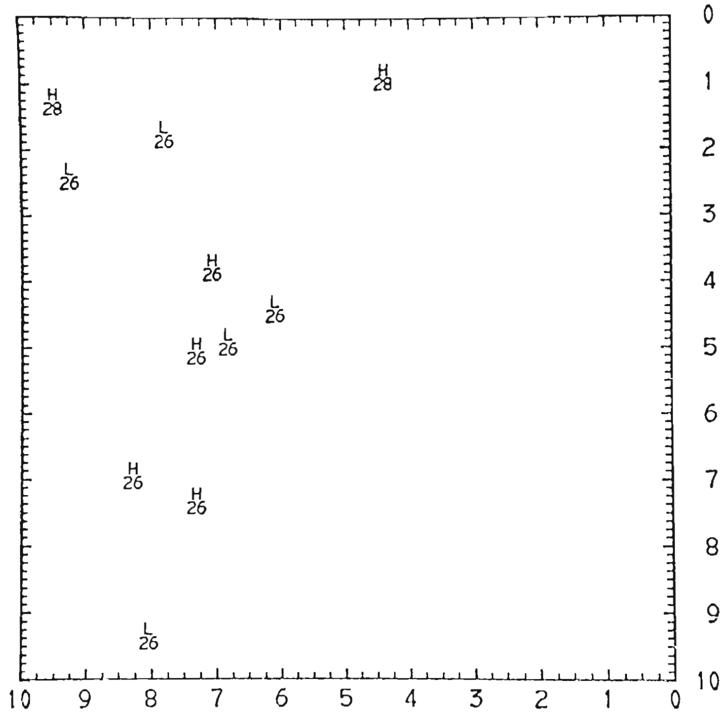

Fig. 23a

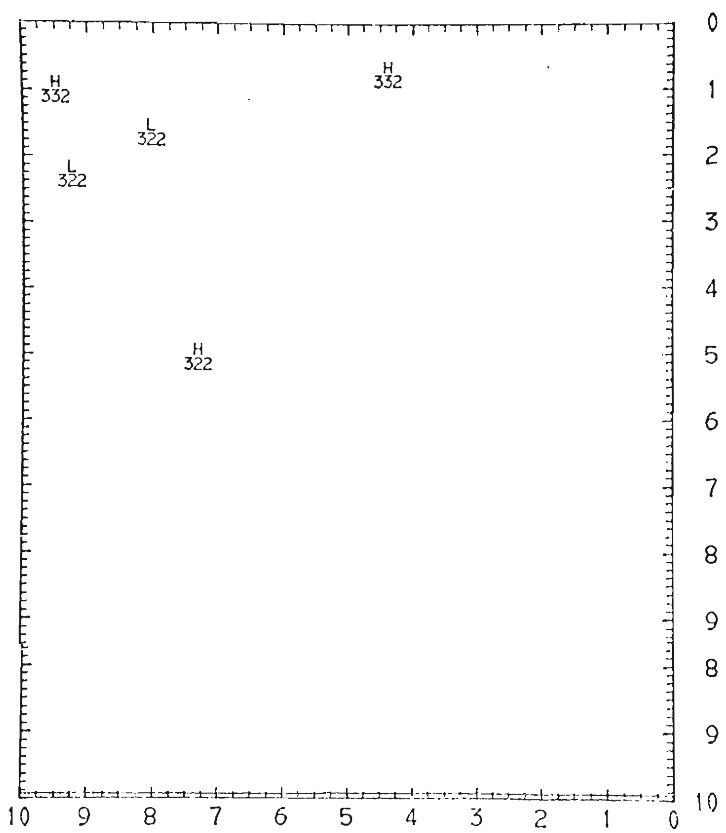

Fig. 23b

Fig. 24a and b. Spatial distribution of the concentration of dissolved limiting nutrient (above) and phytoplankton standing stock (below) at time $t = 4.0$ for an advected, PO_4 limiting sea. Fig. 24a contours from 0.06 to 0.69 by 0.05. Fig. 24b contours from 0.01 to 0.55, contour interval of 0.05.

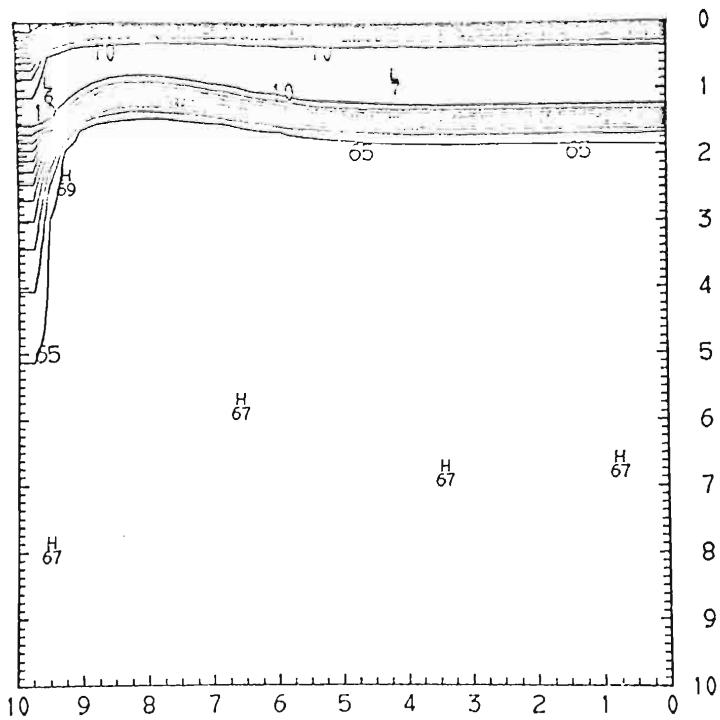

Fig. 24a

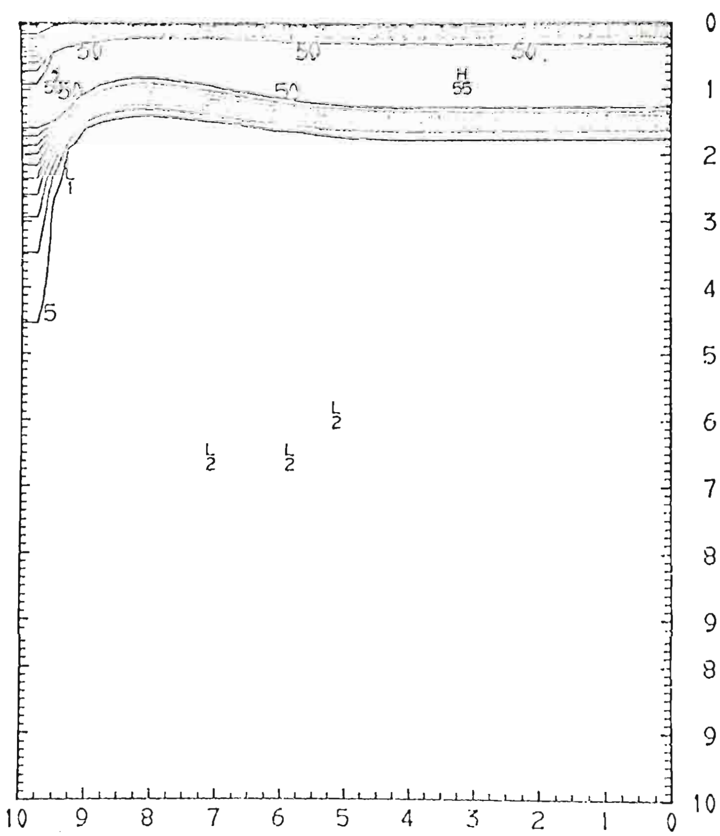

Fig. 24b

Fig. 25a and b. Spatial distribution of the concentration of zooplankton (above) and detritus (below) at time t = 4.0 for an advected, PO_4 limiting sea. Fig. 25a contours from 0.18 to 0.26, contour interval of 0.05. Fig. 25b contours from 0.033 to 0.039, contour interval of 0.002.

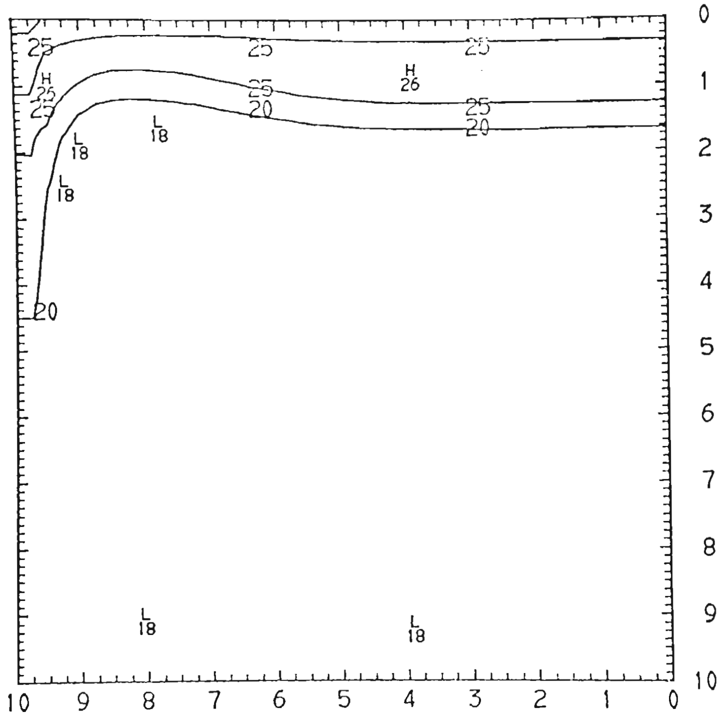

Fig. 25a

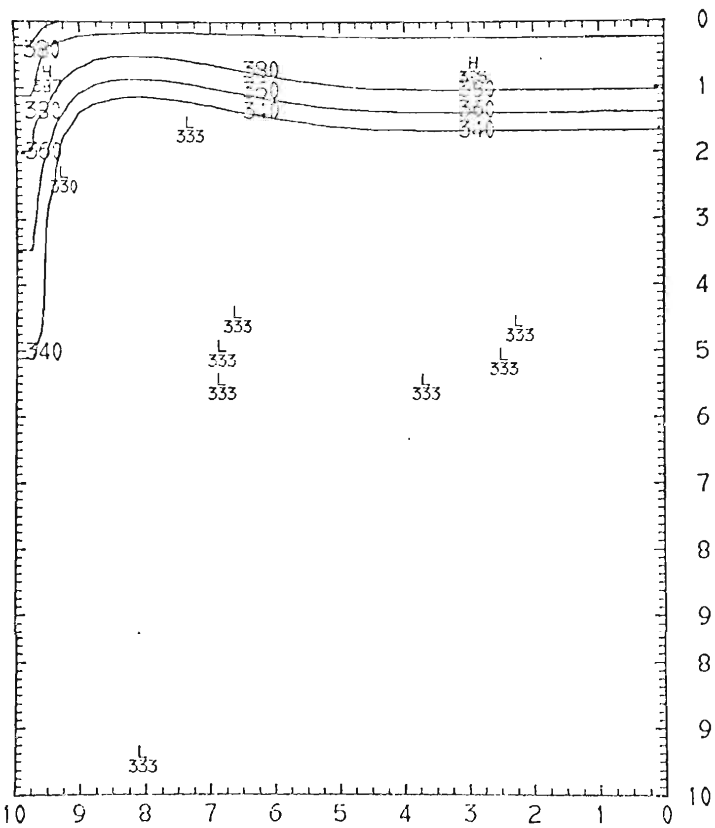

Fig. 25b

Fig. 26a and b. Spatial distribution of the concentration of dissolved limiting nutrient (above) and phytoplankton standing stock (below) at time t = 8.0 for an advected, PO_4 limiting sea. Fig. 26a contours from 0.05 to 0.91, contour interval 0.05. Fig. 26b contours from 0.0 to 0.62, contour interval of 0.05.

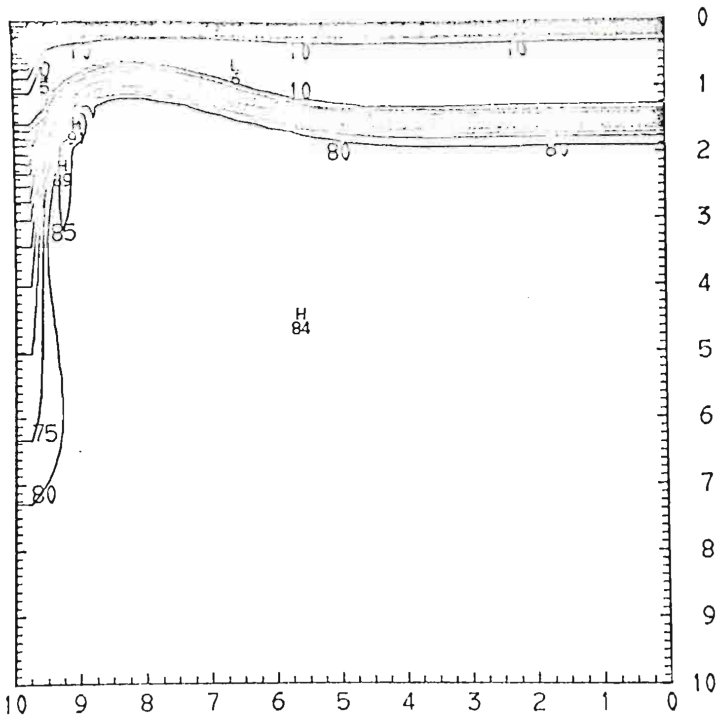

Fig. 26a

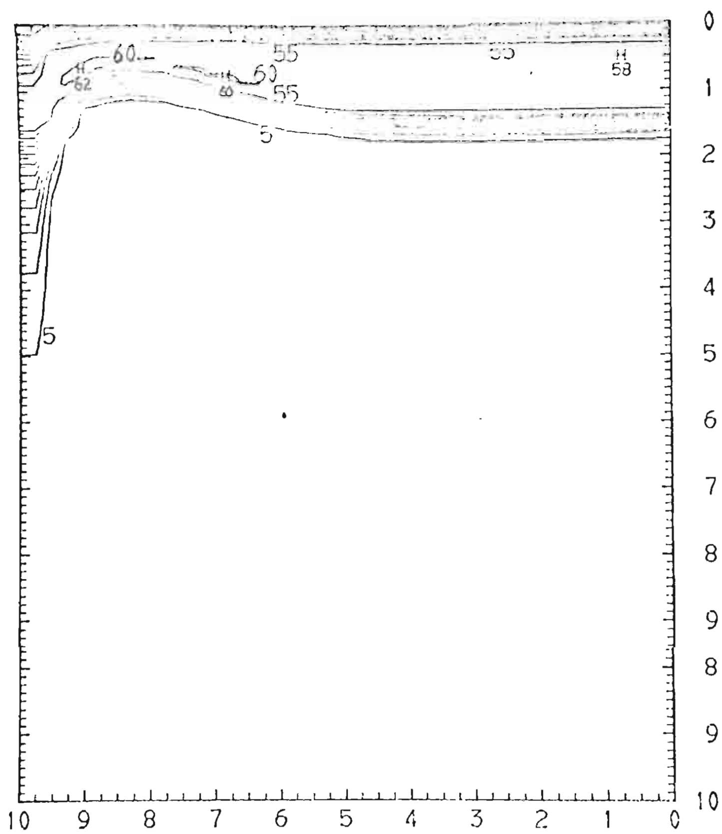

Fig. 26b

Fig. 27a and b. Spatial distribution of the concentration of zooplankton (above) and detritus (below) at time t = 8.0 for an advected, PO_4 limiting sea. Fig. 27a contours from 0.04 to 0.23, contour interval of 0.05. Fig. 27b contours from 0.016 to 0.037, contour interval of 0.002.

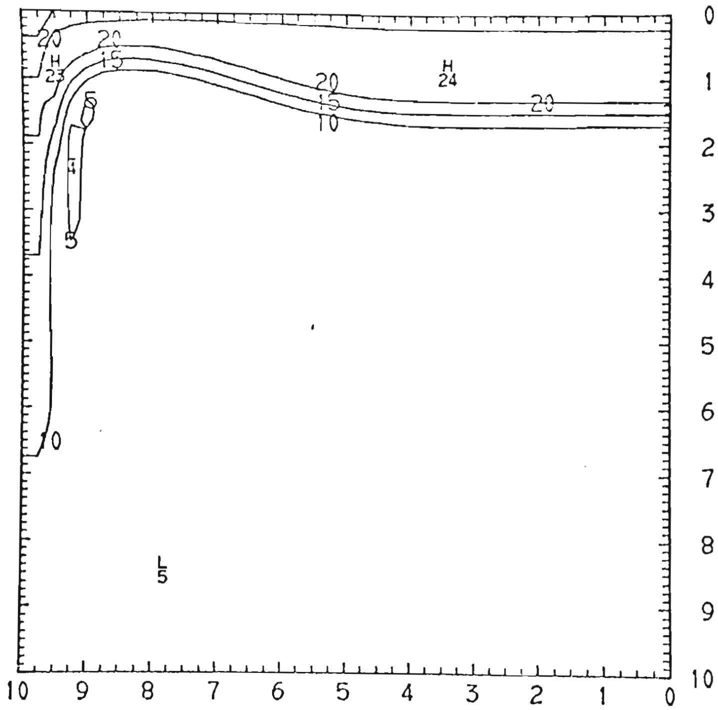

Fig. 27a

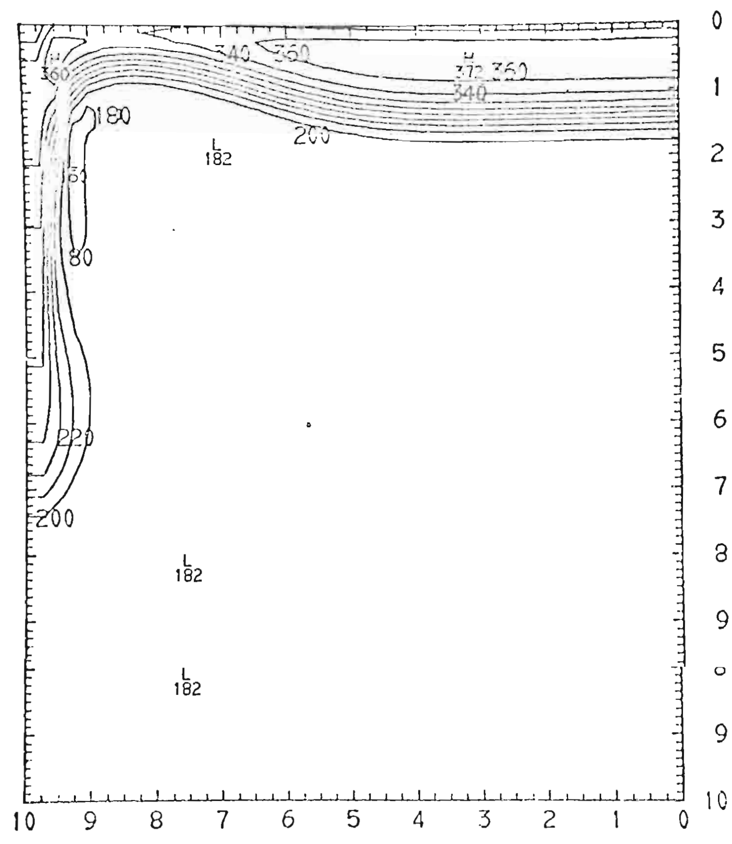

Fig. 27b

At time t = 4, we observe definite zonations in the distribution and concentration of the N, P, Z, and D components. Limiting nutrient has significantly decreased in the euphotic zone. The upwelling of nutrient rich bottom water is evident in Fig. 24a where contour lines indicate an upward advection of water into the euphotic zone. Fig. 24b shows the phytoplankton standing stock at 40 hours. Almost no phytoplankton exists below the euphotic zone, except in regions of strong downwelling at the outer boundary of the shelf. Fig. 25a depicts the highest concentrations of zooplankton in areas where phytoplankton are abundant. Zooplankton continues to decrease in the aphotic zone as the phytoplankton there are grazed to extinction.

The highest concentrations of detritus (Fig. 25b) appear in the euphotic zone. The weakening of the gradient below the euphotic zone is due to the gravitational sinking of detritus.

The steady state P, Z, N, and D standing stock values for phosphate limiting conditions as given by the one box, biological model are

$$P = 0.6190$$

$$Z = 0.2303$$

$$P = 0.6190$$

$$Z = 0.2303$$

$$N = 0.0246$$

$$D = 0.0361$$

$$F = 0.0900$$

These values are being approached by time $t = 8$ (80 hours) in the euphotic zone (Fig. 26 - 27).

The spatial model differs from the one box system in that the biotic components become more concentrated in certain boxes than in others. Each box approaches its own steady state. The concentration of dissolved limiting nutrients (Fig. 26a) for example is greatest in boxes where uptake is nil and regeneration of detritus takes place. Transport of this high concentration into adjacent boxes is dependent on the direction of the circulation pattern. The final steady state within each box is dependent on the biological dynamics occuring within the box, the transport into and out of the box, and the gradient existing between adjacent boxes.

7.3 The Spatial Solutions for an Advected, Nitrate Limiting Sea

The spatial model's response to variation in V_m, N_t, K, and the S parameter was investigated by considering the shelf region to be nitrate limited rather than phosphate limited. The parameter values for this limiting nutrient are given in 6. As solutions to equations
than phosphate limited. The parameter values for this limiting nutrient are given in 6. As solutions to equations

(34) through (37) are highly dependent on the values of these variables, we would expect different values for both the steady state P, Z, N, and D concentrations and their time dependent spatial distributions.

The results are shown in Figures 28 through 29. We begin with the same spatially homogeneous initial values of the biological components as in the phosphate limiting case. We observe major differences in the time dependent solutions.

As in the phosphate limiting case, the model is approaching steady state concentrations for P, Z, N, and D (Fig. 28 -29) by t = 8.0 (160 hours, since V_m for the NO_3 limiting situation is 0.05 hr^{-1}). The steady state values given by the nonspatial biological model using the values of K and N_t for NO_3 are

$$\begin{aligned} P &= 0.6271 \\ Z &= 0.2340 \\ N &= 0.0124 \\ D &= 0.0365 \\ \underline{F} &\underline{= 0.0900} \\ N_t &= 1.000 \end{aligned}$$

Compare Fig. 28b and 26b, the spatial distributions of phytoplankton at t = 8.0 for the two different

Compare Fig. 28b and 26b, the spatial distributions of phytoplankton at t = 8.0 for the two different

Fig. 28a and b. Spatial distribution of the concentration of dissolved limiting nutrient (above) and phytoplankton standing stock (below) at time t = 8.0 for an advected, NO_3 limiting sea. Fig. 28a contours from 0.04 to 0.93, contour interval of 0.05. Fig. 28b contours from 0.0 to 0.68, contour interval of 0.05.

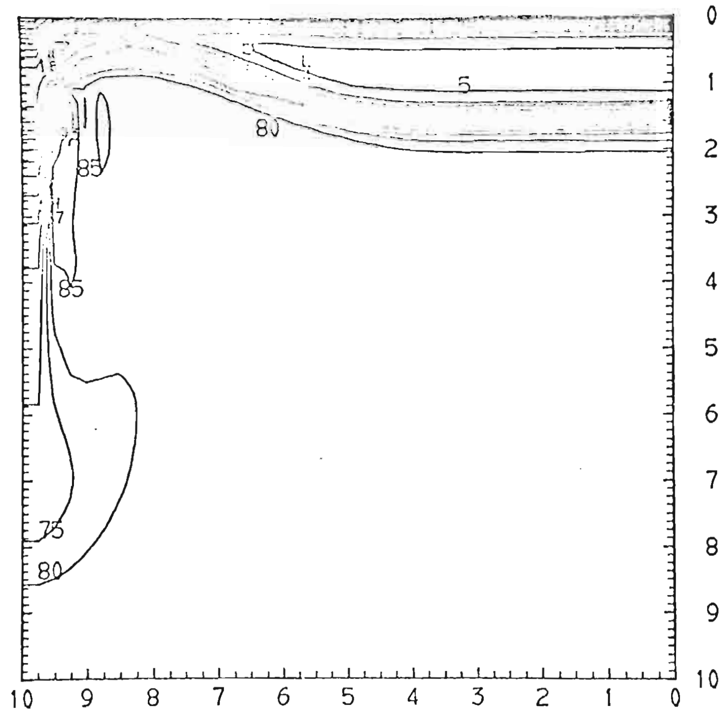

Fig. 28a

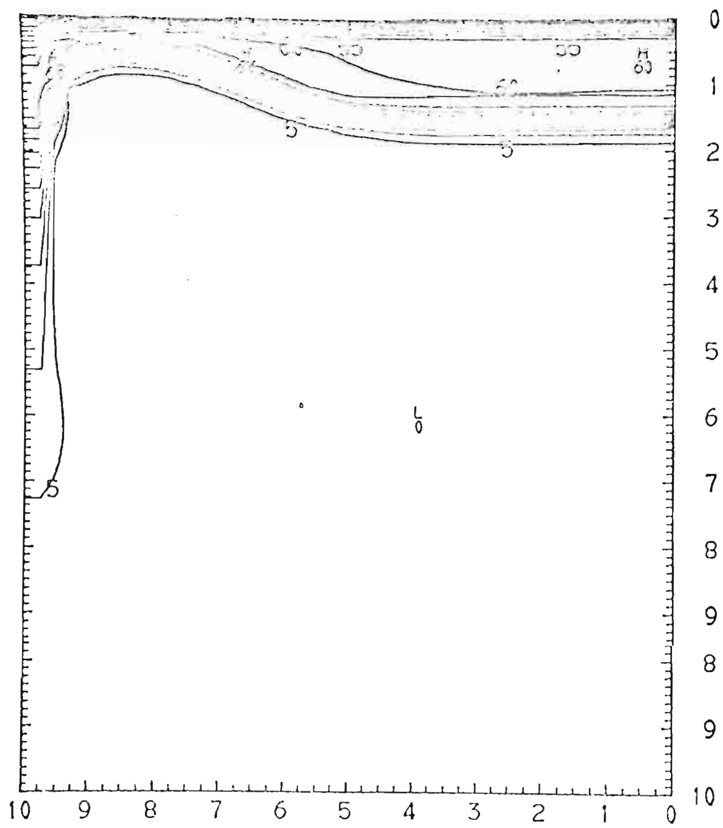

Fig. 28b

Fig. 29a and b. Spatial distribution of the concentration of zooplankton (above) and detritus (below) at time t = 8.0 for an advected, NO_3 limiting sea. Fig. 29a contours from 0.03 to 0.23, contour interval of 0.05. Fig. 29b contours from 0.017 to 0.037, contour interval of 0.002.

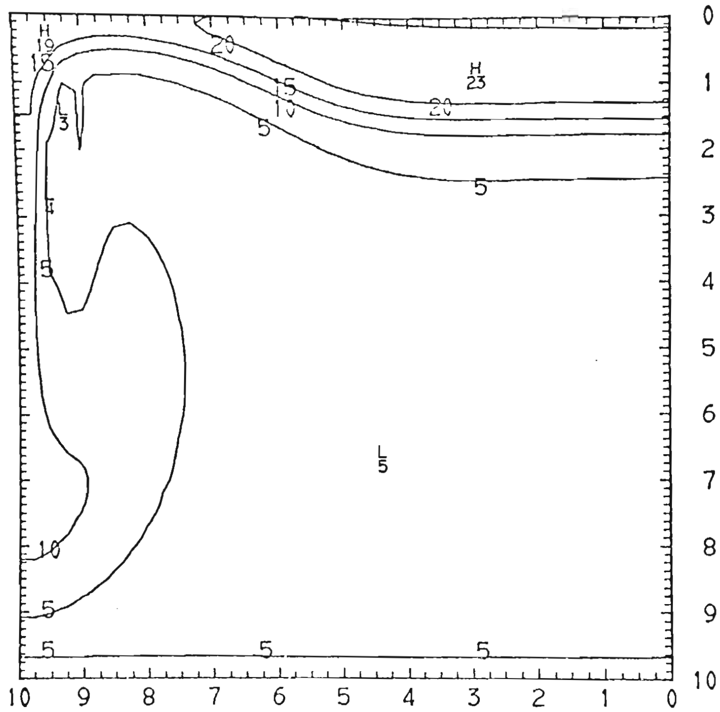

Fig. 29a

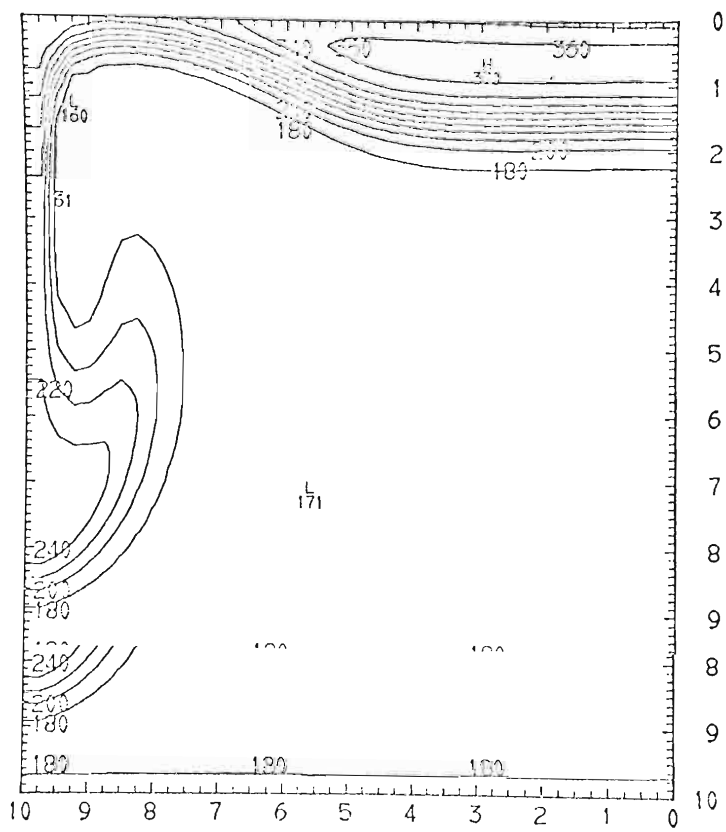

Fig. 29b

nutrient limited cases. We find the phytoplankton euphotic zone concentration is higher in the nitrate limiting case (Fig. 28b) than in the phosphate limiting situation (Fig. 26b). A high of 68% of N_t is found in the region of maximum upwelling of nitrate rich waters as compared to a high level of 62% of N_t in this region in the phosphate case. The higher phytoplankton standing stock results from (1) the slightly lower value of α, enabling the phytoplankton to utilize smaller concentrations of dissolved nutrient, and (2) the greater transport of nutrient rich aphotic zone water into the euphotic zone. The increased width of the gradient band results from an increased rate of diffusion. The extension of the depth to which the phytoplankton are advected below the euphotic zone at the shelf break boundary reflects the increased effect of advection.

A comparison of Fig. 28a and 26a, the two solutions for the dissolved limiting nutrient concentration and distribution at t = 8.0, shows lower N concentrations in the euphotic zone for the nitrate limiting case. This decrease in dissolved nutrient results from its increased uptake by phytoplankton. Zooplankton (compare Fig. 29a

uptake by phytoplankton. Zooplankton (compare Fig. 29a

and 27a) shows higher concentrations in a nitrate limited euphotic zone, a result of the increased phytoplankton standing stock. The greater effects of advection and diffusion in the nitrate limiting sea is made quite evident by the comparison of the spatial distributions of the detritus component at t = 8.0, Fig. 29b and 27b. The increased detritus sinking rate is reflected in the lower depth of the euphotic-aphotic zone gradient band in Fig. 29b.

The response of the spatial model to variation in the parameters V_m, K, N_t, and S is complicated. Different spatial distributions of the biotic components result as advection, scaled by S, and diffusion, scaled by V_m become important. Localities of upwelling of nutrient rich bottom waters show greater phytoplankton and zooplankton production. The steady state standing stock of phytoplankton is dependent on the efficiency of the nutrient uptake parameter K. And finally, the biological turnover rate V_m specifies the time scale of the biological processes such as growth, death, excretion, and regeneration. These variations collectively account for the differences in the phosphate and nitrate spatial solutions after the same elapsed model time.

time.

8. CRITIQUE

We have constructed a time dependent, physical-chemical-biological spatial model of the concentration of the biologically limiting nutrient within the lower marine trophic levels of a continental shelf ecosystem. A theoretical circulation pattern is employed to advect and diffuse the phytoplankton, zooplankton, detritus, and limiting nutrient dissolved in the water column.

An evaluation of the model as an approximation of the real world is in order. The major strength of the model is the formulation of numerous physical and biological processes into a workable framework. A weakness is the knowledge of correct expressions and parameter values which describe the real world ecosystem. A sensitivity analysis indicates which of the included processes strongly influence the system, but we have no measure other than the realism of the solutions of the correctness of the expressions.

Yet our model is encouraging. Reasonable biological production and ecological efficiencies can be simulated using the formulations presented. Spatial distributions of the biotic components simulate zones of biological activity on the mesoscale (10-100 km) x-z plane.

of the biotic components simulate zones of biological activity on the mesoscale (10-100 km) x-z plane.

The limitation of the model is in simulating the complexity of the actual ecosystem. Species composition of the trophic levels is not specified. The food chain is confined to primary and secondary producers with an omnivorous tertiary level. The mobility of fish biomass is neglected. Temperature effects on the biological rates is ignored. Model solutions are toward a steady state, while the real system is in constant flux. More realistic circulation patterns are required by this type of model, as spatial distributions of the biological components are very dependent on advection, especially in nutrient limited seas experiencing upwelling.

The predictive ability of this type of model in locating concentrations of marine food resources is a fundamental goal. A feedback between model theory and field observations is essential. This feedback is a major objective of the Coastal Upwelling Ecosystem Analysis (CUEA) program of the National Science Foundation-International Decade for Ocean Exploration (NSF-IDOE).

9. SUMMARY

The flow of the biologically limiting nutrient through the lower trophic levels of a marine ecosystem has been investigated. A time dependent, spatial model of the distribution of the biological components is constructed which incorporates a theoretical circulation pattern for the West Florida continental shelf region.

A zone of maximum phytoplankton and zooplankton production is located slightly shoreward of the shelf break at the area of maximum upwelling. The model response to increased upwelling is greater phytoplankton and zooplankton standing stocks. Advection of plankton below the euphotic zone occurs in a region of downwelling over the shelf break.

Acceptable food chain ecological efficiencies (approx. 20%) of zooplankton and fish production are attained by the model. Five times as much phytoplankton are produced than zooplankton.

A sensitivity analysis indicates the system is most responsive to changes in the zooplankton dynamics. The model experiences greatest displacements from equilibrium due to variations in the zooplankton grazing, excretion and death parameters. Fish predation
equilibrium due to variations in the zooplankton grazing, excretion and death parameters. Fish predation
is also very important.

The formulation of this model has evolved a parameter S, whose value is dependent on the biological kinetics and organized water motion of a specific area. This parameter scales the effects of advection and diffusion relative to the rate of biological turnover in determining the spatial solutions. The Michaelis-Menton parameter V_m is shown to be a fundamental time scale to which both physical and biological processes can be related.

APPENDIX I

OBSERVATIONAL DATA

In an effort to gain as much information about the model area as possible, Mr. Wroblewski participated in the EGMEX V (Eastern Gulf of Mexico Exploration) program of the State University System of Florida Institute of Oceanography (SUSIO). Sampling of the research area was performed aboard the Research Vessel BELLOWS during mid November, 1971. The portion of the cruise applicable to this study consisted of two parallel transects running due west from Florida's Charlotte Harbor between 83°54' W and 84°39' W longitudes at 27°15' N latitude and between 83°25' W and 84°26' W longitude at 26°45' N latitude (see Fig. 2).

The water over the West Florida continental shelf was sampled in depth profiles for concentrations of chlorophyll a, nitrate-nitrite, ammonia, and water reactive phosphate. Chlorophyll a was regarded as an indicator of phytoplankton standing stock, and the concentrations of NO_3, NH_4, and PO_4 were considered measurements indicative of nutrient availability.

concentrations of NO_3, NH_4, and PO_4 were considered measurements indicative of nutrient availability.

The area sampled was assumed experiencing slow upwelling affected by the presence of the Loop Current off the continental shelf break. Conditions were similar to past seasons when observations indicated upwelling was taking place (Austin, 1971; Bogdanov, 1963; Collier, 1958).

Shallow stations (less than 40 meters) close to shore showed no stratification. However, a thermocline existing between 45 and 55 meters was found for deeper stations over the shelf. Coastal stations registered Secchi disk readings of approximately 13 meters with Secchi depths increasing seaward. Shelf break stations #5 and #9 registered Secchi readings of 20 meters.

Chlorophyll a data for the two transects are shown in Fig. 30 - 31. Fluorometric chlorophyll a calculations were based on the methods given in Strickland and Parsons (1968). From the data it appears the shelf area is moderately productive, with from 0.19 to 0.41 mg chlor a $/m^3$ occuring in the euphotic zone above the thermocline. From Stations #2 to #5 and from #6 to #8 there appeared to be consistently higher

#6 to #8 there appeared to be consistently higher
concentrations of chlorophyll a in the water samples

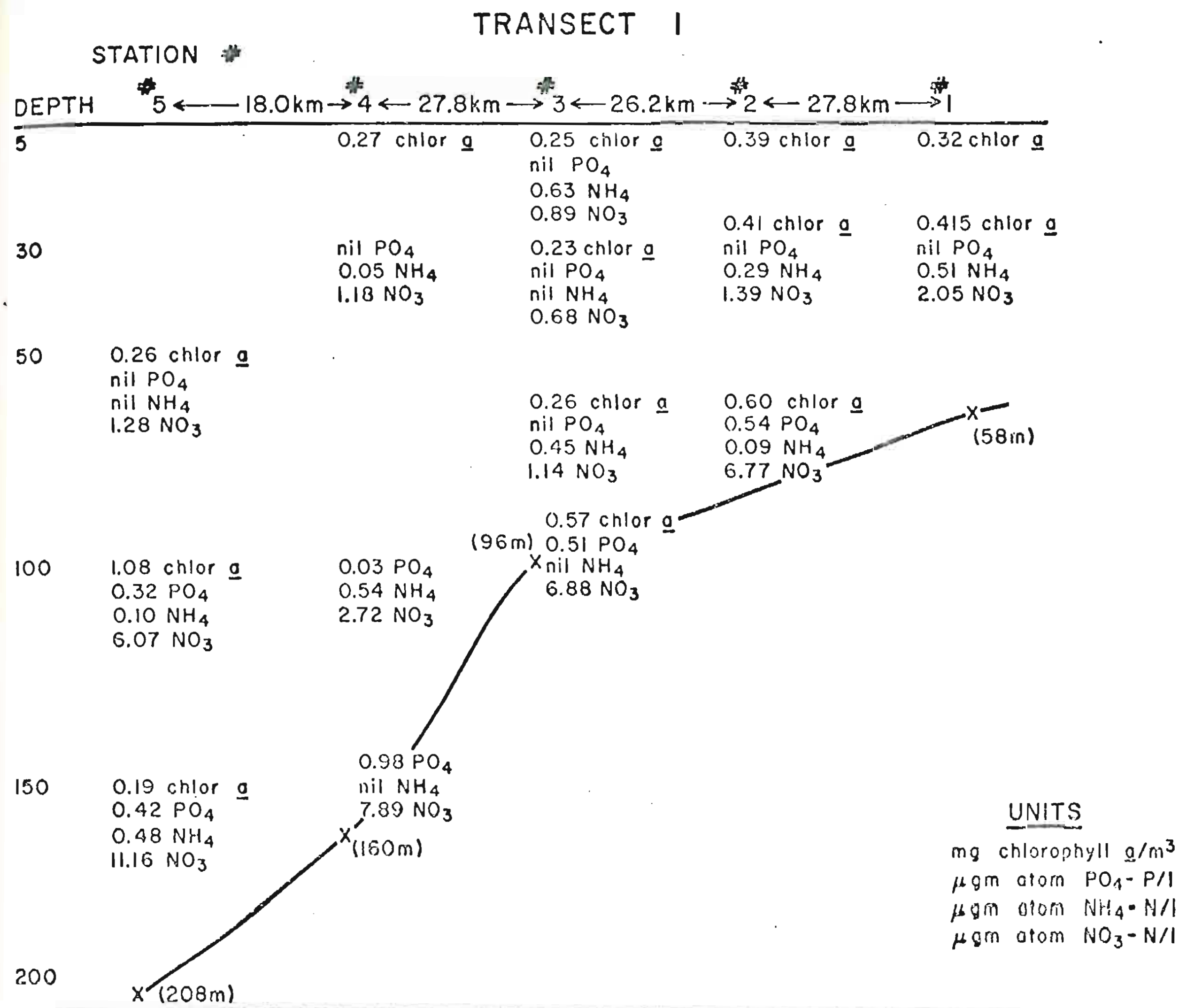

Fig. 30 Transect 1 run from 83° 25' W to 84° 26' W longitude at 26° 45' N latitude (see Fig.2) showing the depth profiles of the chlorophyll *a* and nutrient concentration data collected during November,1971.

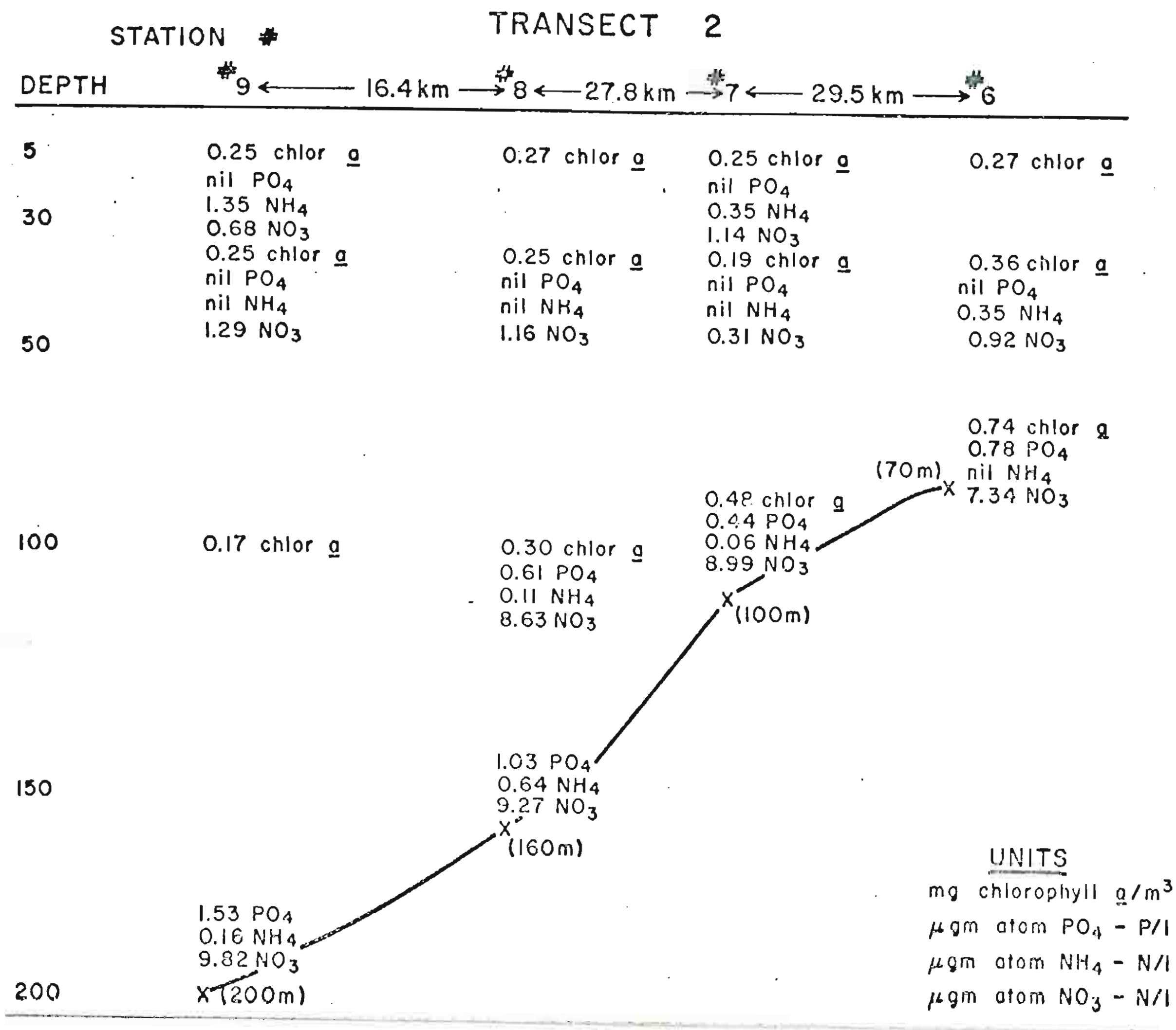

Fig. 31 Transect 2 run from 83° 54' W to 84° 39' W longitude at 27° 15' N latitude (see Fig. 2) showing the depth profiles of the chlorophyll a and nutrient concentration data collected during November, 1971.

below the thermocline. An anomaly occurred at Station #5 at a depth of 100 meters with 1.08 mg chlor a / m^3 being present. Similar anomalies were found by Steele (1964) and Collier (1958) who attributed the high measurements to changes in the carbon/ chlorophyll a ratio in the phytoplankton population. Thus chlorophyll a measurements may be a poor indicator of phytoplankton biomass.

On the other hand the model presented in this study provides a mechanism whereby the phytoplankton may be advected to this depth. The high chlorophyll a concentrations may be an indicator of downwelling off the shelf break.

Of particular interest is the nutrient availability data. Phosphate, nitrate, and ammonia determinations were performed by spectrophotometric techniques. The method of Solorzano (1969) was used in NH_4 determinations. Water reactive phosphate was analyzed according to the technique of Murphy and Riley as presented in Strickland and Parsons (1968). Nitrate-nitrite analysis followed the procedure given in Strickland and Parsons (1968).

Strickland and Parsons (1968).

Concentrations of PO_4 were below measurable levels (0.01 μgm atom/liter) in water samples taken above the thermocline. Nitrate and ammonia were present in concentrations below those specified as V_m concentrations (Thomas, 1970; Thomas and Dodson, 1969). These data indicate the shelf waters are indeed nutrient limited, with phosphate possibly in shortest supply. Nitrate levels are low enough for NO_3 to be a possible limiting nutrient. Shelf break stations (Fig. 30 - 31) held higher values of PO_4 (0.93 to 1.53 μgm atom PO_4-P/liter) and NO_3 (9.82 to 11.16 μgm atom NO_3-N/liter) at depths of 150 meters, which supports the spatial model assumption that nutrient rich bottom water is available from below the shelf break.

The model values chosen for N_t, the average amount of limiting nutrient in the shelf ecosystem, were based on the total PO_4-P and NO_3-N concentrations reported by Collier (1958) for the deeper waters off the shelf break. Samples taken at 85°57' W longitude and 27°00' N latitude showed concentrations of total phosphate increasing from 0.6 μgm atom PO_4-P/liter at the surface to 4.0 μgm atom PO_4-P/liter at a depth of 2100 meters. Nitrate concentra-
0.6 μgm atom PO_4-P/liter at the surface to 4.0 μgm atom
PO_4-P/liter at a depth of 2100 meters. Nitrate concentra-
tion also increased with depth from essentially zero

concentration at the surface to 30 μgm atom NO_3-N/liter at 2100 meters. It was assumed these highest nutrient concentrations are approximately the total amount of phosphate and nitrate available in these waters.

The basic difference between the spatial model simulations and the observational data may have resulted from the time of sampling. The model's circulation pattern assumes a homogeneous ocean, as does the spatial model solutions. Observations were made during a stratified situation. However, bathythermograph measurements taken on SUSIO Cruise #7201 from February 2 - 11, 1972 verify complete mixing of model area waters by late winter.

The value of the observational data lies in the verification of nutrient limiting conditions existing in the model region. The low observed concentrations of phosphate and nitrate indicate these nutrients may be limiting. The V_m, K, N_t, and S parameter values for these nutrients were then used in the spatial model.

APPENDIX II

FINITE DIFFERENCE SCHEMES

This study is concerned with the quantitative description of complicated time dependent processes. The equations predicting the steady state flow field (28) - (30) and those governing the spatial, physical-chemical-biological system (34) - (37) have been developed in 5. These equations are solved numerically. The following is a description of the general procedure.

We create a grid mesh by dividing the cross section of the study area (Fig. 7) into 41 by 82 rectangles in the x and z directions respectively. The vertical grid lines in the x direction are indexed by the letter j and the horizontal lines in the z direction by the letter k. Time is denoted by the index, m. Thus $P^m_{j,k} = P(m\Delta t, j\Delta x, k\Delta z)$ and similarly for the other variables. The steady state values of the u and v velocities are found using the over-relaxation technique (Issacson and Keller, 1966).

In the spatial, time dependent, physical-chemical-biological model, the concentration of a biotic component such as phytoplankton is calculated by considering the amount present in the grid box, the concentration in adjacent boxes, the transport into and out of the box,
the amount present in the grid box, the concentration in adjacent boxes, the transport into and out of the box,

and the biological dynamics occuring within the box. Let us consider a simplified version of (34) describing the concentration of phytoplankton, P(t ,x ,z), where all the biological terms are included in the symbol B,

$$\frac{\partial P}{\partial t} = -S\left(\frac{\partial uP}{\partial x} + \frac{\partial wP}{\partial z}\right) + \nu_h \frac{\partial^2 P}{\partial x^2} + \nu_v \frac{\partial^2 P}{\partial z^2} + B$$

The advection terms are written in flux form by using the continuity equation (30). The change of the phyto-plankton in the center of the box is dependent on the P concentration at its nearest 4 grid neighbors. We refer to the stencil shown in Figure 32. Notice that the values of the u velocities are stored at grid corners, the w velocities at the center of the grid walls, and the calculated average concentrations of P, Z, D, and N at the center of the grid box.

The time difference formulation of the finite difference scheme where the concentration of the biotic component is calculated at the center of the box is:

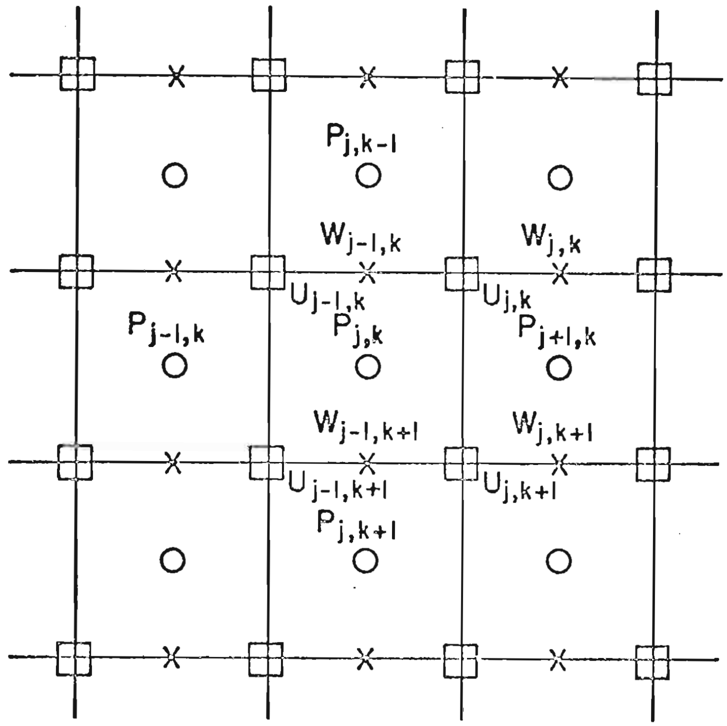

Fig. 32 Stencil showing the grid point location of the u (squares) and w (crosses) velocities and the biotic component P (circles) concentration used in integrating the spatial, physical-chemical-biological model. The vertical grid lines in the x direction are indexed by the letter j and the horizontal lines in the z direction by the letter k.

in the z direction by the letter k.

$$P_{j,k}^{m+1} = P_{j,k}^{m-1} - \frac{\Delta t}{2\Delta x}\left[\overline{u}^{z}\,\overline{P}^{x}\right]_{j,k}^{m} - \frac{\Delta t}{\Delta z}\left[w\,\overline{P}^{z}\right]_{j,k}^{m}$$

$$+ \frac{2\Delta t\,\nu_h}{(\Delta x)^2}\left[P_{j+1,k}^{m} + P_{j-1,k}^{m} - 2P_{j,k}^{m-1}\right]$$

$$+ \frac{2\Delta t\,\nu_v}{(\Delta z)^2}\left[P_{j\,k+1}^{m} + P_{j,k-1}^{m} - 2P_{j,k}^{m-1}\right]$$

$$+ 2\Delta t\,B_{j,k}^{m-1}$$

where the advective terms, are defined as

$$\left[\overline{u}^{z}\,\overline{P}^{x}\right]_{j,k} \equiv \left[(u_{j,k} + u_{j,k+1})(P_{j+1,k} + P_{j,k}) - (u_{j-1,k} + u_{j-1,k+1})(P_{j-1,k} + P_{j,k})\right]$$

and

$$\left[w\,\overline{P}^{z}\right]_{j,k} \equiv \left[w_{j-1,k}\,(P_{j,k} + P_{j,k-1}) - w_{j-1,k+1}\,(P_{j,k} + P_{j,k+1})\right]$$

The advective scheme is a quadratic conservative finite difference method recommended by Grammeltvedt (1969).

difference method recommended by Grammeltvedt (1969).

The time dependent, spatial phytoplankton dynamics represented by the symbol B may be defined as

$$B^{m-1}_{j,k} \equiv (P^{m-1}_{j,k} N^{m-1}_{j,k})/(\alpha + N^{m-1}_{j,k}) - \beta P^{m-1}_{j,k}$$
$$- \epsilon_Z \left[1 - \exp(-\delta_P P^{m-1}_{j,k})\right] Z^{m-1}_{j,k}$$
$$- \phi F \left[\theta P^{m-1}_{j,k} / (\theta P^{m-1}_{j,k} + Z^{m-1}_{j,k})\right]$$

When advection and diffusion are neglected this reduces to the common Euler method.

The maximum time step allowed by linear computational stability is difficult to determine exactly for this complicated model. However necessary conditions for stability are

$$\Delta t < \frac{\Delta x}{\sqrt{2}\, u_{max}} \quad ; \quad u_{max} = \max_{j,k,m} |S u|$$

$$\Delta t < \frac{\Delta z}{\sqrt{2}\, w_{max}} \quad ; \quad w_{max} = \max_{j,k,m} |S w|$$

$$\Delta t < \frac{(\Delta x)^2}{8 \nu_h} \quad ; \quad \Delta t < \frac{(\Delta z)^2}{8 \nu_v}$$

$$\Delta t < \frac{(\Delta x)^2}{8 \nu_h} \quad ; \quad \Delta t < \frac{(\Delta z)^2}{8 \nu_v}$$

In this model the advective criteria are the more stringent.

APPENDIX III

LIST OF SYMBOLS

A_h constant horizontal eddy viscosity, cm^2 sec^{-1}

A_v constant vertical eddy viscosity, cm^2 sec^{-1}

b' width of the continental shelf, km

B coefficient of phytoplankton extracellular release, hr^{-1}

C typical horizontal water velocity, cm sec^{-1}

d' average depth of the continental shelf waters, m.

d_D natural death coefficient of zooplankton, hr^{-1}

d_P constant defining the rate of zooplankton grazing with phytoplankton concentration, conc.$^{-1}$

D detritus conponent, conc.

E_D coefficient of zooplankton grazing on detritus, conc.$^{-1}$ hr^{-1}

E_Z maximum zooplankton phytoplankton-dependent grazing coefficient, hr^{-1}

$E(z)$ nondimensional phytosynthesis-depth function

f Coriolis parameter, sec^{-1}

F pelagic fish component, conc.

g acceleration of gravity, cm sec^{-2}

H fish excretion coefficient, hr^{-1}

j finite differencing index in the x direction

k finite differencing index in the z direction

j finite differencing index in the x direction

k finite differencing index in the z direction

K Michaelis-Menton constant, conc.

ℓ — coefficient of bacterial decomposition rate of detritus, hr^{-1}

N — biologically limiting nutrient component, conc.

N_t — average total amount of limiting nutrient on the continental shelf, amongst all biotic components, conc.

P — phytoplankton component, conc.

P* — concentration of phytoplankton at which zooplankton grazing begins, conc.

Q — average daily amount of the limiting nutrient grazed by one zooplankton, conc. day^{-1} $zooplankter^{-1}$

R_o — Rossby number, $R_o = C\ (A_h\ f)^{-\frac{1}{2}}$

S — nondimensional parameter which categorizes the importance of advection and disorganized water motion in determining the spatial distributions of the biotic components,

$$S = \frac{C}{V_M\ (Ah/f)^{\frac{1}{2}}}$$

t' — time, hr.

Δt — time increment in the numerical integration

u' — x directed component of water velocity, cm sec^{-1}

v' — y directed component of water velocity, cm sec^{-1}

V_M — maximum rate of limiting nutrient uptake by phytoplankton; doubling rate of phytoplankton per 24 hours, hr^{-1}

w' — vertical component of water velocity, cm sec^{-1}

w_s' — average sinking velocity of detritus, cm sec^{-1}

w' — vertical component of water velocity, cm sec^{-1}

w_s' — average sinking velocity of detritus, cm sec^{-1}

x', y', z'	tangent plane Cartesian coordinate; x positive eastward; y positive northward; z positive upward, cm.
Δx	horizontal grid increment
Δz	vertical grid increment
Z	zooplankton component, conc.
Z_n	average number of zooplankton per unit volume
Γ'	zooplankton excretion coefficient, conc.$^{-1}$
ζ'	the deviation of the sea surface from mean sea level, cm.
θ	fish gillraker efficiency coefficient, percent
ν_h'	horizontal eddy diffusivity, cm^2 sec^{-1}
ν_v'	vertical eddy diffusivity, cm^2 sec^{-1}
Φ	fish grazing coefficient hr.$^{-1}$
ψ	streamfunction, cm^2 sec.$^{-1}$
τ'	one day, hr.

REFERENCES

Austin, H. M. 1971. The characteristics and relationships between the calculated geostrophic current component and selected indicator organisms in the Gulf of Mexico Loop Current System. Doctoral Dissertation. Florida State University. 258 pp.

Bogdanov, D. W., V. A. Sokolov, and M. S. Khromov, 1968. Regions of high biological and commercial productivity in the Gulf of Mexico and Caribbean Sea. Oceanology 8(3): 371-381.

Caperon, J. 1967. Population growth in microorganisms limited by food supply. Ecology, 48: 715-722.

Chew, F. 1955. On the offshore circulation and a convergence mechanism in the red tide region off the west coast of Florida. Trans. Amer. Geophys. Union, 36(6): 963-974.

Collier, A. 1958. Gulf of Mexico physical and chemical data from Alaska cruises. U.S. Dept. of Interior, Fish and Wildlife Service, Special Scientific Report: Fisheries 249. 417 pp.

Corner, E. D. S. and C. B. Cowey. 1964. Some nitrogenous constituents of the plankton. Oceanogr. Mar. Biol. Ann. Rev., 2: 147-167.

Curl, H. 1962. Standing crops of carbon, nitrogen, and phosphorus and transfer between trophic levels in continental shelf waters south of New York. Rapp. Proc. Verb. Cons. Perm. Int. Explor. Mer. 153: 183-189.

Cushing, D. H. 1959. The seasonal variation in oceanic production as a problem in population dynamics. J. Cons. Explor. Mer. 24: 455-464.

Cushing, D. H. 1962. An alternative method of estimating the critical depth. J. Cons. Explor. Mer., 27: 131-140.

the critical depth. J. Cons. Explor. Mer., 27: 131-140.

Cushing, D. H. 1963 a. Studies on a Calanus patch. II. The estimation of algal production rates. J. Mar. Biol. Ass. U. K. 43: 339-47.

Cushing, D. H. 1963 b. Studies on a Calanus patch. V. The production cruises in 1954: Summary and conclusions. J. Mar. Biol. Ass. U. K. 43: 387-389.

Cushing, D. H. 1969. Models of the productive cycle in the sea. Morning Review Lectures of the Second International Oceanographic Congress. Paris, UNESCO. p. 103-115.

Davidson, R. S. and A. B. Clymer. 1966. The desirability and applicability of simulating ecosystems. Ann. N.Y. Acad. Sci. 128:790-4.

Ditoro, D. M., D. J. O'Connor, R. V. Thomann. 1970. A dynamic model of phytoplankton populations in natural waters. Envir. Engr. Sci. Prog. Manhatton College, Bronx, NY. 62 pp.

Dugdale, R. C. 1967. Nutrient limitations in the sea: dynamics, identification, and significance. Limnol. Oceanog. 12: 685-695.

Dugdale, R. C. and J. J. Goering, 1967. Uptake of new and regenerated nitrogen in primary productivity. Limnol. Oceanogr. 12, 196-206.

Dugdale, R. C. and J. J. MacIsaac. 1971. A computation model for the uptake of nitrate in the Peru upwelling region. Inv. Pesq. 31(5): 299-308.

Eppley, R. W., and J. L. Coatsworth. 1968. Uptake of nitrate and nitrite by Ditylum brightwellii - kinetics and mechanisms. J. Phycol. 4: 151-156.

Eppley, R. W., J. N. Rogers, and J. J. McCarthy. 1969. Half saturation constants for uptake of nitrate and ammonium by marine phytoplankton. Limnol. Oceanog., 14: 912-920.

Fleming, R. H. 1939. The control of diatom populations by grazing. J. Cons. Explor. Mer., 14: 210-227.

Fogg, G. E. 1966. The extracellular products of algae.
by grazing. J. Cons. Explor. Mer., 14: 210-227.

Fogg, G. E. 1966. The extracellular products of algae. In H. Barnes (ed.) Oceanog. Mar. Biol. Ann. Rev., V. 4, George Allen and Univin Ltd., London. pp. 195-212.

Gerking, S. D. 1962. Production and food utilization in a population of bluegill sunfish. Ecol. Monogr. 32:31-78.

Grammeltvedt, A. 1969. A survey of finite-difference schemes for the primitive equations of a barotrophic fluid. Mon. Wea. Rev., 97:384-404.

Gulland, J. A. 1970. Food chain studies and some problems in world fisheries. in J. H. Steele (ed.), Marine Food Chains, U. of Calif. Press, Berkeley pp. 296-315.

Henrici, P. 1964. Elements of Numerical Analysis. John Wiley and Sons, New York. pp. 271-275.

Hsueh, Y. and J. J. O'Brien, 1971. Steady coastal upwelling induced by an along-shore current. J. Phys. Oceanog. 1:180-186.

Isaacson, E. and H. B. Keller, 1966. Analysis of Numerical Methods. John Wiley and Sons, New York. pp. 467.

Iverson, R. L. 1972. A systems approach to pelagic ecosystem dynamics in an estuarine environment. Doctoral Dissertation. Corvallis, Oregon State University. 107 pp.

Ivlev, V. S. 1945. The biological productivity of waters. Vsp. sovrem. Biol., 19(1):88-120.

Kierstead, H., and L. B. Slobodkin. 1953. The size of water masses containing plankton blooms. J. Mar. Res., 12:141-7.

Kozlovsky, D. G. 1968. A critical evaluation of the trophic level concept. I. Ecological efficiencies. Ecology Vol. 49(1):48-59.

Larkin, P. A. 1964. Canadian lakes. Verh. Int. Verein. Limnol., 15:76-90.

Lasker, R. 1970. Utilization of zooplankton energy by a Pacific sardine population in the California [illegible] Marine Food Chains.

Lasker, R. 1970. Utilization of zooplankton energy by a Pacific sardine population in the California current. in J. H. Steele (ed.) Marine Food Chains, U. of Calif. Press, Berkley, pp. 265-283.

Leipper, D. F., 1970. A sequence of current patterns in the Gulf of Mexico. J. Geophys. Res. 75: 637-658.

Lindeman, R. L. 1942. The trophic dynamics aspect of ecology. Ecology, Vol. 23 (4): 399-418.

Lotka, A. J. 1925. Elements of Physical Biology. Williams and Wilkins, Baltimore. (Also issued as Elements of Mathematical Biology. A. J. Lotka (1956) Dover Publications, Inc. New York. 465 P.).

Macfadyen, A. 1964. Energy flow in ecosystems and its exploitation by grazing. In D. Crisp (ed.), Grazing in terrestrial and marine environments. Blackwell, Oxford.

MacIsaac, J. J., and R. C. Dugdale. 1969. The kinetics of nitrate and ammonia uptake by natural populations of marine phytoplankton. Deep-Sea Res., 16: 415-422.

Mann, K. H. 1969. The dynamics of aquatic ecosystems. Adv. Ecol. Res. 6: 1-81.

McAllister, C. D. 1970. Zooplankton rations, phytoplankton mortality and the estimation of marine production. In J. H. Steele (ed.), Marine Food Chains, Univ. of Calif. Press, Berkeley. pp. 419-457.

Monod, J. 1942. Recherches sur la croissance de cultures bacteriennes. Hermann, Paris. 210 pp.

Murphy. G. I. 1962 Effect of mixing depth on the productivity of freshwater impoundments. Trans. Amer. Fish. Soc. 91: 69-76.

O'Brien, J. J., and J. S. Wroblewski. 1972. On advection in phytoplankton models. J. Theor. Biology. In press.

O'Brien, W. J. 1972. A model demonstrating the development of a single factor limiting phytoplankton algae. Presented at the 35th. Annual Meeting Amer. Soc.

O'Brien, W. J. 1972. A model demonstrating the development of a single factor limiting phytoplankton algae. Presented at the 35th. Annual Meeting Amer. Soc. Limnol. and Oceanog., Tallahassee, Fl.

O'Connor, J. S. and B. C. Patten, 1968. Mathematical models of plankton productivity. Reservoir Fishery Resources Symposium, Amer. Fish. Soc. Publ., Wash. D.C. pp. 207-228.

Odum, E. P. 1962. Relationships between structure and function in the ecosystem. Jap. J. Ecol. 12: 108-118.

Odum, H. T. 1957. Trophic structure and productivity of Silver Springs, Florida. Ecol. Monogr. 27: 55-112.

Odum, H. T. and E. P. Odum. 1955. Trophic structure and productivity of a windward coral reef community on Eniwetok Atoll. Ecol. Monogr., 25: 291-320.

Paloheimo, J. E. and L. M. Dickie. 1970. Production and food supply. In J. H. Steele (ed.) Marine Food Chains U. of Calif. Press, Berkley. pp. 499-527.

Parsons, T. R., LeBrasseur, R. J., and J. D. Fulton. 1967. Some observations on the dependence of zooplankton grazing on cell size and concentration of phytoplankton blooms. J. Oceanogr. Soc. Japan, 23(1): 10-17.

Parsons, T. R., R. J. LeBrasseur, J. D. Fulton, and O.D. Kennedy. 1969. Production studies in the Strait of Georgia. Part II. J. Exp. Mar. Biol. and Ecology, 3: 39-50.

Patten, B. C. 1961. Negentropy flow in communities of plankton. Limnol. Oceanogr., 6: 26-30.

Patten. B. C. 1966. The biocoenetic process in an estuarine phytoplankton community. ORNL - 3946 UC-48, Oak Ridge National Laboratory. 95 pp.

Patten, B. C. 1968. Mathematical models of plankton production. Int. Rev. ges. Hydrobiol. 53(3): 357-408.

Patten, B. C. 1969. Ecological systems analysis
357-408.

Patten, B. C. 1969. Ecological systems analysis and fisheries science. Trans. Amer. Fish. Soc. 98(3): 570-581.

Patten, B. C. (ed.) 1971. Systems Analysis and Simulation in Ecology. Vol. 1. Academic Press, New York. pp. 365.

Pielou, E.C. 1969. An Introduction to Mathematical Ecology. John Wiley and Sons, New York. 286 pp.

Rawson, D. S. 1961. A critical analysis of the limnological variables used in assessing the productivity of northern Saskatchewan lakes. Verb. Int. Verein. Limnol., 14:160-166.

Raymont, J. E. G. 1966. The production of marine phytoplankton. Adv. Ecol. Res. 3:117-204.

Riley, G. W. 1946. Factors controlling phytoplankton population on Georges Bank. J. Mar. Res., 6: 54-73.

Riley, G. A. 1947 a. Seasonal fluctuations of the phytoplankton population in New England coastal waters. J. Mar. Res., 6:114-125.

Riley, G. A. 1947 b. A theoretical analysis of the zooplankton population of Georges Bank. J. Mar. Res., 6:104-113.

Riley, G. A. 1963. Theory of food-chain relations in the ocean. In M. N. Hill (ed.), The Sea, Vol. 2, Interscience Publishers, New York. pp. 438-463.

Riley, G. A. 1965. A mathematical model of regional variations in plankton. Limnol. Oceanogr., 10(Suppl.): R202-15.

Riley, G. A., H. Stommel, and D. F. Bumpus. 1949. Quantitative ecology of the plankton of the Western North Atlantic. Bull Bingham Oceanog. Coll. 12(3):1-169.

Riley, G. A., and R. Von Arx. 1949. Theoretical analysis of seasonal changes in the phytoplankton of Husan Harbor, Korea. J. Mar. Res., 8:60-72.

analysis of seasonal changes in the phytoplankton of Husan Harbor, Korea. J. Mar. Res., 8:60-72.

Russel-Hunter, W. D. 1970. Aquatic Productivity. Collier Macmillan Ltd., London. pp. 52.

Ryther, J. H. 1963. Geographic variation in productivity. In M. N. Hill (ed.), The Sea Vol. 2. Interscience Publishers, New York, pp. 347-380.

Ryther, J. H. 1969. Photosynthesis and fish production in the sea. Science, 166:72-76.

Schaeffer, M. B. 1965. The potential harvest of the sea. Trans. Amer. Fish. Soc. 94:123-8.

Slobodkin, L. B. 1960. Ecological energy relationships at the population level. Am. Nat., 94:213-236.

Slobodkin, L. B. 1962. Energy in animal ecology. Adv. Ecol. Res. 1:69-101.

Smith, E. L. 1936. Photosynthesis in relation to light and carbon dioxide. Proc. Nat. Acad. Sci., Wash., 22:504-511.

Smith, F. E. 1970. Analysis of ecosystems. In D. E. Reichle (ed.) Ecological Studies-Analysis and Synthesis Vol. I. Springer-Verlag, New York. pp. 7-18.

Solorzano, L. 1969. Determination of ammonia in natural waters by the phenolhypochlorite method. Limnol. and Oceanog. 14:799-801.

Steele, J. H. 1956. Plant production on the Fladen Ground. J. Mar. Biol. Ass. U. K. 35:1-33.

Steele, J. H. 1958. Plant production in the northern North Sea. Rapp. Cons. Explor. Mer., 144:79-84.

Steele, J. H. 1959. The quantitative ecology of marine phytoplankton. Biol. Rev., 34:129-158.

Steele, J. H. 1964. A study of production in the Gulf of Mexico. J. Mar. Res. 22(3):211 222.

Strickland, J. D. H. 1960. Measuring the production of
of Mexico. J. Mar. Res. 22(3):211 222.

Strickland, J. D. H. 1960. Measuring the production of marine phytoplankton. Bull. Fish. Res. Bd. Canada, No. 122, pp. 122-131.

Strickland, J. D. H. and T. R. Parsons. 1968. A practical handbook of seawater analysis. Fish. Res. Board Can., Bull. 167, 311 pp.

Sverdrup. H. U. 1953. On conditions for the vernal blooming of phytoplankton. J. Cons-Explor. Mer. 18:287-295.

Talling, J. F. 1957. The phytoplankton population as a compound photosynthetic system. New Phytol. 56:133-149.

Tansley, A. G. 1935. The use and abuse of vegetational concepts and terms. Ecology 16:284-307.

Teal, J. M. 1962. Energy flow intthe salt marsh ecosystem of Georgia. Ecology 43:614-624.

Thomas, W. H. 1970. Effect of ammonium and nitrate concentration on chlorophyll increases in natural tropical Pacific phytoplankton populations. Lmnol. Oceanogr. 15:386-394.

Thomas, W. H. and A. N. Dodson. 1968. Effects of phosphate concentration on cell division rates and yield of a tropical oceanic diatom. Bio. Bull. 134:199-208.

Tomovic. R. 1963. Sensitivity Analysis of Dynamic Systems. McGraw-Hill, New York. 140 pp.

Van Dyne, G. M. 1969. Implementing the ecosystem concept in training in the natural resources sciences. In G. M. Van Dyne (ed.) The Ecosystem Concept in Natural Resource Management, Academic Press, New York. pp. 328-365.

Verhoff, F. H. 1971. Theoretical analysis of a conserved nutrient ecosystem. J. Theor. Biol. 33: 131-147.

Volterra, V. 1926. Variations and fluctuations of the number of individuals in animal species living 131-147.

Volterra, V. 1926. Variations and fluctuations of the number of individuals in animal species living together. (Translated into English by M. E. Wells.) J. Cons. Explor. Mer. 3:1-51.

Walsh, J. J. and P. B. Bass. 1971. OCEANS, a seagoing simulation program. Upwelling Biome Technical Series, Special Report No. 48, Dept. of Oceanog., Univ. of Wash. Seattle, Wash., 46 pp.

Walsh, J. J. and R. C. Dugdale. 1971. A simulation model of the nitrogen flow in the Peruvian upwelling system. Inv. Pesq. 35(1):309-330.

Watt, K. E. F. (ed.) 1966. Systems Analysis in Ecology. Academic Press, New York. 276 pp.

Watt, K. E. F. 1968. Ecology and resource management. McGraw-Hill, New York. 450 pp.

Watt, W. D. 1966. Release of dissolved organic material from the cells of phytoplankton populations. Roy. Soc. (london). Proc. B. 164:521-551.

Whitledge, T. E. and T. T. Packard. 1971. Nutrient excretion by anchovies and zooplankton in Pacific upwelling regions. Inv. Pesq. 35(1):243-250.

Yentsch, C. S. 1963. Primary production. Oceanog. Mar. Biol. Ann. Rev. (1):157-175.

VITA

Mr. J. S. Wroblewski was born June 8, 1948 in Chicago, Illinois. In 1970 he graduated with honors from the University of Illinois, Chicago Circle, with a B.S. in Biological Science. He began his graduate study in the Department of Oceanography at the Florida State University in September, 1970.